GLASS ASSISTED SINTERING OF $BaTiO_3$

By

K. UMESH KUMAR

INTERDISCIPLINARY PROGRAMME IN MATERIALS SCIENCE

INDIAN INSTITUTE OF TECHNOLOGY, KANPUR

JANUARY, 1983

GLASS ASSISTED SINTERING OF $BaTiO_3$

A Thesis Submitted
In Partial Fulfilment of the Requirements
for the Degree of
MASTER OF TECHNOLOGY

By
K. UMESH KUMAR

to the
INTERDISCIPLINARY PROGRAMME IN MATERIALS SCIENCE
INDIAN INSTITUTE OF TECHNOLOGY, KANPUR
JANUARY, 1983

C E R T I F I C A T E

Certified that this work on 'Glass assisted sintering of $BaTiO_3$' by K. Umesh Kumar has been carried out under my supervision and the same has not been submitted elsewhere for a degree.

E.C. Subbarao
Professor
Department of Metallurgical Engineering
Indian Institute of Technology
KANPUR.

ACKNOWLEDGEMENTS

I am greatly indebted to Prof. E.C. Subbarao for the excellent guidance. I esteem very much the invaluable experience gained under his supervision.

I am thankful to Dr. D. Chakravorty for the guidance in the early stages of the work.

I am grateful to Dr. K.P. Gupta and Dr. K.V. Rao for providing certain instruments.

My sincere thanks go to Mr. B. Sharma and Mr. Prasad of A.C.M.S. for allowing me to utilize the central facility. They helped me to speeden up the work in all stages.

I am indebted to Mrs. Padmavathi Sankar, Mr. V.P. Srivastava, Mr. L.M. Arunachalam, Mr. U. Ramakrishna and Mr. Viswanath Singh for their help throughout the work.

I am grateful to Messrs. G.V. Srinivasan, J. Krishnamurthy, M. Krishnamurthy, Suriyanarayana, Manoharan, Gopala Krishnan, G.T. Parthiban, M. Lawrence, V.T. Swamy, Pandian, Chandrashekaran, Y. Ravi Shankar and others for their timely help.

I am thankful to Mr. R.N. Srivastava for the excellent typing and Mr. Jain for the excellent drafting work.

This work was supported by the Department of Electronics, Government of India and their financial assistance is greatly acknowledged.

- K. UMESH KUM

CONTENTS

LIST OF TABLES

LIST OF FIGURES

ABSTRACT

I.	INTRODUCTION	1
I.1.	Electrode Problems	1
I.2.	Liquid Phase Sintering	2
I.3.	Internal Boundary Layer Capacitors	4
II.	STATEMENT OF THE PROBLEM	15
III.	EXPERIMENTAL PROCEDURE	18
III.1.	Sample Preparation	18
III.1.1.	Raw Materials	18
III.1.2.	Preparation of Barium Titanate	18
III.1.2.1.	Carbonate Method	18
III.1.2.1a	Barium Titanate Formation	18
III.1.2.1b	Grinding	19
III.1.2.1c	Formation of Semiconductor Barium Titanate	19
III.1.2.1d	Mixing with $BaCO_3$ + TiO_2 Powder	19
III.1.2.1e	Mixing with 1:1.03 $BaTiO_3$	21
III.1.2.2.	Barium Titanyl Oxalate Method	22
III.1.2.3.	Manganese Addition	23
III.1.2.3.1.	Simultaneous Addition with La	23
III.1.2.3.2.	Separate Addition	24
III.1.3.	Preparation of Glass	24
III.1.4.	Preparation of Samples for Liquid Phase Sintering	25
III.1.4.1.	Insulator $BaTiO_3$	25
III.1.4.2.	Semiconductor $BaTiO_3$	25
III.1.5.	Liquid Phase Sintering	25
III.2.	Characterisation	27
III.2.1.	Thermal Analysis	27
III.2.2.	Density Measurements	28
III.2.3.	Microstructural Observation	

III.2.4.	X-ray Diffraction Studies	29
III.2.5.	Capacitance Vs. Temperature Measurements	30
III.2.6.	Capacitance Vs. Frequency Measurements	30
III.2.7.	Resistivity Vs. Temperature Measurements	31
IV.	RESULTS AND DISCUSSION	33
IV.1.	Insulator $BaTiO_3$	33
IV.1.1.	Density	33
IV.1.2.	Microstructural Observation	34
IV.1.3.	Densification Mechanism	35
IV.1.3.1.	Particle Rearrangement	35
IV.1.3.2.	Solution and Precipitation	36
IV.1.3.3.	Coalescence Process	36
IV.1.4.	X-ray Diffraction Studies	38
IV.1.5.	Temperature Dependence of Dielectric Properties	39
IV.2.	Semiconductor $BaTiO_3$	55
V.	CONCLUSION AND SUGGESTION FOR FURTHER WORK	91
APPENDIX I		93
REFERENCES		96

LIST OF TABLES

II.1.	Dielectric properties of Bi_2O_3-B_2O_3 glasses	17
III.1.	Instrument parameters of derivatograph	27
III.2.	Instrument parameters for X-ray diffraction studies	29
IV.0.	Average grain/agglomerate size values of various samples	34
IV.1.	Room temperature resistivity data of various semiconductor $BaTiO_3$ based samples	69
IV.2.	Room temperature resistivity data 25-30 μ $BaTiO_3$	70
IV.3.	Room temperature dielectric constant and dissipation data of various semiconductor based samples	71
IV.4.	Room temperature dielectric constant data of bigger grain $BaTiO_3$	73

LIST OF FIGURES

I.1.	Schematic representation of a multi layer capacitor	11
I.2.	Ag-Pd phase diagram	12
I.3.	Energy band diagram for an equivalent n-c-i-c-n representation of barrier characteristics in an internal boundary layer capacitor	13
I.4.	Different types of barrier layer capacitors	14
III.1.	Sample holder for high temperature dielectric measurements	32
IV.1.	Effect of particle size on densification of $BaTiO_3$ with G_1 glass addition at different sintering temperatures and times	41
IV.2.	Effect of particle size on densification of $BaTiO_3$ with G_2 glass addition at different sintering temperatures and times	42
IV.3.	Microstructure of liquid phase sintered 10 wt. pct. G_1 glass added samples	43
IV.4.	Microstructure of liquid phase sintered 10 wt. pct. G_2 glass added samples	44
IV.5.	Dihedral angle formed by the liquid phase at the grain boundary	45
IV.6.	Hypothetical densification curve for liquid phase sintering	45
IV.7.	Representative X-ray diffraction patterns of (a) as sintered (b) polished surfaces of 1000°C treated sample	46
IV.8.	Temperature dependence of dielectric constant of 0.65 μ to 0.82 μ $BaTiO_3$ + 4 μ G_1 samples sintered at 950°C	47

IV.9. Temperature dependence of dielectric constant of 0.82 μ to 1.2 μ $BaTiO_3$ + 4 μ G_1 samples sintered at 950°C 48

IV.10. Temperature dependence of dielectric constant of 0.6 μ to 0.82 μ $BaTiO_3$ + 4 μ G_1 samples sintered at 1000°C 49

IV.11. Temperature dependence of dielectric constant of 0.82 μ to 1.2 μ $BaTiO_3$ + 4 μ G_1 samples sintered at 1000°C 50

IV.12. Temperature dependence of dielectric constant of 0.65 μ to 0.82 μ $BaTiO_3$ + 4 μ G_2 samples sintered at 950°C 51

IV.13. Temperature dependence of dielectric constant of 0.82 μ to 1.2 μ $BaTiO_3$ + 4 μ G_2 samples sintered at 950°C 52

IV.14. Temperature dependence of dielectric constant of 0.65 μ to 0.82 μ $BaTiO_3$ + 4 μ G_2 samples sintered at 1000°C 53

IV.15. Temperature dependence of dielectric constant of 0.82 μ to 1.2 μ $BaTiO_3$ + 4 μ G_2 samples sintered at 1000°C 54

IV.16. Resistivity vs. Temperature plots of
A - 0.4 mole pct. La + 0.05 mole pct. Mn (simultaneously) added $BaTiO_3$
B - 0.4 mole pct. La + 0.05 mole pct. Mn (separately) added $BaTiO_3$
C - 0.4 mole pct. La added $BaTiO_3$ + glass G_2 coated, 1100°C/15 min treated sample
D - 0.4 mole pct. La added $BaTiO_3$, crushed, G_2 coated 700°C/1 h treated sample
E - 0.4 mole pct. La added $BaTiO_3$ 73

IV.17. ε vs. T curve for

A - 0.4 mole pct. La + 0.05 mole pct. Mn doped (simultaneously) $BaTiO_3$ + 10 wt. pct. G_2. Heat treated at 1000°C/1 h

B - 0.4 mole pct. La + 0.05 mole pct. Mn added (separately) $BaTiO_3$ + 10 pct. G_2. Heat treated at 1000°C/1 h 74

IV.18. ε vs. T curve for

A - 0.4 mole pct. La doped $BaTiO_3$ crushed and repressed, G_2 coat over one surface. Heat treated at 700°C/1 h 75

IV.19. ε vs. T curve for

A - 0.4 pct. La doped $BaTiO_3$ + glass G_2 coated on one surface and heat treated at 1100°C/15 min

B - 0.4 pct. La doped $BaTiO_3$ + 0.05 pct. Mn doped $BaTiO_3$ (heat treated at 1200°C/1 h) 76

IV.20. ε vs. T curve of

A - 0.4 mole pct. La added S(II) 5-7 μ $BaTiO_3$ + 1 wt. pct. G_2

B - 0.4 mole pct. La added S(II) 5-7 μ $BaTiO_3$ + 3 wt. pct. G_2

C - 0.4 mole pct. La added S(II) 5-7 μ $BaTiO_3$ + 5 wt. pct. G_2 77

IV.21. ρ vs. T curve of

A - 0.4 mole pct. La added S(II) 5-7 μ $BaTiO_3$ + 5 wt. pct. G_2 (1100°C/15 min)

B - 0.4 mole pct. La added S(II) 5-7 μ $BaTiO_3$ + 3 wt. pct. G_2 (1000°C/30 min) 78

IV.22. ε vs. T curve of

A - 0.4 mole pct. La added S(II) 25-30 μ $BaTiO_3$ + 1 wt. pct. Al_2O_3 + 3 wt. pct. G_2 (1100°C/15 min)

B - 0.4 mole pct. La added S(II) 25-30 μ $BaTiO_3$ + 3 wt. pct. G_2 (1100°C/15 min) 79

IV.23. vs. T curve of
A - 0.4 mole pct. La + 1 wt. pct. Al_2O_3 added S(II) 25-30 μ $BaTiO_3$ + 3 wt. pct. G_2 (1100°C/15 min)
B - 0.4 mole pct. La added S(II) 25-30 μ $BaTiO_3$ + 3 wt. pct. G_2 (1100°C/15 min) 80

IV.24. ε vs. T curves of
A - 0.4 mole pct. La + 1 wt. pct. Al_2O_3 added 25-30 μ $BaTiO_3$ + 4 pct. G_2 (1100°C/15 min)
B - 0.4 mole pct. La + 1 wt. pct. Al_2O_3 added 25-30 μ $BaTiO_3$ + 4 pct. G_1 (1100°C/15 min)
C - 0.4 mole pct. La + 1 wt. pct. Al_2O_3 added 25-30 μ $BaTiO_3$ + 3 pct. G_2 (1000°C/30 min) 81

IV.25. P vs. T curve of
A - 0.4 mole pct. La + 1 wt. pct. Al_2O_3 added S(II) 25-30 μ $BaTiO_3$ + 4 wt. pct. G_1 (1100°C/15 min)
B - 0.4 mole pct. La + 1 wt. pct. Al_2O_3 added S(II) 25-30 μ $BaTiO_3$ + 4 wt. pct. G_2 (1100°C/15 min)
C - 0.4 mole pct. La + 1 wt. pct. Al_2O_3 added S(II) 25-30 μ $BaTiO_3$ + 3 wt. pct. G_2 (1000°C/30 min) 82

IV.26. X-ray diffraction pattern of
A - 1000°C treated sample
B - 1100°C treated sample 83

IV.27. Dielectric constant vs. Frequency curves of
A - 0.4 mole pct. La added S(II) 5-7 μ $BaTiO_3$ + 3 wt. pct. G_2 (1000°C/30 min)
B - 0.4 mole pct. La added S(II) 5-7 μ $BaTiO_3$ + 5 wt. pct. G_2 (1100°C/15 min) 84

IV.28. Dielectric constant vs. Frequency curves of
A - 0.4 mole pct. La added S(II) 25-30 μ $BaTiO_3$ + 3 wt. pct. G_2 (1100°C/15 min)

B - 0.4 mole pct. La + 1 wt. pct. Al_2O_3 added S(II) 25-30 μ $BaTiO_3$ + 3 wt. pct. G_2 (1100°C/15 min) 85

IV.29. Dielectric constant vs. Frequency curves of
A - 0.4 mole pct. La + 1 wt. pct. Al_2O_3 added S(II) 25-30 μ $BaTiO_3$ + 4 wt. pct. G_1 (1100°C/15 min)
B - 0.4 mole pct. La + 1 wt. pct. Al_2O_3 added S(II) 25-30 μ $BaTiO_3$ + 4 wt. pct. G_2 (1100°C/15 min)
C - 0.4 mole pct. La + 1 wt. pct. Al_2O_3 added S(II) 25-30 μ $BaTiO_3$ + 3 wt. pct. G_2 (1000°C/30 min) 86

IV.30. ε vs. T curve of
A - 0.4 mole pct. La + 1 wt. pct. Al_2O_3 + 0.025 mole pct. Mn added S(II) 25-30 μ $BaTiO_3$ + 4 wt. pct. G_1 (1100°C/15 min)
B - 0.4 mole pct. La + 1 wt. pct. Al_2O_3 + 0.025 mole pct. Mn added S(II) 25-30 μ $BaTiO_3$ + 4 wt. pct. G_2 (1100°C/15 min) 87

IV.31. ε vs. T curve of
A - 0.4 mole pct. La + 1 wt. pct. Al_2O_3 added S(II) 25-30 μ $BaTiO_3$ + 4 wt. pct. G_1 (+ 0.025 mole pct. Mn) (1100°C/15 min)
B - 0.4 mole pct. La + 1 wt. pct. Al_2O_3 added S(II) 25-30 μ $BaTiO_3$ + 4 wt. pct. G_2 (+ 0.025 mole pct. Mn) (1100°C/15 min) 88

IV.32. ρ vs. T curves of
A - 0.4 mole pct. La + 1 wt. pct. Al_2O_3 + 0.025 mole pct. Mn added S(II) 25-30 μ $BaTiO_3$ + 4 wt. pct. G_1 (1100°C/15 min)
B - 0.4 mole pct. La + 1 wt. pct. Al_2O_3 + 0.025 mole pct. Mn added S(II) 25-30 μ $BaTiO_3$ + 4 wt. pct. G_2 (1100°C/15 min)

C - 0.4 mole pct. La + 1 wt. pct. Al_2O_3 added
S(II) 25-30 μ $BaTiO_3$ + 4 wt. pct. G_1
(+0.025 mole pct. Mn) (1100°C/15 min)
D - 0.4 mole pct. La + 1 wt. pct. Al_2O_3 added
S(II) 25-30 μ $BaTiO_3$ + 4 wt. pct. G_2
(+0.025 mole pct. Mn) (1100°C/15 min) 89

IV.33. ε vs. Frequency curve of above samples 90

ABSTRACT

$BaTiO_3$ ceramics are conventionally sintered at 1300-1400°C. By liquid phase sintering technique, sintering temperature was tried to be reduced and so the cost of preparation. Lower temperature sintering allows the usage of Ag-Pd alloys, silver and nickel electrodes and so the cost of production is reduced further. With $BaTiO_3$ + 74 mole % Bi_2O_3:26 mole % B_2O_3 glass, detailed work was carried out by Ramesh Chowdary (10). For the investigation, 5 and 13 μ $BaTiO_3$ was used. Reasonably dense bodies (greater than 85% of theoretical density) are obtained with 10 to 20 wt. % glass additions by sintering at 1000-1050°C.

In the present investigation, 0.75 and 1 μ $BaTiO_3$ powders were used. These powders were sintered with 10 wt. % of 74 mole % Bi_2O_3:26 mole % B_2O_3 (G_1) and 60 mole % Bi_2O_3:40 mole % B_2O_3 (G_2) glasses at 950°C and 1000°C for the period from 6 min to 2 hrs. 1 μ $BaTiO_3$ powder with both G_1 and G_2 glasses showed reasonably dense bodies (greater than 85% of theoretical density) by sintering at 1000°C.

Various methods of making semiconducting $BaTiO_3$ and of coating these grains with an insulating layers were examined and successful procedures were established. Room temperature dielectric constant of 36000 reaching to 78000 at the Curie point have been obtained with 25-30 μ $BaTiO_3$ and G_2 coating. Reasonably high values of room temperature resistivity with little change at Curie temperature, and reasonably good frequency response of dielectric constant are observed for these

samples. With Mn addition, even though the room temperature dielectric constant value has got reduced to 23000, very high resistivity, $\sim 10^{10}$ ohm-cm, with very little change at Curie point observed. Dielectric constant variation with frequency has got reduced considerably.

I. Introduction

Ferroelectric ceramic materials play a dominant role in the capacitor industry. Barium titanate is one of the few materials widely used in capacitors.

Because of the extensive research, many problems associated with the manufacturing of barium titanate were solved. At present, more or less, it is possible to produce the material to get the required properties. However the cost factor is yet to be solved. By reducing the thickness and increasing the area, high values of capacitance can be achieved. By producing multilayer capacitors (Figure I.1) volumetric efficiency is increased. By means of internal boundary layer capacitors the efficiency is improved further, even though the cost is high because Pt and Pd are used as electrodes.

I.1. Electrode Problems:

The usability of an electrode material is determined by two properties:

1. Its melting point should be higher than the sintering temperature.

2. Its metal/metal oxide equilibrium oxygen vapour pressure should be higher than that of oxygen partial pressure during firing.

Higher firing temperature (1350-1400°C) and the firing atmosphere (air) restricts the usability of other materials. Some time gold is used as Au-Pd alloy. Silver has a

lower melting point (961°C) and transition metals like Ni, Co and Fe have low oxygen equilibrium pressure.

Pt, Pd and Au can be replaced either by developing ceramics which can be fired in an atmosphere with an oxygen partial pressure lower than the equilibrium pressure of one of the transition metals at this temperature or by lowering the firing temperature below the melting temperature of Ag or one of the low melting Ag-Pd alloys.

Mn doping is suitable to sinter the material in reducing atmosphere (1-4). This prevents the reduction of $BaTiO_3$ and so the oxidation of electrodes. So base metals, such as nickel, which have melting temperature higher than the sintering temperature can be used.

I.2. Liquid Phase Sintering:

By reducing the sintering temperature one gets two advantages. From the Ag-Pd phase diagram (5) given in Figure (I. 2) one can see that 30 Pd-70 Ag alloy can be used if the sintering temperature is reduced to 1000-1050°C. If it is further reduced (below 950°C), silver alone can beused. Moreover, by reducing the sintering temperature below 1000°C nichrome furnaces can be used instead of the expensive high temperature furnaces. So manufacturing cost can be reduced enormously.

To reduce the sintering temperature liquid phase sintering was tried. The sintering temperature is lowered by using a transient liquid phase. The liquid phase should

i. It should melt at or below 800-900°C.

ii. It should not react with the dielectric composition.

iii. The crystalline phase, formed on cooling, should preferably have a relatively high dielectric constant, so that the dielectric constant of the composite is not greatly reduced.

iv. The viscosity of the liquid should be low at the sintering temperature so that the amount of liquid phase needed is kept to a minimum.

Lead germanate is one such liquid phase (7,8). Park (7) has developed dielectric ceramics which can sinter at 800-900°C. Ferroelectric nature of the crystalline lead germanate ($Pb_5Ge_3O_{11}$) is the distinct advantage in retaining fairly high dielectric constant of the composite.

Mukherjee and Ravishankar (8) sintered $BaTiO_3$, using 0.6 to 1 mole percent of lead germanate, at 1150-1200°C. Above 1200°C PbO and GeO_2 diffuse into the lattice and due to the partial replacement of Ba by Pb, room temperature dielectric constant is reduced. The toxic nature of lead and the high cost of germanium are the other deterrent factors.

0.5 to 1 mole % CuO was used to reduce the temperature to about 1200°C (9). But with excessive addition, the samples become conductive and thus useless.

Effect of Bi_2O_3-B_2O_3 glasses was studied (10) It is found out that, with 74 mole % Bi_2O_3-26 mole % B_2O_3 glass, reasonable densification occurs with 10 wt. % glass. Better temperature characteristics were observed with upto

20 wt. % glass addition. For this work 13 μ $BaTiO_3$ + 17 μ glass and 5 μ $BaTiO_3$ + 4 μ glass were used.

The next possible way to reduce the cost is using IBL capacitors. Since the room temperature dielectric constant value is, $> 20,000$ and $\tan\delta$ value is < 0.1, very small quantity is needed to get large capacitance value. For many applications $\tan\delta$ value is reasonable. If it is possible to do liquid phase sintering the cost can be reduced further.

I.3. Internal Boundary Layer Capacitors:

This is basically, a semiconducting ferroelectric barium titanate grain, surrounded by the non-conducting grain surface. The effective dielectric constant value depends on ε_1, σ_1, ε_2 and σ_2 where ε stands for dielectric constant and σ stands for conductivity of the two media (11).

The basic problem in the production of IBL capacitor is the preparation of semiconductive barium titanate with low resistivity. The semiconductor is produced either by adding small quantity of aliovalent ions or by heat-treating in reducing atmosphere. Combination of the two are also not uncommon.

The semiconducting property of $BaTiO_3$ was first reported by Sauer and Flaschen (12). Then Saburi (13) reported the usefulness of Ce and La for Ba substitution, Nb, Sb and Ta for Ti substitution. Thereafter many rare earths like Sm, Ga, Ho (14), Sb (15), Y and Sr (16) were found to give good properties.

Mainly carbonate method (15,17) and Barium titanyl oxalate method (13,18,19) were employed. The dopant was added as nitrate (14) or as oxalate (13) etc. after formation of $BaTiO_3$. Before formation of $BaTiO_3$, it was added in chloride form (17-19).

Method of preparation, effectiveness of mixing, heat treatment procedure, Ba/Ti mole ratio and grain size are the important variables in producing good semiconductor $BaTiO_3$.

With some dopant, different concentrations were reported to give lowest resistivity value. For example, with La 0.13 M% (18), 0.3 M% (17), 0.35 to 0.45 M% (18) were used to get lowest possible sensitivity value. The needed amount depends mainly on the degree of mixing. By radioactive tracer technique it is found out that in BTO technique, by which the most effective mixing is achieved, only 20% of La added goes to the material (19).

Heating temperature and heating time also play an important role in the room temperature resistivity value (17). As the heating time is increased the resistivity value is also increased (17). Two competing reactions, namely formation of Barium vacancies and the formation of oxygen vacancies are taking place at the sintering temperature. By increasing the heating time the material is allowed to get equilibrated and so the formation of oxygen vacancies to compensate the excessive charge. Hence a rise in room temperature resistivity is observed. For the same heating time and different temperatures different dopant concentrations are shown to give

Small excess of either Ba or Ti does not alter the properties very much (13,19,20). Small excess of Ti improves the semiconductor properties (19,20). Probable reason is the formation of liquid phase at the sintering temperature and so the uniformity in doping (20).

Effect of grain size is also studied and it is found out that lower the grain size better the semiconductor properties (21). The same relation, namely, lower the initial pelletization pressure better the conductivity and PTC value, is found with the pressure (22).

Very low values of resistivity, say in 10^1 ohm-cm range (compared to 10^{10} ohm-cm range of pure $BaTiO_3$) and the sharp rise in resistivity value at the transition temperature (Curie temperature) are the inherent properties of semiconductor barium titanate. The positive temperature coefficient of resistance (PTCR) effect depends greatly on the preparation technique. Normal firing (13,17,18), firing in different atmospheres (17, 23), halogen treatment (24), and doping with Mn etc. (25, 26) were employed and their effect on PTCR value was studied. Even though, the defective grain boundary is proved to be necessary (27, 28) to produce PTCR effect, certain materials, like B, Al and Si (26) are found to give decreased value of PTCR.

Various models are proposed to explain the PTCR behaviour. Except Saburi's local field mechanism (13, 28) all other models are based on the surface defects. Many models are just improvements over Heywang's barrier layer model (15,29).

Briefly, the barrier layer model is (15, 28, 30) explained as follows (Figure I.3). Crystal grains of two different orientations are in contact, their Fermi level equilibr ated and so a space charge is set up in the grain boundary. This space charge constitutes a potential barrier for conduction electrons from the donor doping ions. The barrier width i.e., its tailing-off distance into the grains on either side, is a function of their dielectric constant. If the dielectric constant value is high, the barrier layer is thin and vice versa.

Many properties (15, 31) are explained by this model. To explain the remaining properties, various improvements are proposed (29). But still the controversy over the presence of defect or extra phase on the boundary is not over. By indirect methods, like Hall effect measurement (27), a.c. field behaviour (15) etc., the importance of defective surface is proved. But by direct observation using electron microscope (29) non-existence of defective surface or extra phase is also proved.

Three types of barrier layer capacitors are produced generally (Figure I.4) (32). First material consists of very thin insulating layer on the surface of the semiconductor. Here the semiconductor material acts mainly as a mechanical support.

In the second case, during the cooling or post treatment period, thin layer of the semiconducting grains are converted to an insulating state (33,36).This mechanism, which also plays an important role in PTC materials, leads to

insulating layers of nearly the same chemical composition as the grains.

In the third case, the grains are coated with an insulating second phase.

Last two types are called grain boundary barrier layer capacitors.

Barrier layer capacitors are mainly produced by reoxidation of H_2 reduced semiconductor $BaTiO_3$ (35). To get lowest resistivity pure (35)or donor doped (36)$BaTiO_3$ or (Ba,Sr) TiO_3 is reduced at higher temperature, typically 1400°C and an insulating layer is formed at lower reoxidation temperature. Reoxidation temperature and the oxygen partial pressure of the heat treating atmosphere along with the heat treating time determines the thickness of the insulating layer and the dielectric constant value.

Grain boundary barrier layer capacitor of first type (Figure I.4b) are produced by one of the following techniques.

1. Sintering $BaTiO_3$ in H_2 atmosphere at 1450°C to produce hexagonal semiconductor $BaTiO_3$, and cooling rapidly to 1000°C to retain the structure, then to room temperature slowly. By this porous pellets are formed. By reoxidation between 650 and 1000°C thin insulating grain boundary layers are found (37). Hexagonal form is chosen because of its low dissipation factor and the absence of the Curie point. Since the material is porous it is not used commercially.

2. This method, namely, preparation of thin insulating layer by metal ion dopant, is commercially used to produce

GBBL capacitors. First such material was produced by Waku (38,39) Dy_2O_3 was doped to produce semiconductive $BaTiO_3$ grain. Grain boundary insulation was accomplished by painting onto the faces of the specimen a slurry of the oxide of copper or manganese or other metals, or any of 18 other elements or their oxides. CuO was found to be one of the most effective. Thereupon many patents were taken (40,41). Semiconductor $BaTiO_3$ of 20-40μ m grain size and 1 to 2 μ m grain boundary thickness gives a dielectric constant value, typically, 20000. The true resistivity of the grain boundary material is estimated to be $\simeq$ 2 - 3 x 10^{12} ohm-cm. Much higher values are achieved by selecting $Ba(TiSn)O_3$ as the base material and Dy_2O_3 and CuO as the respective dopants.

Second type of GBBL capacitors are produced by diffusing a glass at around 1000°C. Such materials of $BaTiO_3$ have serious disadvantages like, high loss and poor temperature dependence (32,42). But GBBL capacitors of $SrTiO_3$ with PbO-Bi_2O_3-B_2O_3 glass show very good properties (32). This glass is selected because of its low melting point and the high dielectric constant value of the layered pervoskite type of Pb-Bi-Ti compound forming as a thin coating.

Some general conditions and properties are (36,43):

1. An effective dielectric constant that, below the relaxation frequency range, exceeds the intrinsic value by the factor of the ratio of grain dimension to grain boundary thickness; above the relaxation frequency it drops to the intrinsic value.

2. An effective resistivity, that at low frequencies, is smaller than the grain boundary resistivity by the factor of the inverse dimensional ratio and that decreases, above the relaxation, to the grain resistivity.

3. An effective time constant that is the intrinsic RC product is increased by the factor $(d_g/d_{gb})^{1/2}$.

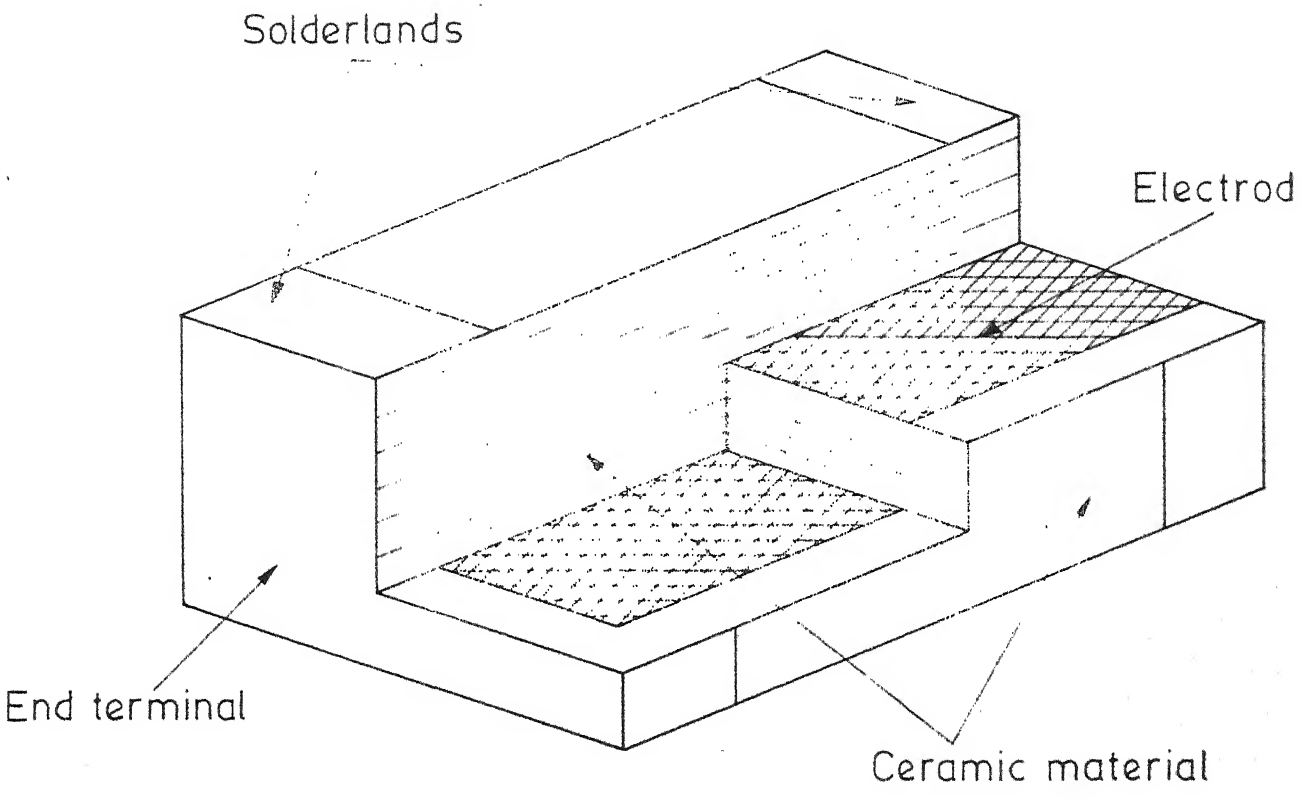

Fig. I .1. Schematic representation of a multilayer capacito

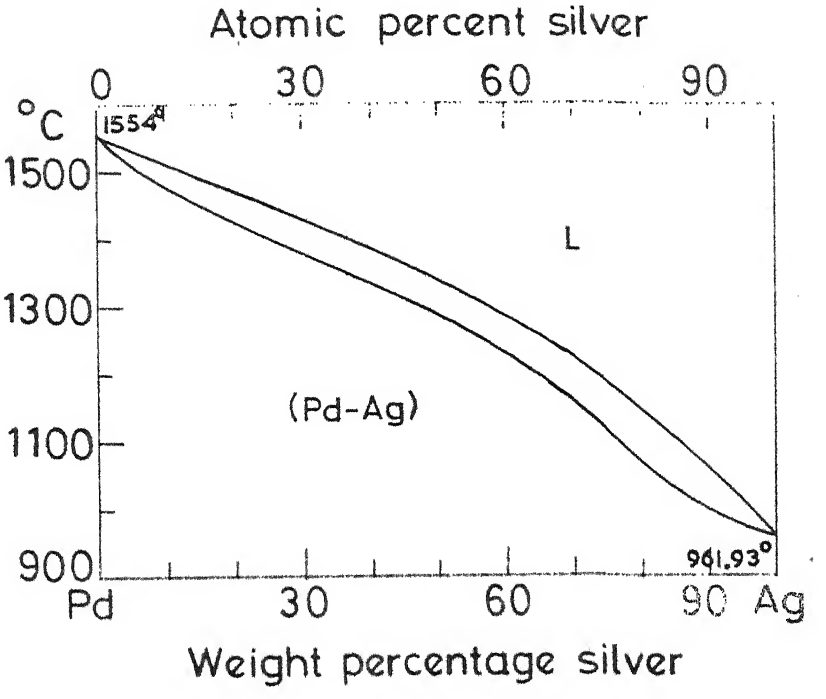

Fig. I.2 Ag-Pd Phase diagram.

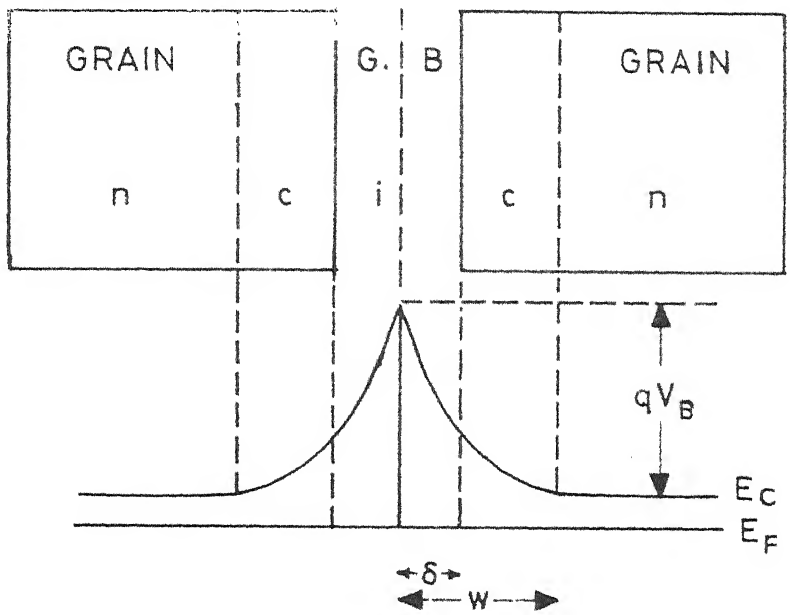

Fig.I.3 Energy band diagram for an equivalent n-c-i-c-n representation of barrier characteristics in an internal boundary layer capacitor

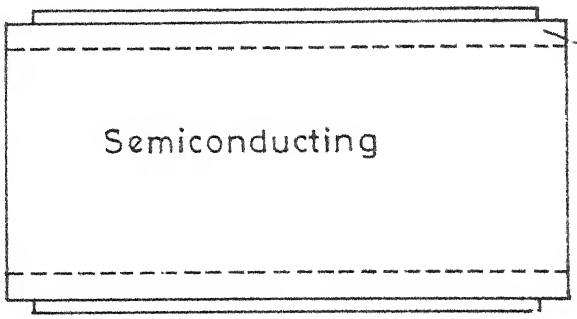

Insulating surface layers formed by reoxidation

$d_1 = 2 - 20\,\mu m$

$K_1 = 1000$

a) Surface layers

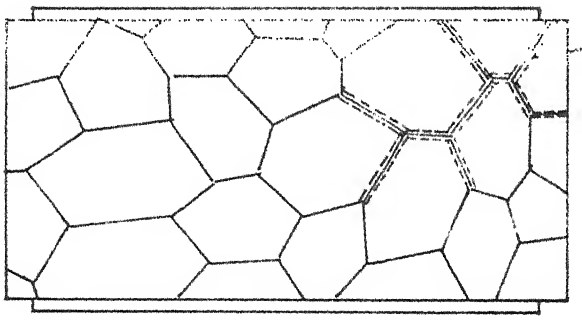

Insulating grain boundary layers formed by diffusion of defects

$d_1 = 0.5 - 2\,\mu m$

$K_1 = 500 - 1000$

b) Internal grain boundary layer

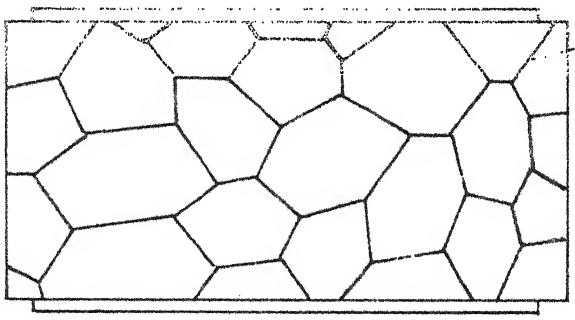

Insulating grain boundary layers formed by second phases

$d_1 = 0.1 - 2\,\mu m$

$K_1 = 50 - 300$

c) Second phase layers

Fig I.4 Different types of barrier layer capacitors. Typical values for the thickness d_1 and the dielectric constant K_1 of the insulating layers are given on the right.

II. STATEMENT OF THE PROBLEM

From (10), one can conclude the following:

1. With 10 wt. % of the 74% Bi_2O_3 and 26% B_2O_3 glass and 1050 to 1100°C sintering reasonable properties were achieved.

2. For both particle sizes of $BaTiO_3$, 5 μ and 13 μ, the sintering temperature and the amount of glass needed, to get reasonable properties are the same.

In the present work the effect of lower particle size ($\leq$1 μm) is investigated. The glass 74% Bi_2O_3:26% B_2O_3 (G_1) has a melting temperature of approximately 650°C (44). Effect of another glass with more boron and with reasonably good dielectric properties on the sintering behaviour of $BaTiO_3$ is worth investigating. So a glass of 60% Bi_2O_3:40% B_2O_3 (G_2) is selected. The dielectric properties of this glass is given in Table II.1).

In short, the effect of following variables on densification and dielectric properties are studied.

1. Particle size of $BaTiO_3$, 0.75 and 1 μ.
2. Two glasses G_1 and G_2
3. Sintering temperature, 900, 950 and 1000°C
4. Sintering time - 6, 10, 15, 30, 60 and 120 minutes.

Having studied the effect of glass to reduce the sintering temperature of insulator barium titanate, its effect on the sintering of the semiconductor $BaTiO_3$ is also studied. For this, various methods are tried to dope La to

produce good reproducable semiconductor $BaTiO_3$ and their final properties are studied. Addition of an acceptor type impurity, Mn, and its effect is also studied. Bulk diffusion of Mn grain surface coatings are tried and the final properties are studied. In all the cases, the effect of glass addition and the dielectric properties of sintered products are examined.

Table II.1. Dielectric Properties of Bi_2O_3-B_2O_3 Glasses

(Dielectric constant at room temperature and resistivity (ohm-cm) at 130°C and 230°C)

Glass No.	Composition mole %		Dielectric constant				100 tanδ		ρ_{130}	ρ_{230}
	Bi_2O_3	B_2O_3	10^3 c/s	10^5 c/s	10^7 c/s	9.6x 10^9 c/s	10^3 c/s	9.6x 10^9 c/s	($x10^{14}$) ohm-cm	($x10^{11}$) ohm-cm
19	26	74	14.1	13.9	13.6	10.3	0.13	0.84	34	340
25	32	68	21.8	21.8	21.4	16.1	0.15	1.24	6.4	10
26	40	60	28.0	28.0	26.6	19.1	0.14	2.88	1.3	5.9
27	46	54	31.0	31.1	29.8	22.1	0.18	3.29	0.55	0.70
22	54	46	31.1	31.1	29.9	21.5	0.32	2.41	0.16	0.25
60	60	40	37.6	37.1	36.2	24.3	0.22	1.72	0.023	0.042
28	66	34	38.8	38.7	36.5	26.6	0.22	1.98	0.013	0.022
29	74	26	42.5	42.5	41.2	31.1	0.21	1.90	0.0017	0.0058

III. Experimental Procedure

III.1. Sample Preparation:

III.1.1. Raw materials:

Raw materials used were (all of them are AR grade, more than 99 percent purity) barium carbonate (Reanal, Hungary), titanium dioxide (Baker Analysed Reagent, U.S.A.), boric acid (Sarabhai Chemicals, India), bismuth oxide (Mayfair and Raydon, England), barium chloride (British Drug Houses, India), oxalic acid (British Drug Houses, India), titanium tetrachloride (Riedel-De Haen Ag Seelze-Hannover, Germany), lanthanum oxide (Indian Rare Earths Ltd., India) and Manganese carbonate (Baker Analysed Reagent, U.S.A.).

III.1.2. Preparation of barium titanate:

Two different methods, namely carbonate and barium titanyl oxalate methods, were employed to prepare barium titanate.

III.1.2.1. Carbonate method:

III.1.2.1a. Barium titanate formation:

1:1.03 $BaCO_3$ and TiO_2 (45) powders were mixed in acetone media using Fritsh pulveriser in agate jar using agate balls for 4 to 5 hrs. In the pulverizer, four agate jars are fixed on a rotating wheel. Each jar is fixed in such a way, that while the wheel is rotating, the jar also rotates but with a spin. Agate balls, of 1" dia and 1/4" dia, are used to grind the material. By the combination of rotation and spin the

efficiency of breaking the particle is improved. Every time 100 gms of the mixture was taken. The mixed powder was then compacted at 4 tonnes of pressure using a hydraulic press to improve reaction during calcination. Calcination was carried out in an alumina crucible at 1200°C for 6 hrs. After calcination the material was pulverized for 48 hrs. in water media using Fritsh pulveriser. The fine powder was repeatedly washed to remove Ba_2TiO_4 phase using distilled water (46). The operation was carried out till the pH of the filtrate shows 7.2 to 7.4. These washings were done to remove $Ba(OH)_2$ which forms as a by-product of Ba_2TiO_4 and H_2O reaction (45).

$$Ba_2TiO_4 + H_2O \longrightarrow BaTiO_3 + Ba(OH)_2 \qquad \text{(Eq. 1)}$$

III.1.2.1b. Grinding:

To get 4 μ $BaTiO_3$ wet grinding was employed using Fritsh pulveriser. Then to get, 0.65 to 0.82 μ $BaTiO_3$ dry grinding was employed using Fritsh pulveriser (Ultrasonic vibrator). Agate jar and ball were used. Every time around 6 gms of powder was ground for 13 hrs. To get 0.82 to 1.2 μ $BaTiO_3$ powder, 6 gms of powder was ground for 6 hrs.

III.1.2.1c. Formation of semiconductor barium titanate:

Two different procedures were tried.

III.1.2.1d. Mixing with $BaCO_3$ + TiO_2 powder:

A stock solution of lanthanum nitrate was prepared by reacting lanthanum oxide with concentrated nitric acid. First, the amount of La_2O_3 present in the $La_2O_3.xH_2O$ powder was

determined by TG and chemical analysis (Appendix I). By both methods it was found that 86% of the material is La_2O_3 and the remaining is water. So after correcting to 86%, 1.7135 gm of $La_2O_3.xH_2O$ powder was dissolved in concentrated nitric acid. The solution was slowly evaporated to remove excess nitric acid. Twice or thrice distilled water was added to the remaining powder and the solution was reevaporated. This $La(NO_3)_2.xH_2O$ powder was dissolved in 100 ml of distilled water, using a standard flask. This solution was kept as stock solution. The amount of solution to be added to the $BaCO_3$ + TiO_2 mixture was calculated for different concentrations of dopants. For example, for 0.3 mole % of La addition, the amount added to the 25 gm of $BaCO_3$ + TiO_2 mixture was 3.5 ml.

After adding lanthanum nitrate to the $BaCO_3$ + TiO_2 mixture, the powders were mixed thoroughly in Fritsh pulverizer for 12 to 15 hrs. in acetone media. The dried mixture was made into cakes using 4 tonnes of pressure. The mixture was heat treated, at 150°C for 2 to 3 hrs. to dissociate $La(NO_3)_2$ and to form La_2O_3, either before forming cakes or after forming.

The cakes with 0.3, 0.4, 0.5 and 0.6 mole % of La were subjected to different heat treatment shedules to find out the resistivity value. They were heat treated first at 1250°C, 1300°C and 1325°C for 3 hrs. and it was found that 1300°C heat treatment yielded uniform blue coluration. So, they were subjected to 1300°C/0, 1, 2, 3, 4 and 5 hrs. heat treatments. Among them 0.4 mole % La doped sample heat treated at 1300°C/5 hrs. gave uniform blue colouration.

The resistivity value was found by using In-Hg electrode (47). Mercury dipped Indium metal was firmly rubbed on both faces and the resistence value was found using a multimeter. Using the standard formula $\rho = R \frac{A}{l}$ ohm-cm, where ρ- resistivity, R - resistance, A - area in cm^2 and l - thickness in cm, the resistivity value was calculated. The above mentioned sample had $\rho = 3.07 \times 10^3$ ohm-cm. But since the value is high and the reproducibility is very poor this method was dropped altogether.

III.1.2.1e. Mixing with 1:1.03 $BaTiO_3$:

$BaTiO_3$ is prepared by calcining the mixture of 1:1.03 of $BaCO_3$:TiO_2 mixture using the procedure given in Section III.1.2.1a.

With 4 μ $BaTiO_3$ powder, lanthanum was mixed as follows. 0.406 gms of $La_2O_3.xH_2O$ was used to form lanthanum chloride solution. Lanthanum oxide was treated with concentrated hydrochloric acid and the excess acid was evaporated thorough repeated addition of distilled water. The lanthanum chloride powder was then dissolved in water and the solution was made up to 100 ml using a standard flask. From this stock solution necessary amount of solution was pipetted out. For example, to add 0.4 mole % La to 5 gms $BaTiO_3$, 4 ml of solution was used.

$BaTiO_3$ after adding La solution was made into slurry by vigorous stirring after adding 50 ml of water. After 5 minutes of mixing concentrated ammonia solution was added slowly. Lanthanum hydroxide was formed and by stirring for 5 more minutes it was mixed thoroughly. The powder was filtered

out and lightly washed to remove excess ammonia (22). The powder was oven dried and made into cakes by applying 4 tonnes of pressure using a hydraulic press. Using an alumina crucible the cakes were heat treated.

The cakes with 0.3, 0.4 and 0.5 mole % of La were heat treated to 1350°C/1 hr. and 1400°C/1 hr. using alumina crucibles. 0.4 mole % La and 1400°C/1 hr. treatment gave lowest room temperature resistivity value, ρ = 400 ohm-cm. For consistency, at least four batches were prepared and resistivity values were checked. The maximum value obtained was ρ = 450 ohm-cm. So these samples were used for further sintering experiments.

III.1.2.2. Barium titanyl oxalate method:

Semiconductor $BaTiO_3$ alone was prepared by this method. Desired quantities were taken for a 30 gm batch. Same procedure as reported by Clabaugh et al. (48) was used here also.

Titanium tetrachloride was diluted using deionized water with the help of ice bath. 250 ml of $TiCl_4$ was added to 250 ml of water and that was further diluted to 1250 ml. The concentration of $TiCl_4$ was found out to be 0.223 gms per ml. (Appendix I).

The following amounts were taken to prepare 0.3% La doped BTO:

1. 23.125 gm of oxalic acid was dissolved in 125 ml of water.
2. 71.03 ml of $TiCl_4$ solution was taken.
3. 9.35 ml of La chloride solution (III.1.2.1e) was pipetted out.

4. 20.559 gms of $BaCl_2 2H_2O$ was dissolved in 200 ml of water. 2, 3 and 4 were mixed (18). This solution was slowly dripped into oxalic acid which was vigorously stirred and maintained at 80 to 83°C. White flocculent precipitate was formed, as soon as the $BaCl_2.2H_2O$ + $TiCl_4$ mixture touched the oxalic acid, and redissolved. After 10 to 15 minutes white precipitate started forming. As soon as the reaction is over the salt was separated (1°) and washed with hot water (80 to 85°C) repeatedly to remove excess oxalic acid, and to avoid low temperature unwanted reactions (18). Then it was washed with acetone a few times to remove the last traces of water. The powder was dried in an air oven.

Formation of $BaTiO_3$ was carried out at 900°C/1 hr. using a platinum crucible (22). Then cakes were formed by applying 4 tonnes of pressure in a hydraulic press and they were heat treated at 1400°/1 hr using a ZrO_2 crucible.

By this method 0.2 mole % and 0.3 mole % of La added samples were prepared.

III.1.2.3. Manganese addition:

Two different techniques were employed.

III.1.2.3.1. Simultaneous addition with La:

In case of 0.4 μ, 1:1.03 $BaTiO_3$ along with lanthanum chloride, manganese chloride was also added in the required quantity. Manganese oxide was treated with concentrated HCl and manganese chloride was prepared. This was diluted to 0.00308 gms of Mn/ml concentration.

0.4 mole % La and 0.05 mole % Mn were simultaneously added to the slurry and the hydroxides were precipitated by ammonia addition. The cakes were heat treated at 1400°C/1 hr.

In case of BTO, 0.02 mole % of Mn and 0.3 mole % La were added to $BaCl_2.2H_2O$ + $TiCl_4$ mixture and the reaction was carried out.

III.1.2.3.2. Separate addition:

In both cases, semiconductor powder was prepared as a slurry and then Mn solution was added. Manganese hydroxide was precipitated and the cakes were heat treated at 1200°C/1 hr.

III.1.3. Preparation of glass:

Two different compositions of glasses were prepared. 20 gm batches of 74 pct. Bi_2O_3, 26 pct. B_2O_3 (G_1) and 60 pct. Bi_2O_3, 40 pct. B_2O_3 (G_2) were prepared as follows. Required amount of Bi_2O_3 and H_3BO_3 were measured and mixed in an agate mortar using acetone. The dried mixtures were heated in alumina crucibles to 750°C. Then the molten glass was poured into a tray containing distilled water. The glass pieces were collected and grounded in Fritch pulveriser (ultrasonic vibrator) for 6 hrs. The final particle sizes were measured as 4 μ using Fisher subsieve sizer.

The concentrations were cross checked by chemical analysis.

For G_1 and G_2 glasses the chemical analysis values for Bi_2O_3 are 73.8% and 59.6% respectively (Appendix I).

III.1.4. Preparation of samples for liquid phase sintering:

III.1.4.1. Insulator $BaTiO_3$:

Four different samples were prepared. Two particle sizes (0.75 and 1 μ) with two glasses G_1 and G_2. Each time 5 to 6 gms of $BaTiO_3$ powder was mixed with 10 wt. % of glass using acetone in agate mortar for about 30 minutes. The mixture was pressed into discs using 3/8" dia die, after mixing it with PVA binder. Pressing was carried out using Bimco double acting automatic hydraulic press at 8 tonnes of pressure. The thickness of the pellets was maintained between 1 to 1.5 mm.

III.1.4.2. Semiconductor $BaTiO_3$:

Different semiconductor powders were used. As explained above, they were mixed with 10 wt. % of glass and pressed into 3/8" dia discs. Few pellets were pressed using hand operated hydraulic press at 2.5 tonnes of pressure.

III.1.5. Liquid phase sintering:

A globar horizontal tube furnace was used to sinter the samples. Samples were stocked in two alumina boats which were connected to each other. The boats were pulled by a stainless steel rod from one end to the other end. Constant temperature zone was found out and the first boat was pulled to that place in 1 hr. 45 minutes. The next boat at that time would be in the heating zone. After the set soaking period the next boat was pulled to the soaking zone in 1 hr. The first boat by this time came to the cooling zone. After the set soaking period, the boats were pulled out of the furnace in 2 hrs.

The heating and cooling rates were maintained 10°C/min. for 950°C treatment and 10.5°C/min. for 1000°C treatment. The boats were pulled approximately 1 cm per every 3 minutes. Soaking time was varied as 6, 10, 15, 30, 60 and 120 minutes.

In the case of semiconductor pellets, few sinterings were carried out at 1100°C, 1200°C and 1250°C. These experiments were carried out using a globar muffle furnace. The set temperature was achieved in 5½ to 6 hrs. period. After necessary heating the furnace was switched off and allowed to cool to the room temperature before removing the sintered samples.

Some semiconductor pellets were flash fired (FF). In the horizontal furnace, the boat was pulled to soaking zone in 1/2 to 1 minute and after allowing soaking time, it was pulled out in 1/2 to 1 minute. Within 3 to 5 minutes the samples attained the room temperature.

For higher temperature (1100°C, 1200°C etc.) flash firing, muffle furnace was used. After heating the furnace to the set temperature, the alumina crucibles with the samples were lowered into the furnace. After specified heating time, the samples were taken out. Within 3 to 5 minutes, temperature came down to room temperature value.

Some semiconductor samples were sintered in N_2 atmosphere. 1/2 m length, one end closed, alumina tube was used for this purpose. Open end was closed with copper flanges. A stainless steel tube of 1/2 m length was introduced to 3/4th of the length of alumina tube through the top flange. This well sealed tube was used as gas inlet. Outlet was provided in the bottom flange. Samples were kept in a small alumina

crucible and the crucible was lowered to the bottom of the alumina tube. After providing gas connections, the tube was slowly introduced inside the horizontal furnace. In one hour, the bottom portion was pushed to soaking zone. After the soaking period, the tube was pulled out in 1 hr. period. The rate of pulling and pushing was 5 cms per 12 minutes.

III.2. Characterisation:

III.2.1. Thermal Analysis:

Simultaneous DTA, DTG and TG studies were carried out on $La_2O_3.xH_2O$ sample using MOM Derivatograph. By this, the amount of La_2O_3 present in the commercially available lanthanum oxide powder was determined. The instrument parameters are given in Table III.1.

Table III.1: Instrument Parameters of Derivatograph

1.	Heating rate :	5°C/min.
2.	Reference sample :	Alumina powder
3.	Sensitivity of DTA :	1/5
	DTG :	1/100
4.	Maximum temperature :	1000°C
5.	Amount of sample :	1.732 gms.

III.2.2. Density Measurements:

Geometrical densities were measured. The pellets were weighed (w) in a Mettler single pan, electric balance. The volume (V) was calculated by measuring thickness and diameter of the samples using screw gauge. Density was calculated as (W/V). Average value, of three measurements, was reported as density.

III.2.3. Microstructural Observation:

Samples were mounted in a thermosetting plastic such that one face of the disc was exposed. They were polished using silicon carbide powder, over a glass plate, in liquid paraffin media. They were polished successively on 600 and 800 mesh size SiC powders. Then they were polished on a rotating cloth using diamond paste for 24 hrs. The polished samples were etched approximately for 30 seconds with a solution containing 5 pct. HCl and 0.5% HF (49). The microstructure was observed under a Carl Zeiss NU 20 microscope using reflected light. Microstructural study of sintered discs was used to examine the thoroughness of glass coating over the $BaTiO_3$ grains and the effect of sintering time and temperature on microstructure development.

Grain size measurement was carried out using the same microscope. For the following microscope settings filar micrometer eye-piece was precalibrated.

Eye-piece	-	15X
Objective	-	25X
Zoomlens dia	-	12.5

It was found that each division on the specimen of thermocrometer corresponds to 0.417 microns.

Approximately 125 grains were measured and from the statistical distribution average grain size was determined.

III.2.4. X-ray Diffraction Studies:

To determine the phases present, X-ray diffraction patterns were taken with Philips X-ray diffractometer (Type PW 1730/10) and the instrument parameters are given in Table III.2.

Table III.2

Instrument parameters for X-ray diffraction studies

Radiation	CuK_α with Ni filter
Excitation voltage	30 KV
X-ray current	20 mA
Divergent slit	1°
Soller slit for incident beam	0.2R
Soller slit for diffracted beam	0.2R
Detector slit	0.1°
Scanning speed	2°/min.
Chart speed	2 cm/min.
Time constant	4 sec.
Range	400 c/s.

By these patterns, the purity of calcined $BaTiO_3$ powder, the different reaction products in the sintered glass

added $BaTiO_3$, relative amount of the different phases with respect to sintering time and temperatures were studied.

Sintered pellets were fixed on an aluminum specimen holder, provided with the instrument. Top surface of the pellet is aligned with the top surface of the specimen holder. By adjusting the slit width etc., X-rays are made to fall only on the specimen. The calcined material was studied in powder form.

III.2.5. Capacitance Vs. Temperature Measurement:

Capacitance and dissipation factor were measured using GR-1620 A capacitance bridge assembly at 1 KHz and 0.3 V. Flat, fire skin removed discs were electroded with air dry silver paint, after measuring thickness. Electroded area was calculated using a transparent graph sheet.

Schematic representation of the high temperature sample holder is given in Figure III.1. The details are described earlier (10).

III.2.6. Capacitance Vs. Frequency Measurements:

Using 1311 A oscillator unit, with the help of GR 1620 A capacitance bridge, the frequency dependence of dielectric properties of the samples was measured. Frequency was varied from 1 KHz to 100 KHz at 0.3 V. The semiconductor samples were electroded with In-Hg electrode (47) and mounted in the sample holder described in Section III.2.5.

III.2.7. Resistivity Vs. Temperature Measurements:

Using the sample holder of Section III.2.5, and GR 1320 A D.C. amplifier and Electrometer assembly, resistance vs. temperature values were measured. Using the standard formula resistivity values were calculated.

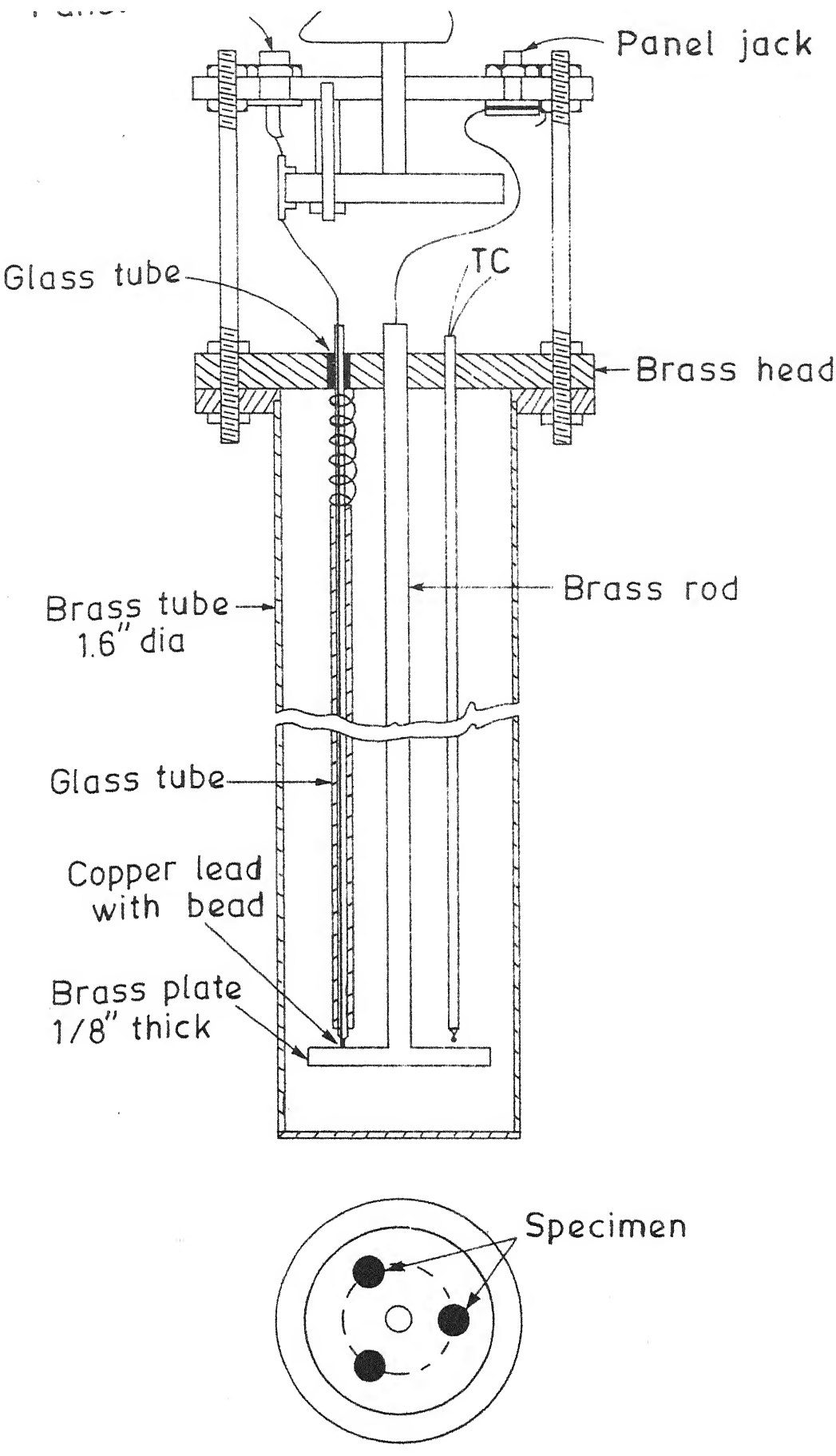

Fig. III.1 Sample holder for high temperature dielectric measurements

IV. RESULTS AND DISCUSSION

IV.1. Insulator $BaTiO_3$:

As mentioned in earlier portions, detailed work on 5 μ and 13 μ $BaTiO_3$ with 74 mole % Bi_2O_3:26 mole % B_2O_3 glass (G_1 glass) was done by Ramesh Chowdary (10). Glass composition was varied from 0.4 wt. % to 40 wt. % and the sintering experiments were carried out from 850°C to 1200°C. Optimum properties were obtained with 10 wt. % glass addition for 1000°C to 1050°C sintering. By X-ray diffraction studies, presence of $BaBi_4Ti_4O_{15}$ in all sintered samples was confirmed. Based on the amount present in different samples heat treated at different temperature, and on microstructural behaviour, a theory of densification was proposed after performing many confirmatory experiments.

Effect of smaller particles of $BaTiO_3$ with fixed composition of glass (10 wt. %) and the effect of another glass on these smaller particles were investigated and the results are discussed here.

IV.1.1. Density:

Pellets formed with 0.75 μ and 1 μ $BaTiO_3$ powder, as mentioned in Section III.1.4.1, were sintered at 900°C, 950°C and 1000°C for 6, 10, 15, 30, 60 and 120 minutes, as mentioned in Section III.1.5. For all samples geometric density was calculated. Since 900°C treated samples showed

IV. RESULTS AND DISCUSSION

IV.1. Insulator $BaTiO_3$:

As mentioned in earlier portions, detailed work on 5 μ and 13 μ $BaTiO_3$ with 74 mole % Bi_2O_3:26 mole % B_2O_3 glass (G_1 glass) was done by Ramesh Chowdary (10). Glass composition was varied from 0.4 wt. % to 40 wt. % and the sintering experiments were carried out from 850°C to 1200°C. Optimum properties were obtained with 10 wt. % glass addition for 1000°C to 1050°C sintering. By X-ray diffraction studies, presence of $BaBi_4Ti_4O_{15}$ in all sintered samples was confirmed. Based on the amount present in different samples heat treated at different temperature, and on microstructural behaviour, a theory of densification was proposed after performing many confirmatory experiments.

Effect of smaller particles of $BaTiO_3$ with fixed composition of glass (10 wt. %) and the effect of another glass on these smaller particles were investigated and the results are discussed here.

IV.1.1. Density:

Pellets formed with 0.75 μ and 1 μ $BaTiO_3$ powder, as mentioned in Section III.1.4.1, were sintered at 900°C, 950°C and 1000°C for 6, 10, 15, 30, 60 and 120 minutes, as mentioned in Section III.1.5. For all samples geometric density was calculated. Since 900°C treated samples showed very low values, they are not discussed further.

From Figures IV.1 and IV.2 following results are derived.

1. 0.75 μ particles show poorer densification at both temperatures, 950°C and 1000°C, with both glasses compared to 1 μ particles.

2. 1 μ particles sintered at 1000°C have ≥85% of theoretical density for both glass additions. With G_2 glass the densification is relatively independent of time.

IV.1.2. Microstructural Observation:

Samples sintered at 950°C/1 hr, 2h and 1000°C/6 min, 15 min and 1 h were polished as mentioned in Section III.2.3. Microstructures were observed for all samples. Samples sintered at 950°C/1 h and 2 h, 1000°C/6 min did not have well developed microstructure.

Remaining samples showed better structure and the grain/agglomerate sizes were measured. Results are provided in Table IV.0.

Table IV.0

Average grain/agglomerate size values of various samples

Heat treatment	0.75 μ $BaTiO_3$ + 10 wt. % G_1	0.75 μ $BaTiO_3$ + 10 wt. % G_2	1 μ + $BaTiO_3$ 10 wt.% G_1	1 μ +BaTi 10% G_2
1000°C/ 15 min	2-3 μ (0.5-1.0 μ)	8-12 μ (2-2.5 μ)	5-7 μ (2-2.5 μ)	5-7 μ (1.5-2.5 μ)
1000°C/ 1 h	3-5 μ (0.4-0.8 μ) & (2-2.5 μ)	6-8 μ (2-2.5 μ)	5-7 μ (2-2.5 μ)	5-7 μ (1.5-2.5 μ)

Values appeared inside the brackets are glass thickness.

IV.1.3. Densification Mechanism:

Generally three stages of densification occur in liquid phase sintering corresponding to three mechanisms (10,50).

1. Particle rearrangement, 2. solution-precipitation and 3. coalescence.

In the first stage liquid phase formation will be there. The liquid will flow and fill up the pores, and the solid particles will get rearranged, resulting in close packing. In the second stage the fine particles will dissolve and get precipitated on the bigger particles. In the third stage the substance is slowly consolidated. Most of the densification is achieved in first stage itself(51). The dominance of one mechanism over another depends on the nature of process and the amount of liquid present.

First condition to be satisfied is the perfect penetration of liquid between the grains. The extent of penetration depends on the dihedral angle formed by the liquid phase at the boundary with two grains of the solid (Figure IV.5)

IV.1.3.1. Particle Rearrangement:

After melting, capillary pressure will tend to rearrange the particles in such a way as to give maximum packing and minimum resulting pore surface. This process occur very rapidly and is the principal reason for densification.

IV.1.3.2. Solution and Precipitation:

Limited solubility of solid in the liquid phase is necessary for this mechanism to occur. The densification rate is lower compared to first stage. Here smaller particles dissolve and precipitate on larger particles, thereby leading to densification (52).

IV.1.3.3. Coalescence Process:

During sintering process a certain number of grains will be oriented such that the grain boundary energy is smaller than twice the solid liquid interface energy ($\sigma_{S_1-S_2} < 2\,\sigma_{S-L}$). So the value φ increases. Now, solid-solid contact will be formed and the sintering will be simply solid state sintering. The change in the density value with respect to time will be less (Figure IV.6).

In general it can be stated that (1) an appropriate amount of liquid, (2) a limited solubility of the solid and (3) complete melting are the necessary requirements for good densification.

Results mentioned in Sections IV.1.1 and IV.1.2 are discussed here. In Figures IV.1 and IV.2 higher densification of $BaTiO_3$ with both glasses are observed for 1 μ particle. In grain size measurement, constant average grain size was observed for both 15 min. and 1 hr treated samples.

From these results one can infer that the solution and precipitation stage predominates in 1 μ particle densification. With G_2 glass because of its lower viscosity expected

dependency on time is relatively less. This is observed in Figure IV.2.

With smaller particles, the densification takes place in a different way. As mentioned in Section IV.1.3.3, if the dihedral angle Ø is more solid-solid contact will be more stable. This observation is reflected in density curves (Figures IV.1 and IV.2 and Table IV.1). For lower sintering time, higher average agglomerate size was observed with G_2 sample confirm the result two different samples treated at 1000°C/ 15 min were polished repeatedly but same results were observed. So it was concluded that the glass did not penetrate fully so as to surround the grain thouroughly. With 0.75 μ $BaTiO_3$ + 10 wt. % G_1 sample treated at 1000°C/1 h, two glass thicknesses, were observed, one in 0.4 to 0.8 μ range and another in 2-2.5 μ range. First one was very feeble and the later one was bright. With G_2 added samples only one grain boundary thickness in 2-2.5 μ range was observed. Generally, a big area covered with thick glass coating with small subdivisions (with thin glass coating) was observed.

This observation shows that with higher sintering time G_1 penetrates further and surrounds the grains. In this stage solution and precipitation mechanism will be dominating, Section IV.1.3.2.

This argument is reflected in the densification curves. With G_1 glass the curve rises gradually. With G_2 glass after some time the density value is constant. Moreover final density of G_2 added glasses are less than that of G_1 added glass.

With above observation and from the nature of density curves (Figure IV.1 and Figure IV.2) one can conclude that coalescence process is playing dominant role. If solid-solid contact is more stable, further densification will not be there with higher sintering time (50). This is observed with G_2 glass. Further penetration with larger sintering time in G_1 glass added samples explains the presence of other stages of sintering and so the nature of density curve.

From the nature of the density curve for 950°C sintered samples, one can conclude that combination of all three mechanisms of sintering takes place.

For a quantitative explanation of the densification nature at both temperatures many parameters like viscosity and surface tension of glasses at the sintering temperatures, interfacial energy between solid-solid, solid-liquid contacts, contact angles between solid-liquid-gas interface, capillary force, capillary energy, etc. are needed to be measured/calculated.

IV.1.4. X-ray Diffraction Studies:

X-ray diffraction patterns were taken for all sintered samples. Following results are observed.

1. No appreciable angular shift in diffraction peaks is observed. This lead to the conclusion that no solid solutions are formed.

2. Extra peaks corresponding to $BaBi_4Ti_4O_{15}$ and $Bi_4Ti_3O_{12}$ are observed. $Bi_4Ti_3O_{12}$ phase is present mainly on the surface only (Figure IV. 7).

These two results are in accordance with the results observed by Ramesh Chowdhary (10).

IV.1.5. Temperature Dependence of Dielectric Properties:

Dielectric properties (dielectric constant and dissipation factor) were measured as a function of temperature for all the sintered samples.

Reported values are corrected for porosity using the relation given by Rushman and Strivens (53).

$$k = \bar{k} \frac{2 + v}{2(1 - v)}$$

where v - volume fraction of pores

$\bar{k}$ - dielectric constant measured with porosity

k - dielectric constant corrected for porosity.

Dielectric constant vs. temperature curves of 10 wt. % G_1 added samples are produced in Figures IV.8 to IV.11 and of 10 wt. % G_2 added samples in Figures IV.12 to IV.15.

Following results are observed:

1. Room temperature dielectric constant of all the samples are $\geq$ 1000. At higher sintering temperature irrespective of sintering time, most of the samples show a value $\geq$ 1500.

2. Variation of dielectric constant with temperature is relatively less and the peak value for all samples are less than twice the value at room temperature.

3. Within experimental error, all samples have the Curie temperature at 120°C.

4. Room temperature dissipation factor for most of the samples are ≤ 0.1 and their variation with temperature is very less.

As mentioned, with 5 μ and 13 μ $BaTiO_3$ and various G_1 glass combination detailed work was carried out by Ramesh Chowdhary(10)

Similar results were reported and a detailed account was given to explain the behaviour.

Unshifted Curie point conclusively proves that no solid solution has formed. The behaviour $\varepsilon_{peak} \leq 2\ \varepsilon_{RT}$, may be compared with the variation of the dielectric constant of hot pressed $BaTiO_3$ samples as a function of heat treatment temperature (59).

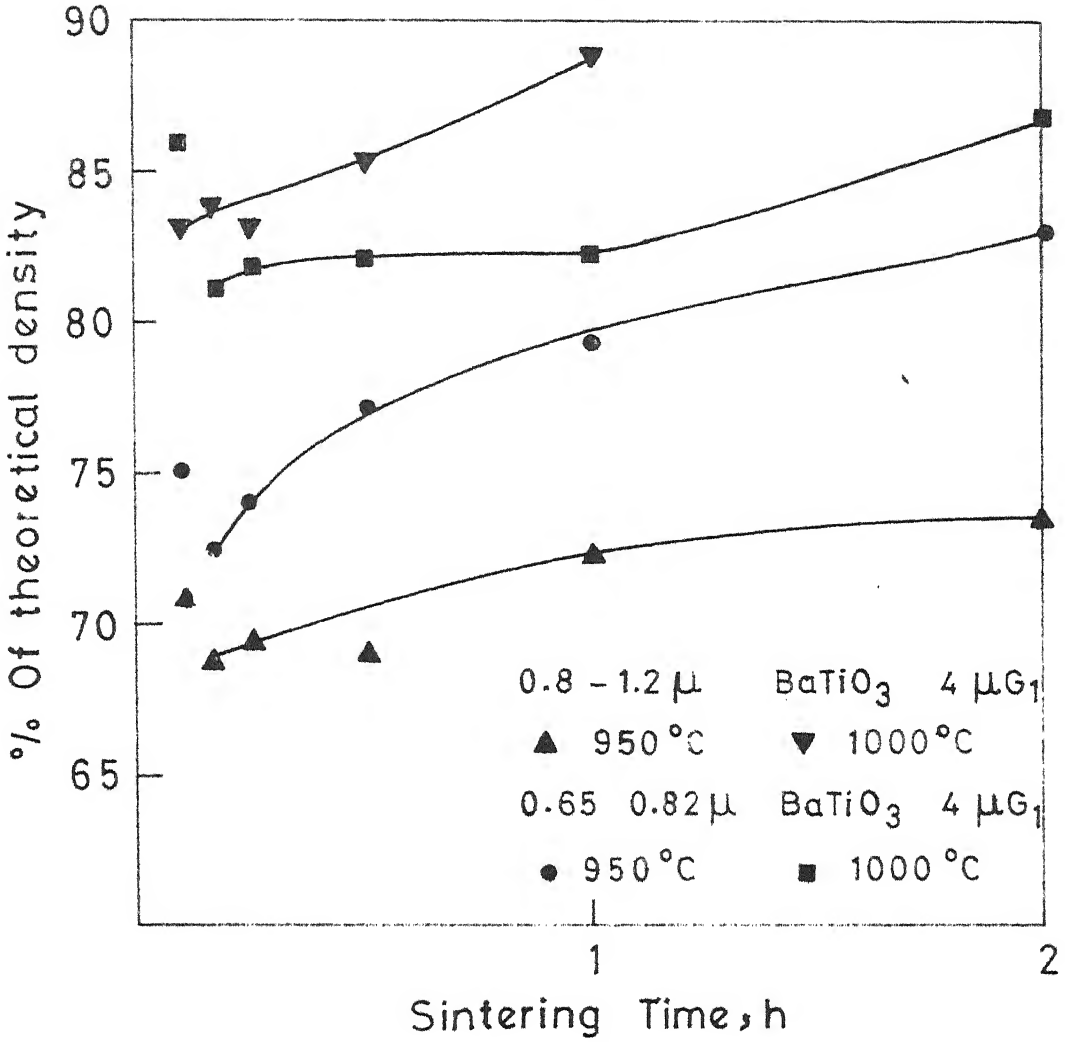

Fig. IV.1 Effect of particle size on densification of $BaTiO_3$ with G_1 glass addition at different sintering temperatures and times

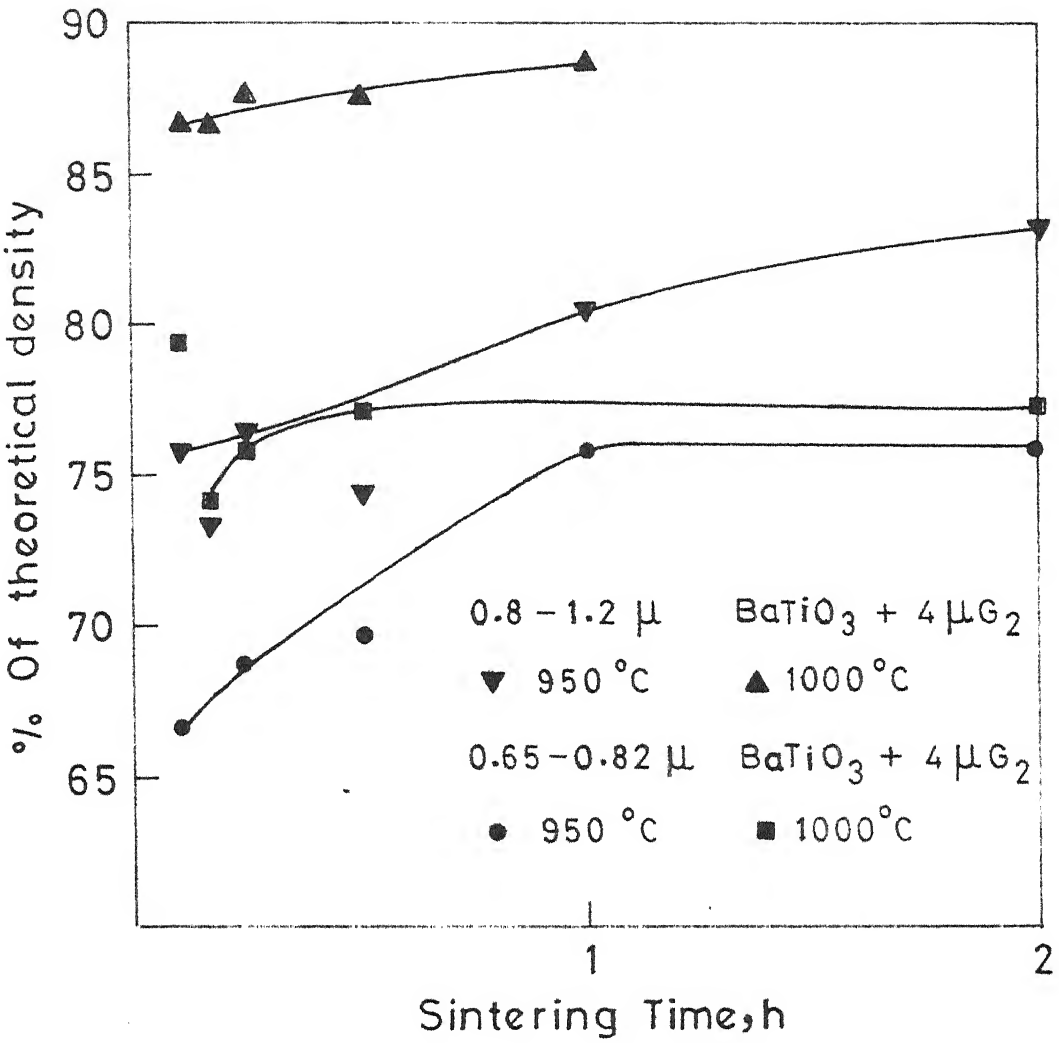

Fig. IV.2 Effect of particle size on densification of $BaTiO_3$ with G_2 glass addition at different sintering temperatures and times

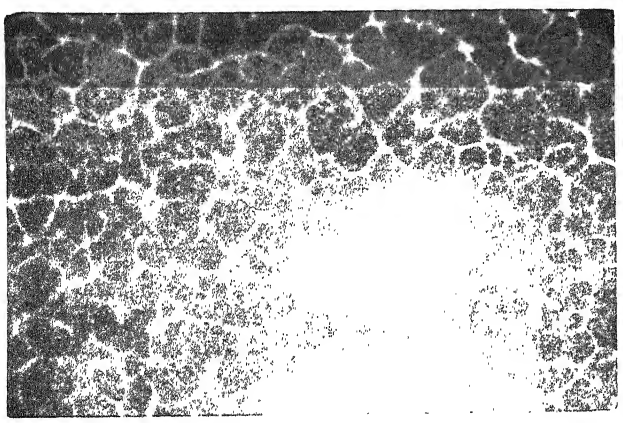

0.75 μ $BaTiO_3$. 950°C/1 h

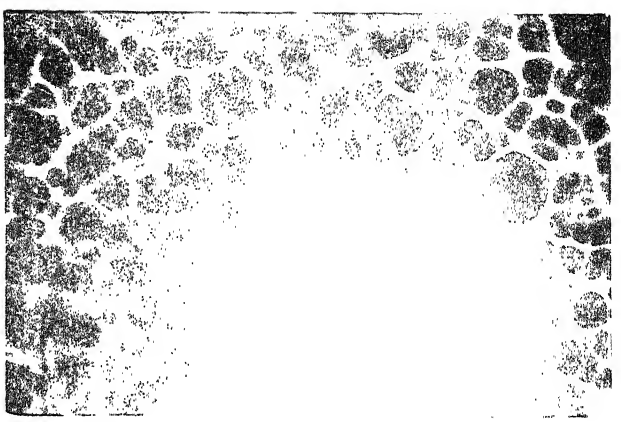

0.75 μ $BaTiO_3$. 1000°C/1 h

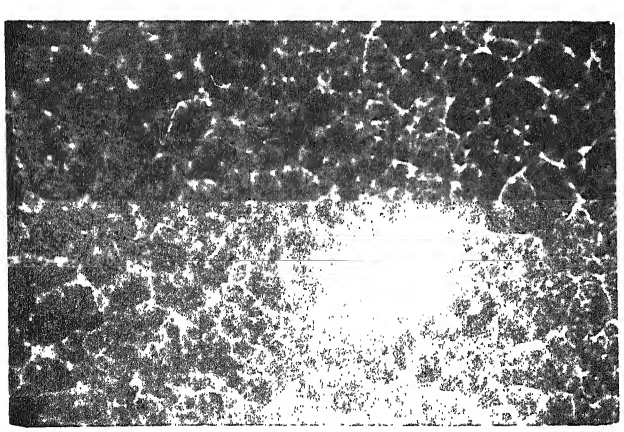

1 μ $BaTiO_3$. 950°C/1 h

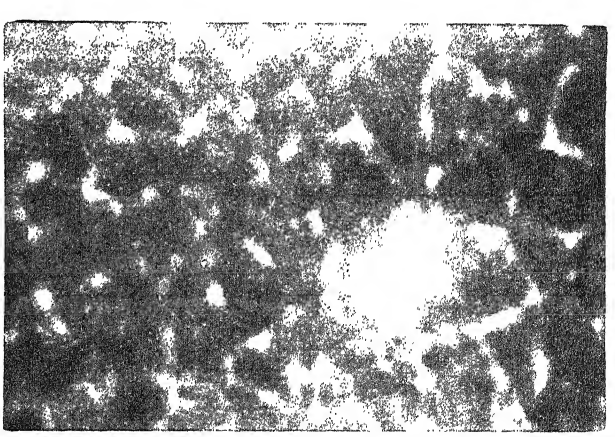

1 μ $BaTiO_3$. 1000°C/1 h

Figure IV.3. Microstructure of liquid phase sintered 10 wt. % G_1 glass added samples.

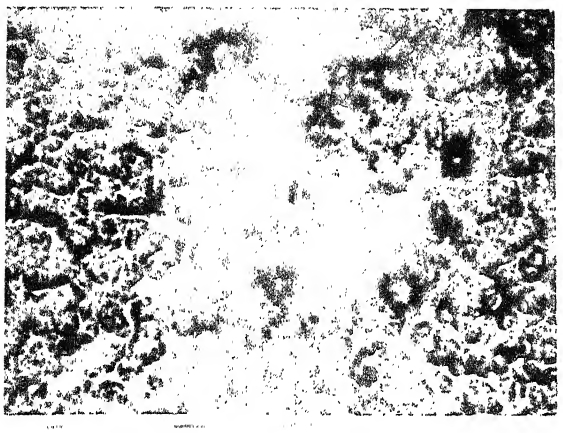

0.75 μ $BaTiO_3$. 950°C/1 h

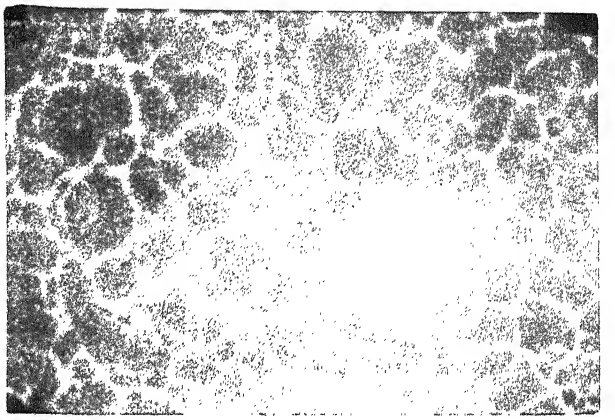

0.75 μ $BaTiO_3$. 1000°C/1 h

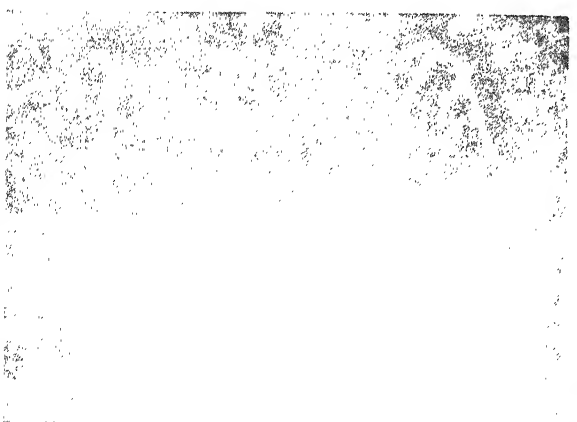

1 μ $BaTiO_3$. 950°C/1 h

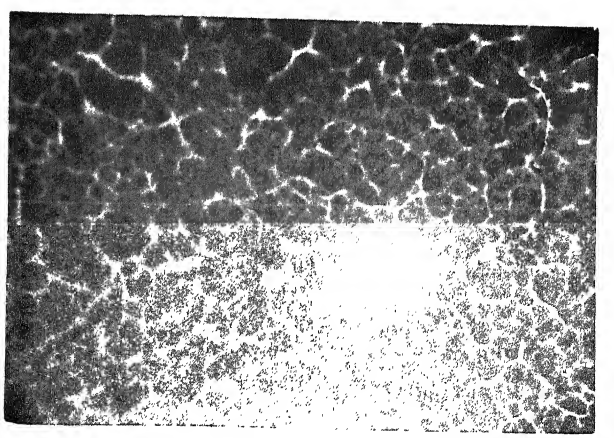

1 μ $BaTiO_3$. 1000°C/1 h

Figure IV.4. Microstructure of liquid phase sintered 10 wt. % G_2 glass added samples.

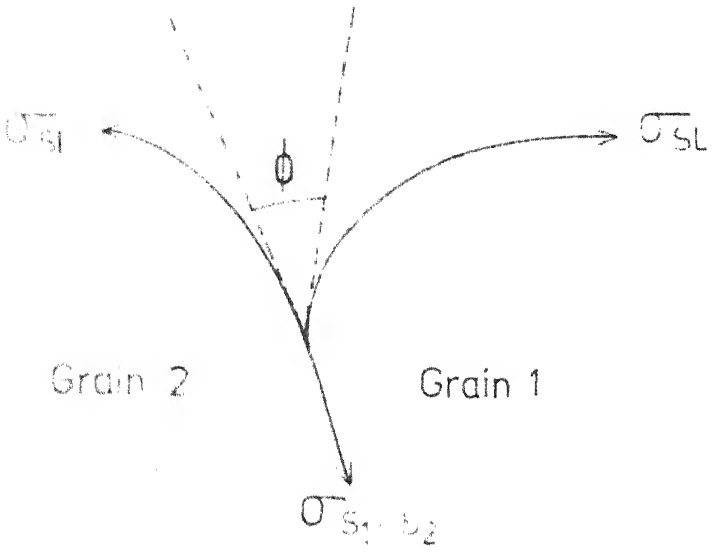

Fig. IV.5 Dihedral angle formed by the liquid phase at the grain boundery.

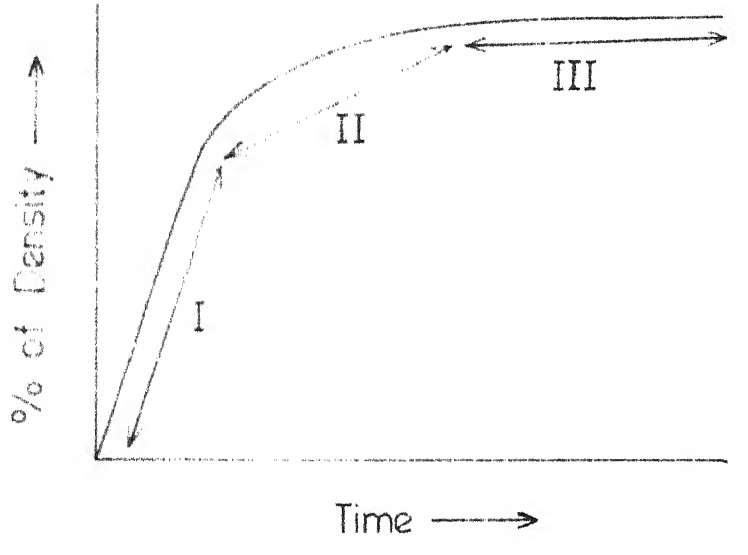

Fig. IV.6 Hypothetical densification curve for liquid phase sintering.

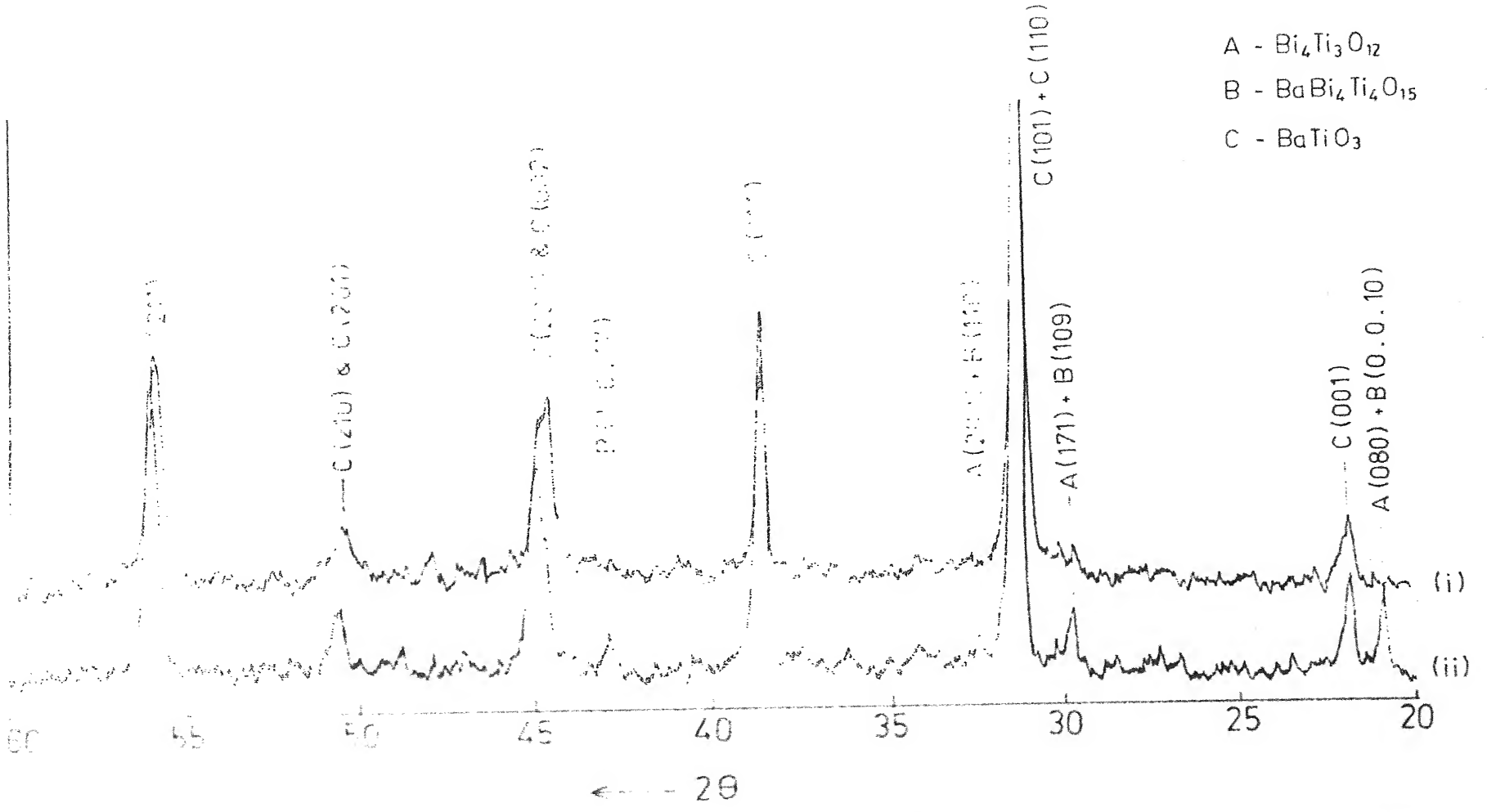

Fig. IV 7 Representation of X-ray diffraction patterns of $BaTiO_3$ + 10 wt % Glass added (i) as sintered (ii) polished surfaces of 1000°C treated samples.

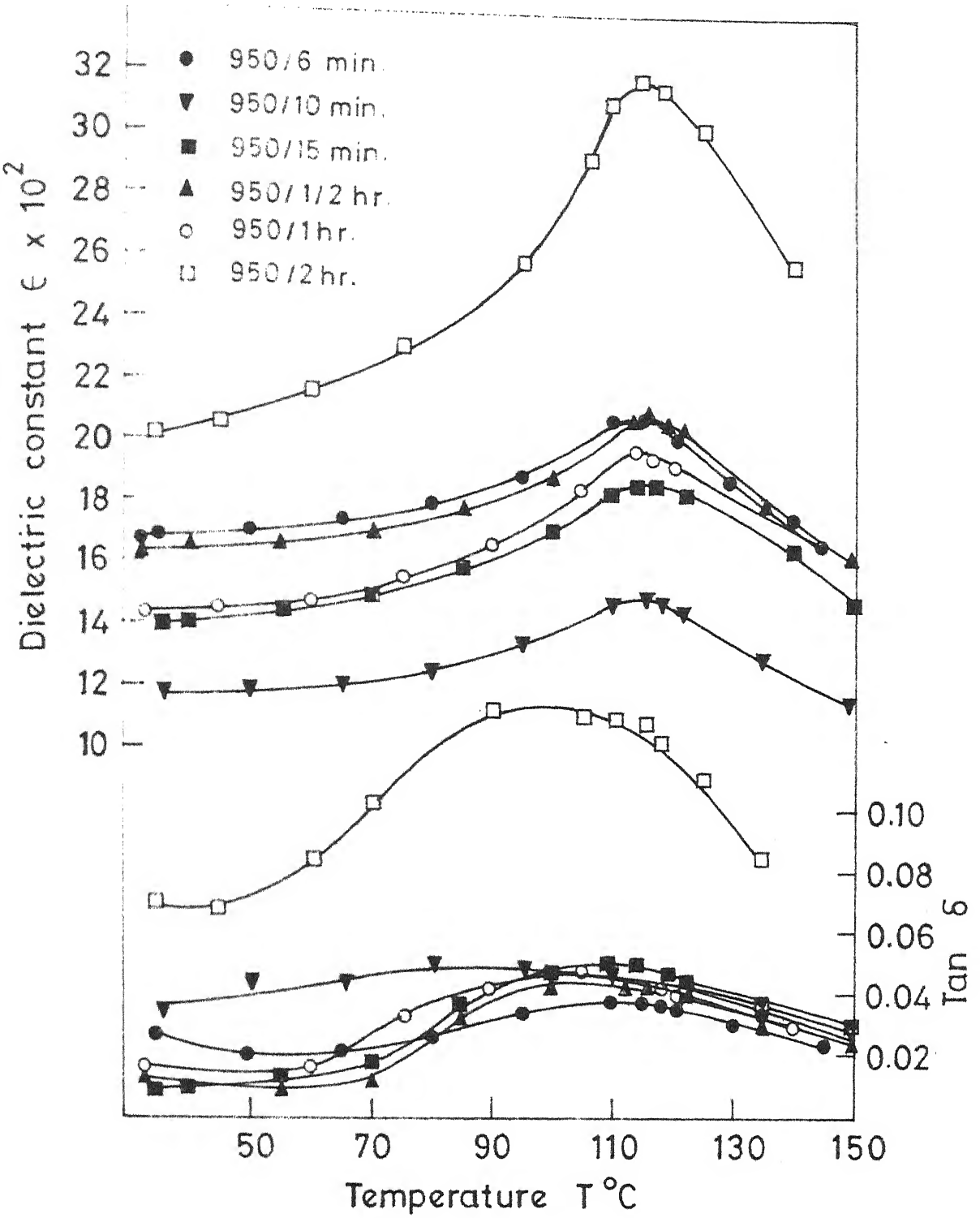

Fig. IV. 8 Temperature dependence of dielectric constant of 0.65 μ to 0.82 μ $BaTiO_3$ + 4 μ G_1 samples sintered at 950 °C

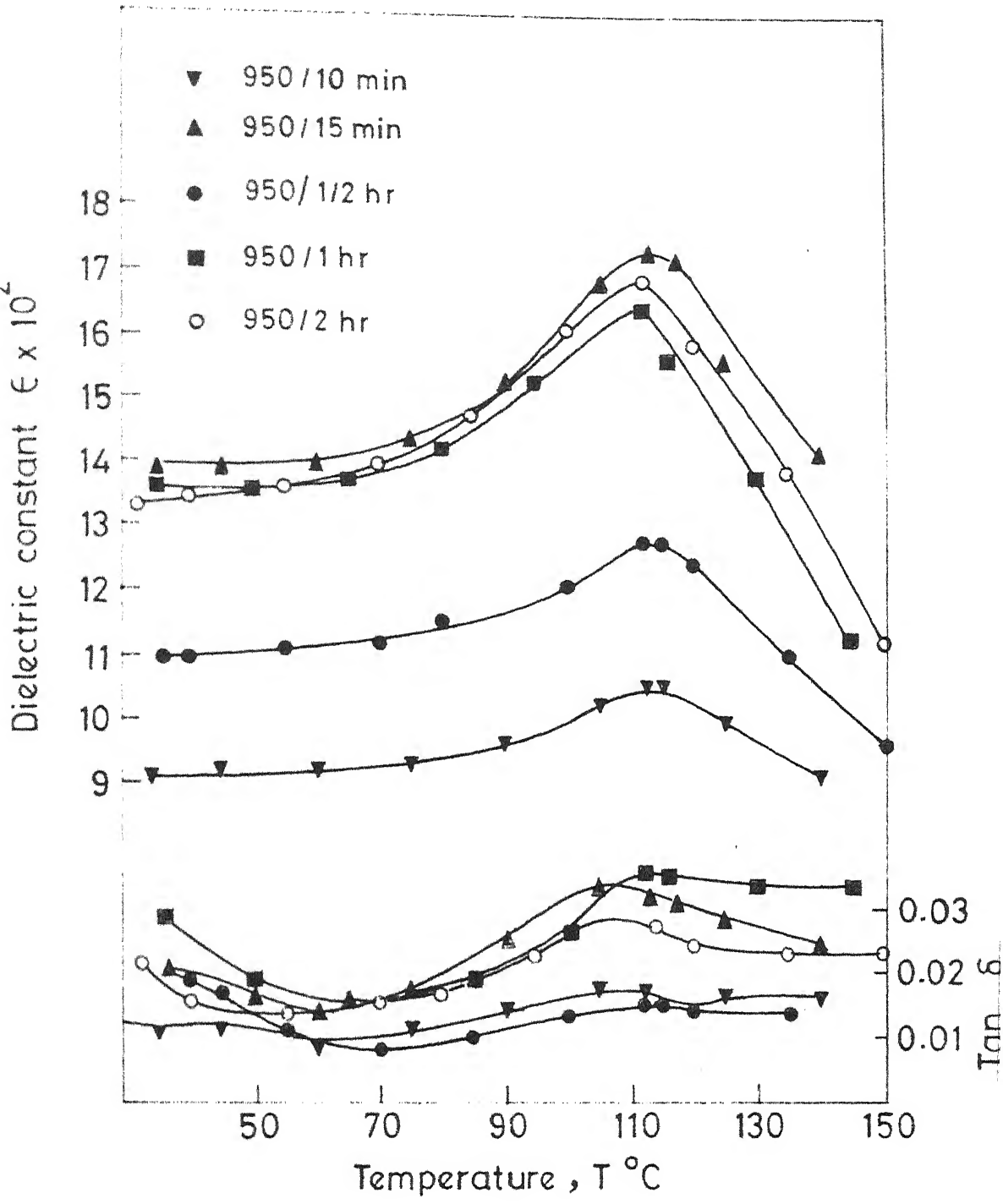

Fig.IV.9 Temperature dependence of dielectric constan of 0.82 μ to 1.2 μ $BaTiO_3$ + 4 μ G_1 samples sintered at 950 °C

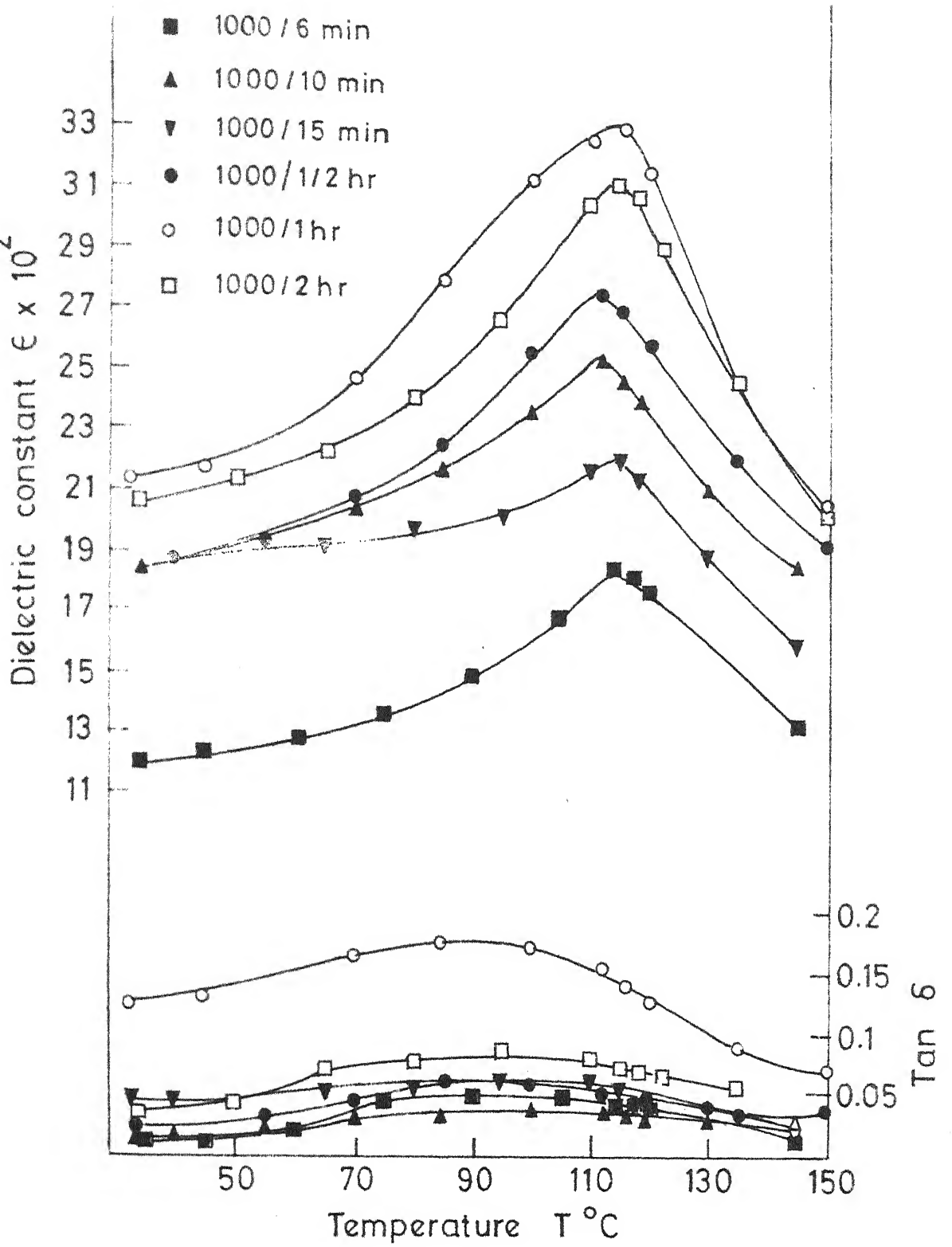

Fig. IV. 10 Temperature dependence of dielectric constant of 0.65 to 0.82 μ $BaTiO_3$ + 4 μ G_1 samples sintered at 1000 °C

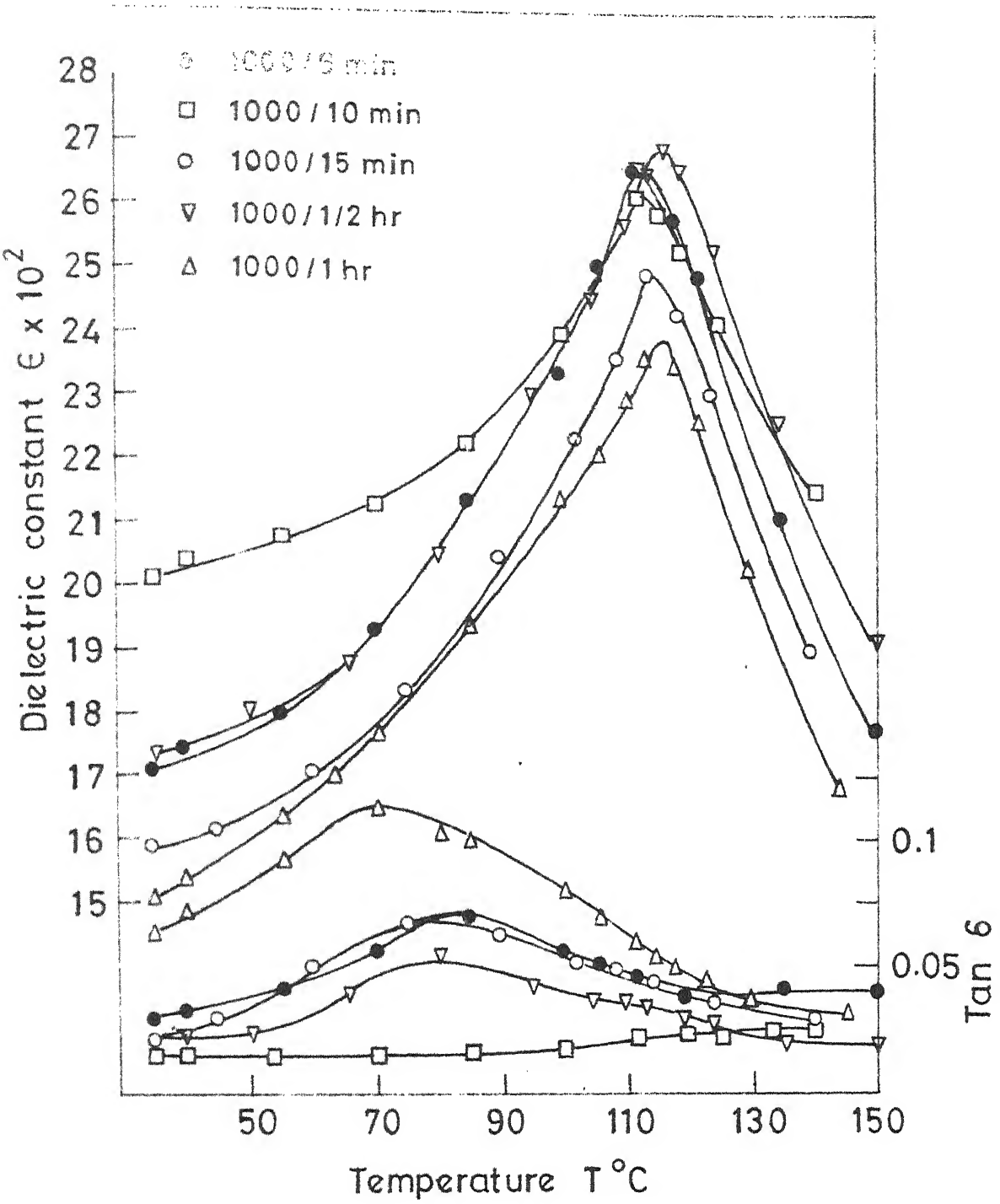

Fig. IV. 11 Temperature dependence of dielectric constant of 0.82 to 1.2 μ $BaTiO_3$ + 4 μ G_1 samples sintered at 1000 °C

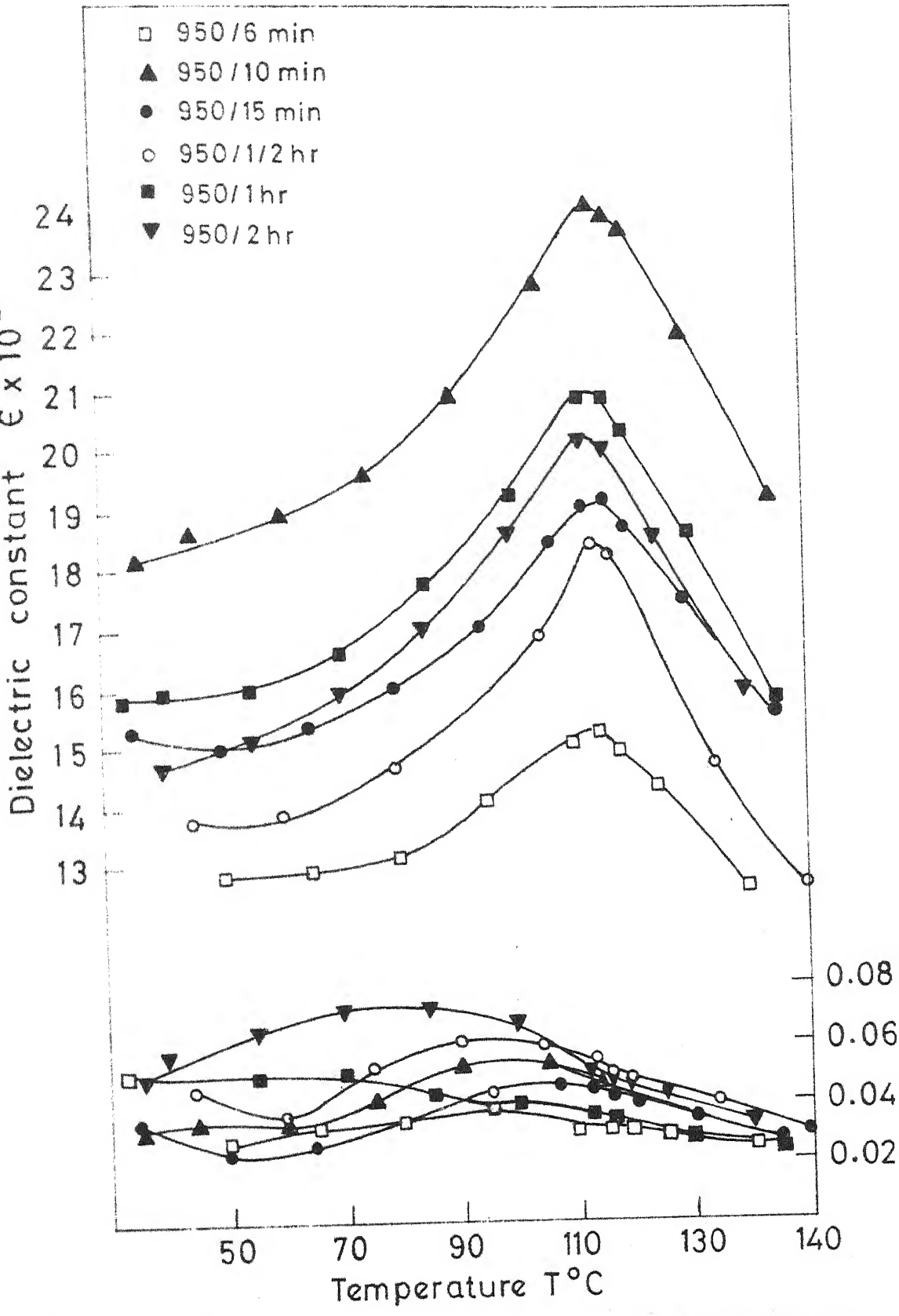

Fig. IV. 12 Temperature dependence of dielectric cons
of 0.65 μ to 0.82 μ $BaTiO_3$+4 μ G_2 sample
sintered at 9[illegible]°C

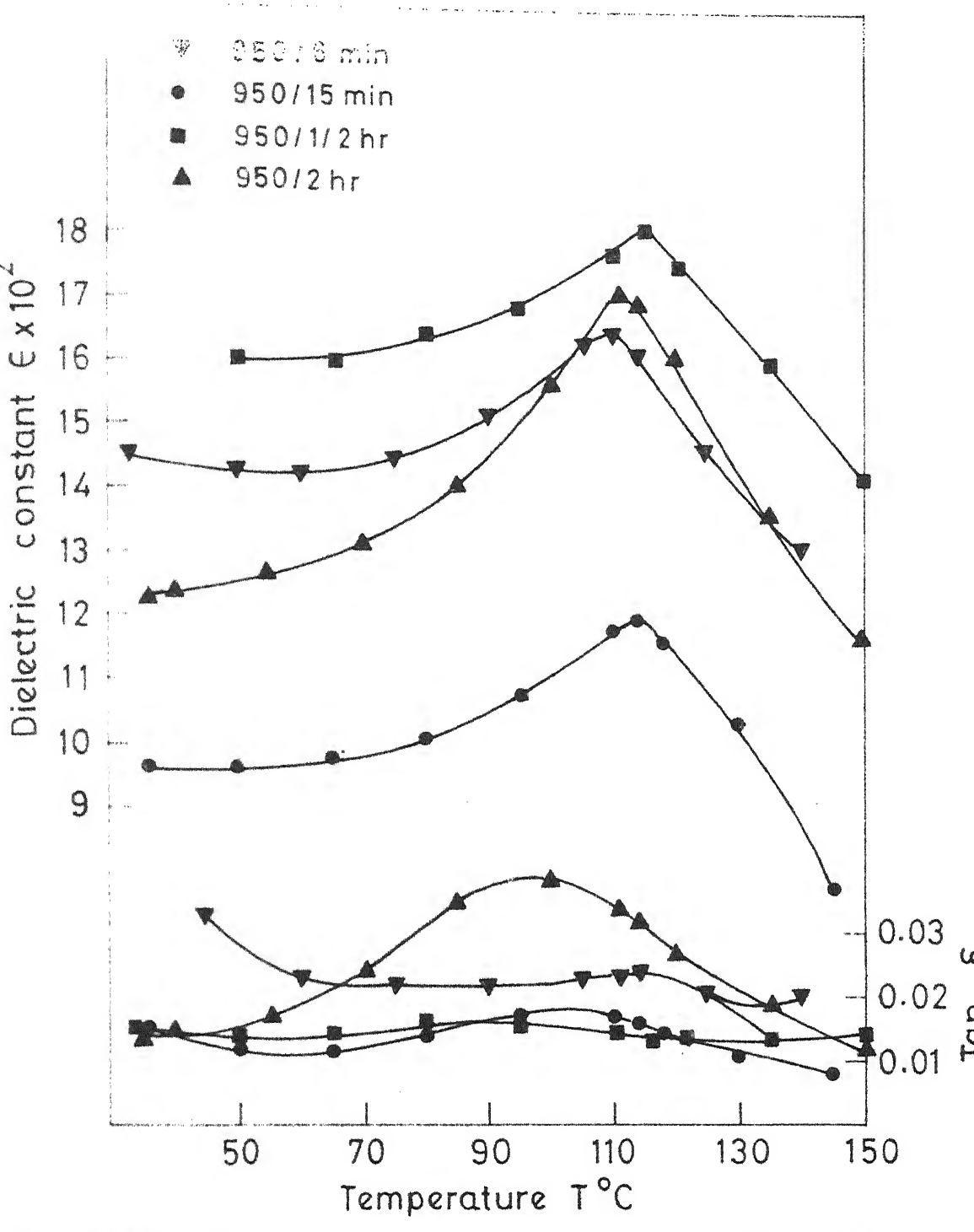

Fig. IV.13 Temperature dependence dielectric constant of 0.82 μ to 1.2 μ $BaTiO_3$ + 4 μ G_2 samples sintered at 950 °C

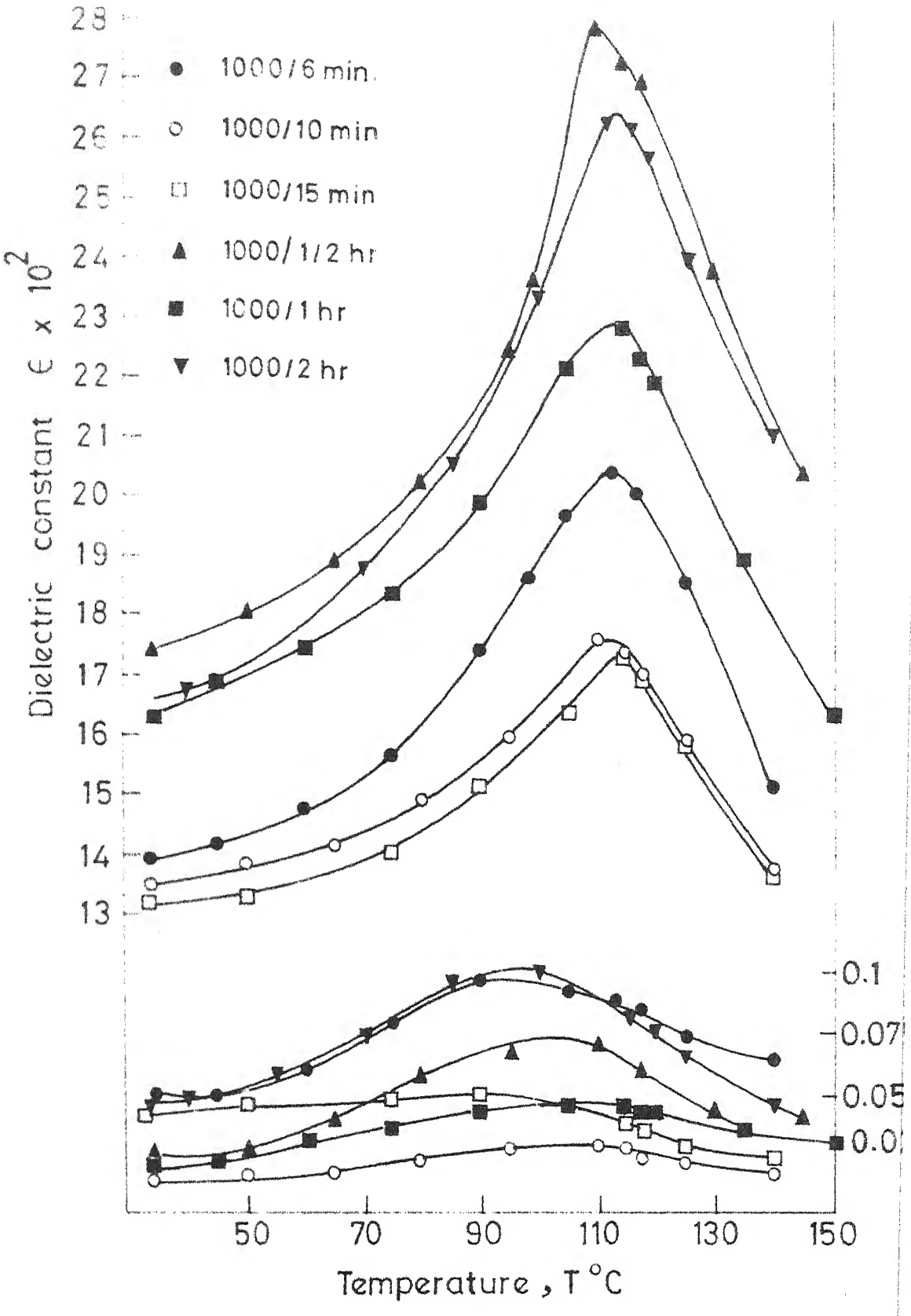

Fig.IV.14 Temperature dependence of dielectric constant of 0.65 μ to 0.82 μ $BaTiO_3$ + samples sintered at 1000 °C

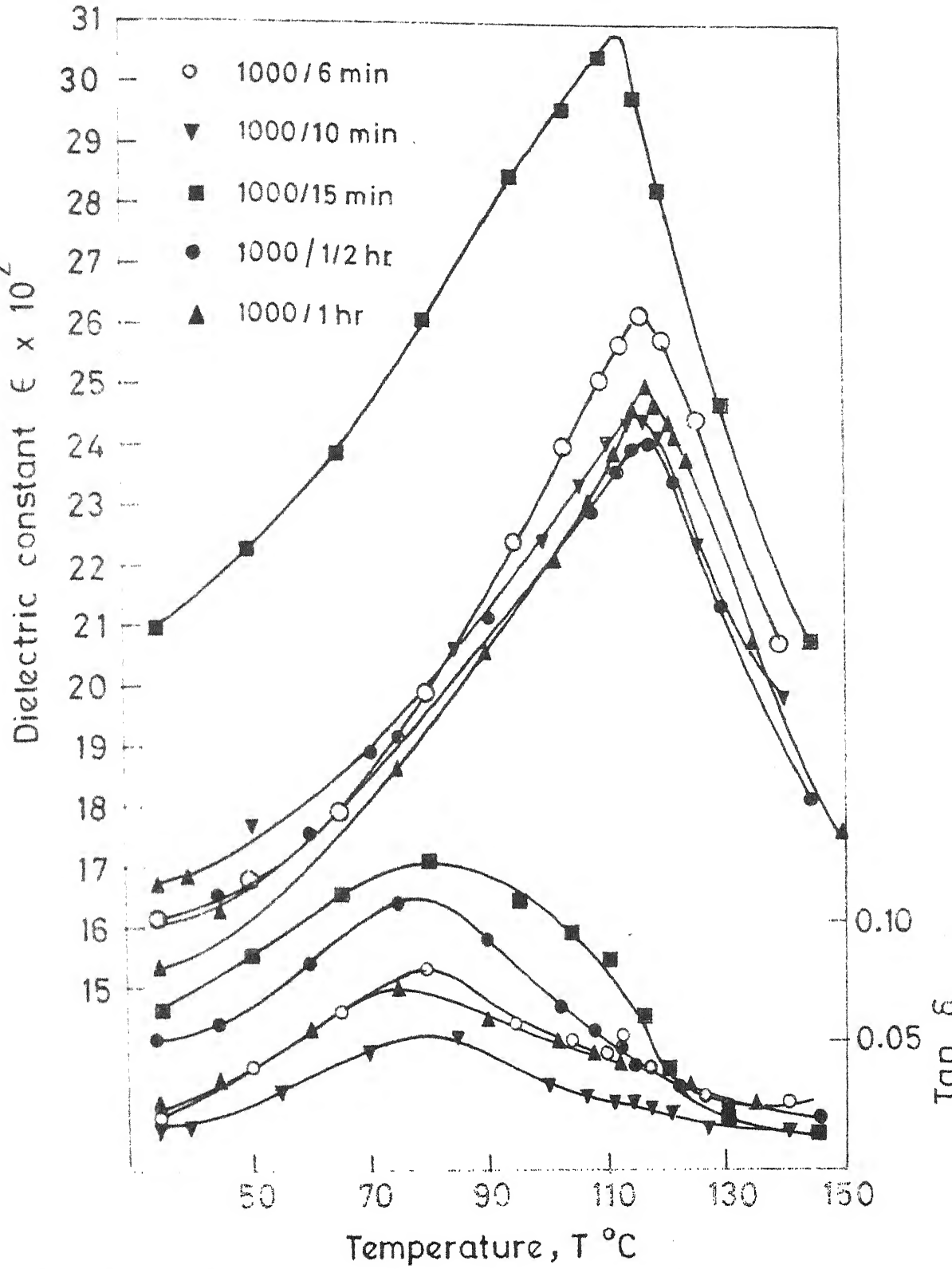

Fig. IV. 15 Temperature dependence of dielectric constant of 0.82 μ to 1.2 μ $BaTiO_3$ + 4 μG samples sintered at 1000 °C

IV.2. Semiconductor $BaTiO_3$:

As mentioned in Section III, the semiconductor samples were prepared by three different methods.

Samples prepared by mixing Lanthanum nitrate with barium carbonate, titanium dioxide are designated as S(I) $BaTiO_3$, and that prepared by Lanthanum chloride addition to the $BaTiO_3$ powder was called as S(II) $BaTiO_3$. Samples prepared by BTO technique are designated as S(III) $BaTiO_3$.

Room temperature resistivity values of various semiconducting samples prepared are shown in Tables IV.1 and 2. Room temperature values of dielectric constant and tan δ are shown in Table IV.3. The dielectric constant values are corrected for porosity.

S(I) semiconductor powder was mixed with 10 wt. % of G_2 glass and the pellets were heat treated in a tubular furnace adopting the procedure mentioned in Section III.1.5. Since the room temperature dielectric constant value was very low, Table IV 3:1 the next set of experiments were tried with S(II) $BaTiO_3$.

First the effect of particle size of the semiconductor $BaTiO_3$ was studied. Basically, the semiconductor $BaTiO_3$ grain was to be surrounded by insulating glass and thereby the barrier layer was expected to be created. So to produce larger barrier layer surface area, various particle sizes of semiconductor $BaTiO_3$ were tried.

Semiconductor pellets were crushed into powder using agate mortar and pestle and the powder was ground further

5 hr and 10 hr. Every time exactly 3 gms of powder was used. They were mixed with 10% G_2 and sintered at 1100°C/1 h using the tubular furnace. Again the room temperature dielectric constant values of the sintered pellets are very low (Table IV.3:6).

To see the effect of other glass G_1 (74 wt. % Bi_2O_3 - 26 wt. % B_2O_3) another experiment was carried out. But this pellet also has very low ε value. (Table IV 3:3)

It was assumed that the semiconductor is becoming insulator because of some reason. To check the possibility of reoxidation, i.e. effect of flash firing and the effect of inert atmosphere were studied.

In flash firing (FF), the pellets were pulled to hot zone in 1 minute and after specified sintering period it was removed to room temperature. The samples got cooled within 5 minutes. (Table IV. 3:5,7)

Procedure for N_2 atmosphere sintering is discussed in Section III.1.5.

The density and room temperature dielectric constant values are shown in Table IV.3:9,10. All the samples have low values of dielectric constant. So flash firing as well as inert atmosphere were ineffective in restricting the reoxidation.

But, to confirm the reoxidation possibility a direct experiment was carried out. A semiconductor pellet, without glass, was heat treated to the same temperature, 1100°C/1 h. It was found out that the room temperature resistivity had

increased slightly to 1200 ohm-cm, but still the value is very low compared with that of insulator $BaTiO_3$.

Next possible reason one could think of is the purity. It is well known that the most effective method of preparation, to avoid impurities, is barium titanyl oxalate method.

The semiconductor, S(III) $BaTiO_3$, was prepared as mentioned in Section III.1.2.2 (Third method). After powdering, using mortar and pestle, and mixing it with G_2, pellets were prepared. The pellets were sintered in the tubular furnace at 1000°C/1 h. But again the room temperature dielectric constant value is very low. For this experiment 0.2 mole % La added samples were used.(18). (Table IV. 3:11)

Above experiments proved that the poor value of dielectric constant is neither because of reoxidation due to higher temperature reheating, nor because of the presence of unwanted impurities.

So, as a next step, the basic assumption itself was modified. Instead of taking a simple semiconductor grains and then surrounding them by insulator glass, it was planned to take barrier layered grains themselves and then sintering the material at lower temperature with the help of glass as a liquid phase.

Many methods were employed to produce barrier layered grains (36). Among them, addition of acceptor ions like ions of Mn, Cu, Fe etc. were found to be the most effective one. Ions of Mn and Cu are found to be suitable for commercial production.

Using manganese, the preparation of barrier layered grains was tried. The amount of Mn should be few hundred ppm only (26). So very small quantity was added. To get very pure material (with Mn alone), BTO technique was used.

With 4 μ $BaTiO_3$ slurry, necessary amount of La and Mn solutions were added and the hydroxides were precipitated. Details were given in Section III.1.2.3.1. These samples were designated as S(II) (0.4 mole % La + 0.05 mole % Mn) $BaTiO_3$ (added simultaneously). With BTO also simultaneous addition was carried out. Here since the preparation is carried out by precipitation, more effective mixing is expected. So smaller quantity (0.02 mole % Mn) was used. Since 0.2 mole % La added $BaTiO_3$ pellets had shown larger value of resistivity, 0.3 mole % of La was added for this preparation.

Both pellets had shown higher values of room temperature resistivity owing to the presence of manganese. But still, the loss is very high and so the room temperature dielectric constant value could not be measured with the capacitance bridge of type 1615-A of General Radio.

The materials were mixed with glass G_2 as described and the pellets were sintered at 1000°C/1 h using the tubular furnace. For these pellets also, the room temperature dielectric constant is very low. (Table. IV.3: 12, 15).

These experiments proved one point. Very high purity is not the criterion.

By measuring resistivity vs. temperature using an electrometer of the type 1230-A of General Radio some additional information was obtained.

From Figure IV.16 one infers the rise in resistivity value from around 100°C to 130°C for simultaneous addition of La and Mn in S(II) $BaTiO_3$. So the material is yet to cross the PTC behaviour, that is, the addition of acceptor ions has produced surface defects but not to a large enough extent so that a well defined barrier layer can be found.

So, as a next step, separate addition of Mn was tried. In simultaneous addition, the defective boundary layer was expected to be formed because of differential diffusion rate of La and Mn. La is expected to diffuse in at a faster rate than Mn. Positive temperature coefficient resistance (PTCR) behaviour of the final product confirms the validity of the above statement. But still, to produce barrier layer larger concentration of Mn at the surface is essential. These materials are characterized by larger values of room temperature resistivity of the order of 10^9 ohm-cm and smaller variation, either in positive side or in negative side, of reactivity at Curie temperature (55). To produce this material separate addition was tried.

Experimental details were given in Section III.1.2.3.2. The resistivity behaviour with temperature was plotted in Figure IV.16. Room temperature dielectric constant and the % of theoretical density value is given in Table IV.3. Larger value of dielectric constant proves the formation of barrier layer. All this work was carried out with S(II) $BaTiO_3$. With S(III) $BaTiO_3$ also, the same work was carried out. Since the density value was very low (58.7% of theoretical density)

and since the material turned thoroughly brown in colour detailed work was not pursued.

Above mentioned S(II) $BaTiO_3$ with Mn was powdered and mixed with glass G_2 and sintered as mentioned previously. The lower value of room temperature dielectric constant led to further speculations. (Fig 10 17)

Two explanations can be thought of for the lower values. Either the starting material should be non barrier layered one, or the existing barrier layer is destroyed by some reaction. Resistivity behaviour and the higher dielectric constant values rules out the first possibility. So, the second possibility may be true.

Generally with liquid phase sintering, if the precipitation and rearrangement stage predominates over the other stages, the grain growth will be larger (10). Since the growth is larger in this system (10). the modification of grain surface will be there. So the defective grain surface which was produced deliberately to the requirement by Mn addition is changed. Moreover, MnO and Mn_2O_3 which are the two probable forms existing for the above heat treatments, forms compounds with Bi_2O_3 and B_2O_3 (44). But since the amount of Mn is very small the compound cannot be detected by X-ray diffraction studies. Lower value of dielectric constant may be due to these effects.

Grain growth may be the reason for the observed behaviour of S(II) 0.4 mole % La added $BaTiO_3$ + glass G_2 combination. By material transportation the same La concentration as well as the distribution of La ions, cannot be expected

with deposited material, i.e., concentration of dopants will be, generally, high in the liquid phase than in the solid phase formed and the concentration profile in the solid phase varies with thickness (56).

To confirm whether this line of reasoning is correct or not, an experiment was planned. Glass G_2 was spread over the surface and by heating, it was allowed to diffuse inside the pellet. This procedure was successfully employed to produce $SrTiO_3$ barrier layer capacitors (32).

To see the effect S(II) La doped $BaTiO_3$ was used. Since the Mn added S(II) $BaTiO_3$ is already having high value of room temperature dielectric constant, (Table IV. 3:16) the final result with glass may mislead to a wrong conclusion. Without Mn, even though the material is not a barrier layered one, covering the semiconductor grain with glass without grain growth may produce necessary results. By smearing glass over the surface and heating will definately lead to grain growth at the surface, but after certain depth the grain growth may not be there. To ensure this, either the temperature or the time of treatment should be low.

With this reasoning the next set of experiments were designed. Pores will be helpful for quicker penetration. So powder was pelletized with 4 tonnes of pressure using a hydraulic press and the pellet was heat treated at 1200°C/1 h

to impart strength. This temperature is just below the temperature for the on set of sintering(17). The density value is 57.3% of theoretical value.

One pellet of this, and another pellet of starting material (non powdered one, density $\simeq$ 91% of theoretical value) were used for this experiment. G_2 glass was spread over a surface of the pellets and the pellets were heat treated at 600°C/6 hr. But after cooling, it was found out that, the glass did not get penetrated, even though there was slight colour change. So the pellets were again heat treated to 700°C/1 h. With porous pellet, the penetration was complete but with denser one, it was not. (Fig IV.18) So this pellet was heated to 1100°C/15 min. in a globar rod furnace. The penetration was complete now.

The resistivity behaviour and dielectric constant behaviour are shown in Figures IV.16 and IV.19. This proves the above assumptions and lead to the formation of grain boundary barrier layer (GBBL) material (Table IV.3 : 17).

Amount of glass used with this pellet is approximately 0.5 wt. %. From Figure IV.16 it is clearly seen that there is a rise in resistivity at around Curie temperature. So with another set of pellets 1 wt. % G_2 glass was used and the pellets were sintered again at 1100°C/15 min. and ε vs. T curve was shown in Figure IV.20. In Figure IV.21 ρ vs. T curve appears. Lower values of dielectric constant and the rise in resistivity in Curie point region are observed. To check the effectiveness of lower temperature of sintering

and still higher glass addition, samples with 3 wt. % G_2 were heat treated at 1000°C/30 min. But by X-ray diffraction studies, it was found out that, the glass had not penetrated fully. Still the lower value of dielectric constant and the rise in resistivity at around Curie point is observed.

So, again the higher temperature heat treatment was utilized. This time 5 wt. % G_2 was used. But the dielectric constant value was lowered further and the presence of PTC effect was observed.

Lower value of RT dielectric constant can be explained As it was observed by many workers (36) dielectric constant value, below relaxation frequency is directly proportional to grain diameter to grain boundary thickness. Since the grain size of the pellet is relatively smaller (5-7 μ) the ratio also is expected to be small.

So, it has been decided to carry out the experiments with bigger grains. It is mentioned in literature (57,58) that the optimum grain size is 20-50 μ. Optimum BaO to TiO_2 ratio is 1.01:1 to 1.02:1. Former is to avoid poor humidity and voltage effects and the latter is to improve the capacitor life.

So two batches, one with 1.02:1 $BaCO_3$:TiO_2 mixture and other with 1:1.03 $BaCO_3$:TiO_2 mixture were prepared. Excess titanium oxide provides liquid phase at the heat treatment temperature (1400°C) and so better La distribution and grain growth were expected. They were calcined at 1200°C/6 h and then powdered with morter and pestle. To improve homogenity, every time 6 gms of powder was powdered with ultrasonic vibrator for 1 hr.

With 0.4 mole % La solution the semiconductor was tried to be formed at 1400°C/1 h. $BaTiO_3$ from 1.02:1 $BaCO_3$: TiO_2 readily gave semiconductor behaviour. The blue colouration was almost uniform whereas, with the other powder, highly non uniform pellets were obtained. To get uniform blue colouration with 1:1.03 powder also, 0.35, 0.45, 0.5 mole % La additions were tried. The improvement with 0.45 was not sufficient. Then the effect of Al_2O_3 was tried. With both powders 1 wt. % Al_2O_3 was added along with La solution. Uniformity has increased considerably, but still with 1:1.03 powder thorough uniformity was not obtained. Average grain size of the final dense pellet is 25-30 μ.

With 3 wt. % of G_2 over the surface, alumina added samples of 1.02:1 composition showed higher room temperature dielectric constant value (ε = 33,000) and so for all further experiments this powder was used (Figure IV.22).

Alumina added pellets showed around 9000 ohm-cm as room temperature resistivity value where without alumina the value is around 11,000 ohm-cm.

Even though the dielectric constant value of the glass added sample is high, the PTC effect is still observed (Figure IV.23). At higher temperature reaction is expected to be more. If so the grain diameter to grain boundary thickness ratio will reduce. To avoid this 1000°C/30 min. heat treatment was tried. With 3 wt. % G_2 glass and 1000°C/30 min. heat treatment the properties were not improved (Figures IV.24 and IV.25).

By visual examination, glass coating was observed on the surface. X-ray diffraction pattern was taken for the glass coated surface. No $BaTiO_3$ peak was observed. Peaks characteristic of $Ba\ Bi_4\ Ti_4\ O_{15}$, and $Bi_4\ Ti_3\ O_{12}$ were found (Figure IV.26). These two compounds are the reaction products of $BaTiO_3$ with the glass. Since no $BaTiO_3$ peaks were observed it was concluded that the penetration of glass inside the specimen was not complete.

So still higher concentration as well as higher temperature effect was studied next. With these samples a rise in room temperature dielectric constant is obtained. But still the PTC effect exists. By X-ray diffraction full penetration of glass into the sample was confirmed.

Then the effect of G_1 glass was studied. This glass having higher dielectric constant and higher resistivity value, compared to G_2 glass (Table II.1) is expected to give better properties. By X-ray diffraction studies, complete penetration was confirmed. Final pellets had lower tanδ value and higher room temperature resistivity value (Figures IV.24 and IV.25). But the dielectric constant value is also low (ε = 27,250).

With this glass also PTC effect was observed. A good grain boundary barrier layer capacitor should have the following characteristics (59).

1. Room temperature resistivity should be of the order of insulator $BaTiO_3$. The temperature behaviour should be similar to that of insulator $BaTiO_3$.

2. Peak height of dielectric constant at Curie temperature should be as small as possible.

3. Dissipation factor value should be less than 0.1 at room temperature and should not vary much with temperature.

4. Dielectric constant should not vary much with frequency-constant value is ideal.

5. Dissipation factor value reaches a minimum at around 1 MHz and then rises. The minimum should be shifted to higher frequency value as much as possible.

Resistivity vs. temperature plots of all the samples showed PTC behaviour. Frequency characteristics (Figures IV.27 to 29) showed variation in dielectric constant. Since with the capacitance bridge 1615 A, it is not possible to tune beyond 100 KC, the dip in tanδ value was not observed. 5 to 7 μ $BaTiO_3$ showed relatively flat frequency response. But the dielectric constant value is very less.

From Table IV.2 and Table IV.4 and from resistivity vs. temperature plots, one can conclude that above mentioned properties were obtained more or less. Higher value of dielectric constant, very little variation (around one order only) in resistivity near the Curie temperature, reasonably high value of room temperature resistivity ($\sim 10^6$ ohm-cm), and smaller variation of dielectric constant with frequency (few thousands only) are observed. To improve the properties further, higher glass concentration may be utilized. But reaction between $BaTiO_3$ and glass also will increase and so the necessary result may not be produced.

Better way of tackling the problem may be the utilization of one of the well explored acceptor ions like Mn, Cu etc. (36,39,59). As some work was done using Mn ions with 5-7 μ $BaTiO_3$ its effect with bigger grains was tried.

In Figure IV.16 effect of 0.05 mole % of Mn on 5 to 7 μ $BaTiO_3$ can be observed. Simultaneous addition with La produced a PTC material and with separate addition the PTC effect got reduced considerably. So the effect of 0.05 mole % of Mn on bigger particles may be studied.

But simultaneous addition of 0.05 mole % of Mn with La and subsequent heat treatment at 1400°C for 1 h produced brownish blue pellets. Many pellets were fully brown in colour, i.e., with the bigger particle $BaTiO_3$ produced from 1.02:1 $BaCO_3$:TiO_2 mixture, the diffusion is faster and the amount of Mn is also more.

So in the next experiment 0.025 mole % Mn was used. These pellets were heat treated with 4 wt. % of G_1 and G_2 glasses on one surface at 1100°C/15 min. and the ε vs. T, ρ vs. T and ε vs. frequency were studied (Figures IV.30, IV.32 and IV.33). Peak hight in ε vs. T curve has reduced considerably. Relatively flatter frequency response is obtained. Higher resistivity value (in 10^9 ohm-cm range) is also observed. Lower room temperature tanδ (in 10^{-2} range) value is also an additional result. But room temperature dielectric constant value got reduced (ε = 18,000) and the PTC effect is still observed. Moreover nearly overlapping curves showed the relative independence of the glass

composition. Lower change in resistivity at Curie point showed advantage of using G_1 glass.

In 1400°C/1 h treatment, some manganese ions will diffuse inside the lattice. This will increase the bulk resistivity. As the effective dielectric constant is inversely proportional to the bulk resistivity value (36) the lower value of dielectric constant can be explained. Moreover from PTC behaviour one can conclude that the lower amount of Mn at the surface is ineffective to produce material with proper resistivity behaviour.

If Mn is added at lower temperature the above drawbacks may get rectified. So calculated amount of Mn solution (Section III.1.2.3) was added to measured quantity of G_1 and G_2 glasses and the excess amount of water was evaporated. Concentration of Mn is chosen in such a way that for 4 wt. % addition of glass 0.025 mole % of Mn will be consumed.

So with next set of pellets, 4 wt. % of glass G_1 and G_2 with Mn was spread over a surface and the pellets were heat treated to 1100°C/15 min. Various behaviours are shown in Figures IV.31, IV.32 and IV.33. Room temperature dielectric constant value got improved (ε = 23,000) compared to the other case. Flatness with frequency is also improved slightly. With G_1 glass the rise in sensitivity value at Curie temperature has reduced considerably.

Table IV.1

Room temperature resistivity data of various semiconductor $BaTiO_3$ based samples

	Sample	Temperature and time	Room temperature resistivity ohm-cm
1.	S(I) 0.4 mole % La doped $BaTiO_3$	1300/6 h	3.56×10^3
2.	S(II) 0.4 mole % La doped $BaTiO_3$	1400°C/1 h	400
3.	S(III) 0.2 mole % La doped $BaTiO_3$	1400°C/1 h	12000
4.	S(III) 0.3 mole % La doped $BaTiO_3$	1400°C/1 h	1400
5.	S(II) 0.4 mole % La and 0.05 mole % Mn doped $BaTiO_3$ (Added simultaneously)	1400°C/1 h	10^7
6.	S(II) 0.4 mole % La and 0.05 mole % Mn doped $BaTiO_3$ (Added separately)	-	3×10^9
7.	S(III) 0.3 mole % La + 0.02 mole % Mn doped $BaTiO_3$	1400°C/1 h	1500
8.	S(II) 0.4 mole % La doped $BaTiO_3$ + glass G_2 coated	1100°C/15 min	4.5×10^9
9.	S(II) 0.4 mole % La doped $BaTiO_3$, crushed, repressed, G_2 coated	700°C/1 h	3×10^{10}
10.	S(II) 0.4 mole % La doped $BaTiO_3$ + 1 wt. % G_2 coated	1100°C/15 min	2.1×10^{10}
11.	S(II) 0.4 mole % La doped $BaTiO_3$ + 3 wt. % G_2 coated	1000°C/30 min	1.9×10^8
12.	S(II) 0.4 mole % La doped $BaTiO_3$ + 5 wt. % G_2 coated	1100°C/15 min	1.74×10^{10}

Table IV.2

Room temperature resistivity data of 25-30 μ $BaTiO_3$
All samples are prepared from 1.02:1 $BaCO_3$:TiO_2 mixture
average grain size = 25-30 μ

	Samples	Temperature and time	Room temperatur resistivity ohm-cm
1.	S(II) 0.4 mole % La + 1 wt. % Al_2O_3 added $BaTiO_3$	1400°C/1 h	9000
2.	S(II) 0.4 mole % La added $BaTiO_3$ + 3 wt. % G_2 coated	1100°C/15 min	6.85×10^7
3.	S(II) 0.4 mole % La + 1 wt. % Al_2O_3 added $BaTiO_3$ + 3 wt. % G_2 coated	1100°C/15 min	3.77×10^7
4.	S(II) 0.4 mole % La + 1 wt. % Al_2O_3 added $BaTiO_3$ + 3 wt. % G_2 coated	1000°C/30 min	6×10^6
5.	S(II) 0.4 mole % La + 1 wt. % Al_2O_3 added $BaTiO_3$ + 4 wt. % G_1 coated	1100°C/15 min	2.7×10^7
6.	S(II) 0.4 mole % La + 1 wt. % Al_2O_3 added $BaTiO_3$ + 4 wt. % G_2 coated	1100°C/15 min	4.7×10^6
7.	S(II) 0.4 mole % La + 1 wt. % Al_2O_3 + 0.025 mole % Mn added $BaTiO_3$ + 4 wt. % G_1	1100°C/15 min	7.3×10^9
8.	S(II) 0.4 mole % La + 1 wt. % Al_2O_3 + 0.025 mole % Mn added $BaTiO_3$ + 4 wt. % G_2	1100°C/15 min	8×10^9
9.	S(II) 0.4 mole % La + 1 wt. % Al_2O_3 added $BaTiO_3$ + 4 wt. % G_1 (+ 0.025 mole % Mn)	1100°C/15 min	9.6×10^{10}
10.	S(II) 0.4 mole % La + 1 wt. % Al_2O_3 added $BaTiO_3$ + 4 wt. % G_2 (+ 0.025 mole % Mn)	1100°C/15 min.	1.1×10^{11}

Table IV.2

Room temperature resistivity data of 25-30 μ $BaTiO_3$
All samples are prepared from 1.02:1 $BaCO_3$:TiO_2 mixture
Average grain size = 25-30 μ

	Samples	Temperature and time	Room temperatu resistivity ohm-cm
1.	S(II) 0.4 mole % La + 1 wt. % Al_2O_3 added $BaTiO_3$	1400°C/1 h	9000
2.	S(II) 0.4 mole % La added $BaTiO_3$ + 3 wt. % G_2 coated	1100°C/15 min	6.85×10^7
3.	S(II) 0.4 mole % La + 1 wt. % Al_2O_3 added $BaTiO_3$ + 3 wt. % G_2 coated	1100°C/15 min	3.77×10^7
4.	S(II) 0.4 mole % La + 1 wt. % Al_2O_3 added $BaTiO_3$ + 3 wt. % G_2 coated	1000°C/30 min	6×10^6
5.	S(II) 0.4 mole % La + 1 wt. % Al_2O_3 added $BaTiO_3$ + 4 wt. % G_1 coated	1100°C/15 min	2.7×10^7
6.	S(II) 0.4 mole % La + 1 wt. % Al_2O_3 added $BaTiO_3$ + 4 wt. % G_2 coated	1100°C/15 min	4.7×10^6
7.	S(II) 0.4 mole % La + 1 wt. % Al_2O_3 + 0.025 mole % Mn added $BaTiO_3$ + 4 wt. % G_1	1100°C/15 min	7.3×10^9
8.	S(II) 0.4 mole % La + 1 wt. % Al_2O_3 + 0.025 mole % Mn added $BaTiO_3$ + 4 wt. % G_2	1100°C/15 min	8×10^9
9.	S(II) 0.4 mole % La + 1 wt. % Al_2O_3 added $BaTiO_3$ + 4 wt. % G_1 (+ 0.025 mole % Mn)	1100°C/15 min	9.6×10^{10}
10.	S(II) 0.4 mole % La + 1 wt. % Al_2O_3 added $BaTiO_3$ + 4 wt. % G_2 (+ 0.025 mole % Mn)	1100°C/15 min.	1.1×10^{11}

Table IV.3

Room temperature dielectric constant and dissipation factor data of various semiconductor $BaTiO_3$ based samples

	Sample	Sintering temperature/time	% of theoretical density	Room temperature dielectric constant	RT tanδ
1.	S(I) 6 hg* $BaTiO_3$ + 10% G_2	1100°C/ 1 h	80%	1920	0.057
2.	S(I) 6 hg $BaTiO_3$ + 10% G_2	FF 1100°C/ 15 min	78%	1930	0.05
3.	S(II) 2 hg $BaTiO_3$ + 10% G_1	1100°C/ 1 h	80.8%	2500	0.067
4.	S(II) 5 hg $BaTiO_3$ + 10% G_2	1100°C/ 1 h	90.27%	2061	0.27
5.	S(II) 5 hg $BaTiO_3$ + 10% G_2	FF 1200°C/ 1 h	92.4%	1680	0.04
6.	S(II) 10 hg $BaTiO_3$ + 10% G_2	1100°C/ 1 h	83%	1849	0.14
7.	S(II) 10 hg $BaTiO_3$ + 10% G_2	FF 1200/ 5 min	80%	1486	0.061
8.	S(II) 10 hg $BaTiO_3$ + 10% G_2	1200°C/ 1 h	93.3	2343	0.256
9.	S(II) 10 hg $BaTiO_3$ + 10% G_2	N_2 1100°C/ 1 h	69.09%	2263	0.058
10.	S(II) 5 hg $BaTiO_3$ + 10% G_2	N_2 1100°C/ 1 h	80.58%	1634	0.057
11.	S(III) (0.2 mole % La) $BaTiO_3$ + 10% G_2	1000°C/ 1 h	53.14%	1748	0.058
12.	S(III) (0.3 mole % La + 0.02 mole % Mn) $BaTiO_3$ + 10% G_2 (Added simultaneously)	1000°C/ 1 h	54.36%	3276	0.097
13.	S(III) (0.3 mole % La + 0.05 mole % Mn) $BaTiO_3$ + 10% G_2 (Added separately)	1000°C/ 1 h	54.03%	3912	0.079

Contd...

Table IV.3 (Continued)

	Sample	Sintering temperature/time	% of theoretical density	Room temperature dielectric constant	RT tanδ
15.	S(II) (0.4 mole % La + 0.05 mole % Mn) $BaTiO_3$ + 10% G_2 (Added separately)	1000°C/ 1 h	83.96%	2936	0.12
16.	S(II) 0.4 mole % La + 0.05 mole % Mn $BaTiO_3$ + 10% G_2 (Added simultaneously)	1000°C/ 1 h	84.78%	2858	0.11
17.	5-7 μ S(II) (0.4 mole % La + 0.05 mole % Mn) $BaTiO_3$ (Added separately)	-	62.68%	11892	0.042
18.	5-7 μ S(II) (0.4 mole % La) $BaTiO_3$ + G_2 spread on the surface	1100°C/ 15 min	91%	14121	0.080
19.	S(II) 0.4 mole % La added $BaTiO_3$ + 1 wt. % G_2 coated	1100°C/ 15 min	89.98%	8690	0.04
20.	S(II) 0.4 mole % La added $BaTiO_3$ + 3 wt. % G_2 coated	1000°C/ 30 min	91.44%	10243	0.074
21.	S(II) 0.4 mole % La added $BaTiO_3$ + 5 wt. % G_2 coated	1100°C/ 15 min	89.95%	6070	0.041

* 6 hg - 6 hour grinding using ultrasonic vibrator.

Table IV.4

Room temperature dielectric constant data of bigger grain $BaTiO_3$

All samples were prepared from 1.02:1 $BaCO_3$:TiO_2 mixture. Particle size = 25-30 μ

	Sample	Temperature/ time	% of theoretical density	Room temperature dielectric constant ε	RT tan δ
1.	S(II) 0.4 mole % La added $BaTiO_3$ + 3 wt. % G_2 coated	1100°C/ 15 min	88.94	25995	0.077
2.	S(II) 0.4 mole % La + 1 wt. % Al_2O_3 added $BaTiO_3$ + 3 wt. % G_2 coated	1100°C/ 15 min	88.1	33468	0.095
3.	S(II) 0.4 mole % La + 1 wt. % Al_2O_3 added $BaTiO_3$ + 3 wt. % G_2 coated	1000°C/ 30 min	89.61	15577	0.063
4.	S(II) 0.4 mole % La + 1 wt. % Al_2O_3 added $BaTiO_3$ + 4 wt. % G_1 coated	1100°C/ 15 min	90.94	27251	0.135
5.	S(II) 0.4 mole % La + 1 wt. % Al_2O_3 added $BaTiO_3$ + 4 wt. G_2 coated	1100°C/ 15 min	88.1	36352	0.154
6.	S(II) 0.4 mole % La + 1 wt. % Al_2O_3 + 0.025 mole % Mn added $BaTiO_3$ + 4 wt. % G_1 coated	1100°C/ 15 min	89.78	18689	0.075
7.	S(II) 0.4 mole % La + 1 wt. % Al_2O_3 + 0.025 mole % Mn added $BaTiO_3$ + 4 wt. % G_2 coated	1100°C/ 15 min	88.9	18097	0.063
8.	S(II) 0.4 mole % La + 1 wt. % Al_2O_3 added $BaTiO_3$ + 4 wt. % G_1 (+ 0.025 mole % Mn)	1100°C/ 15 min	89.94	23651	0.069
9.	S(II) 0.4 mole % La + 1 wt. % Al_2O_3 added $BaTiO_3$ + 4 wt. % G_2 (+ 0.025 mole % Mn) coated	1100°C/ 15 min	88.94	22669	0.068

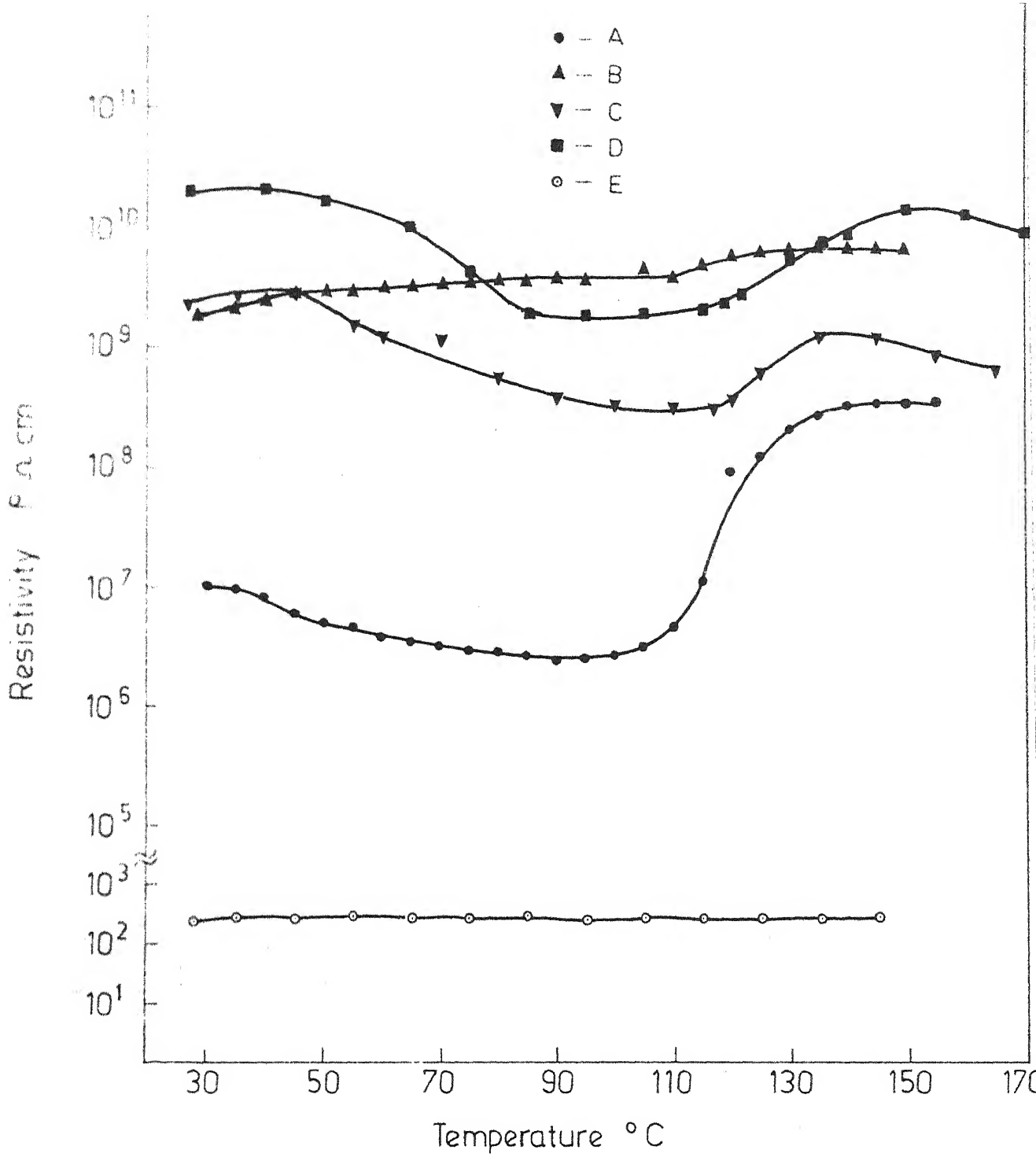

Fig. IV.16 Resistivity Vs temperature plots of

A - 0.4 mole % La + 0.05 mole % Mn (Simultaniously) added $BaTiO_3$.

B - 0.4 mole % La + 0.05 mole % Mn (Seperately) added $BaTiO_3$.

C - 0.4 mole % La added $BaTiO_3$ + Glass G_2 coated, 1100°C/15min treated sample.

D - 0.4 mole % La added $BaliO_3$, crushed, G_2 coated 700°C/1hr treated

E - 0.4 mole % La added $BaTiO_3$.

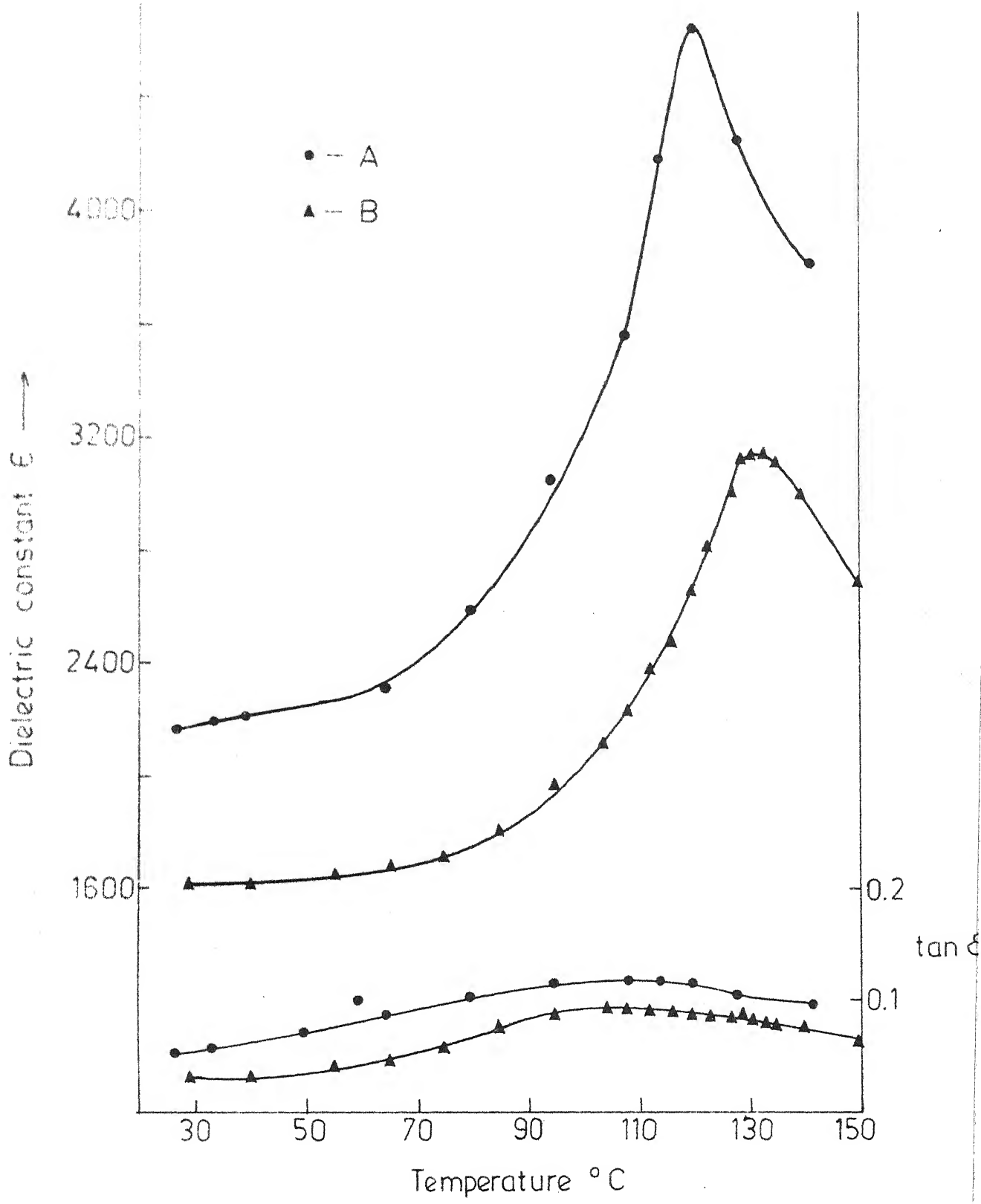

Fig. IV.17 ϵ Vs T curve for

A - 0.4 mole % La + 0.05 mole % Mn doped (Simultaniously) $BaTiO_3$ + 10 % G_2 heat treated at 1000°C/1h.

B - 0.4 mole % La + 0.05 mole % Mn doped (Seperately) $BaTiO_3$ + 10 % G_2 heat treated at 1000°C/1h.

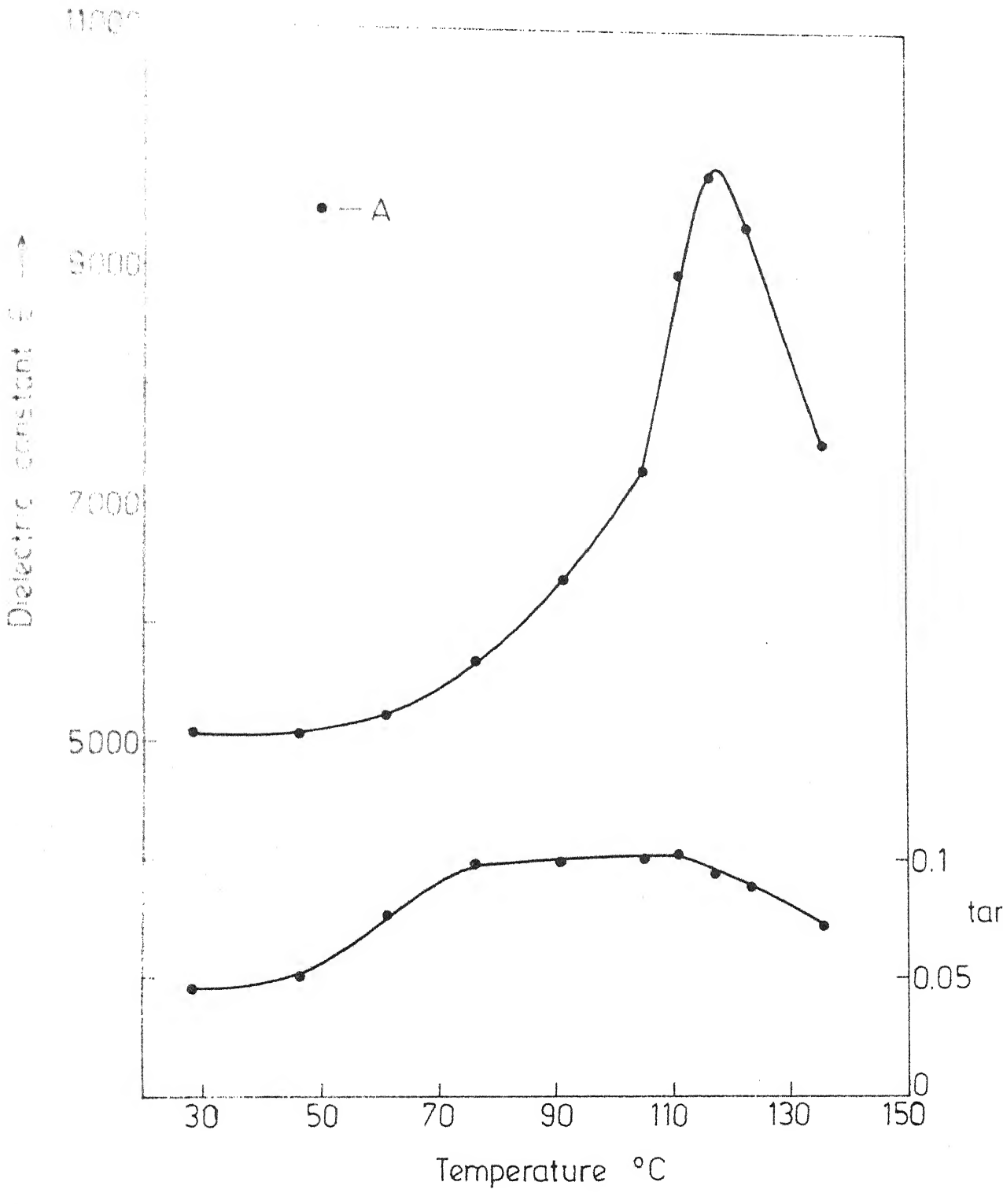

Fig. IV.18 ϵ Vs T curve for

A - 0.4 mole % La doped $BaTiO_3$ crushed and repressed, G_2 coating over one surface. Heat treated at 700 °C / 1 h.

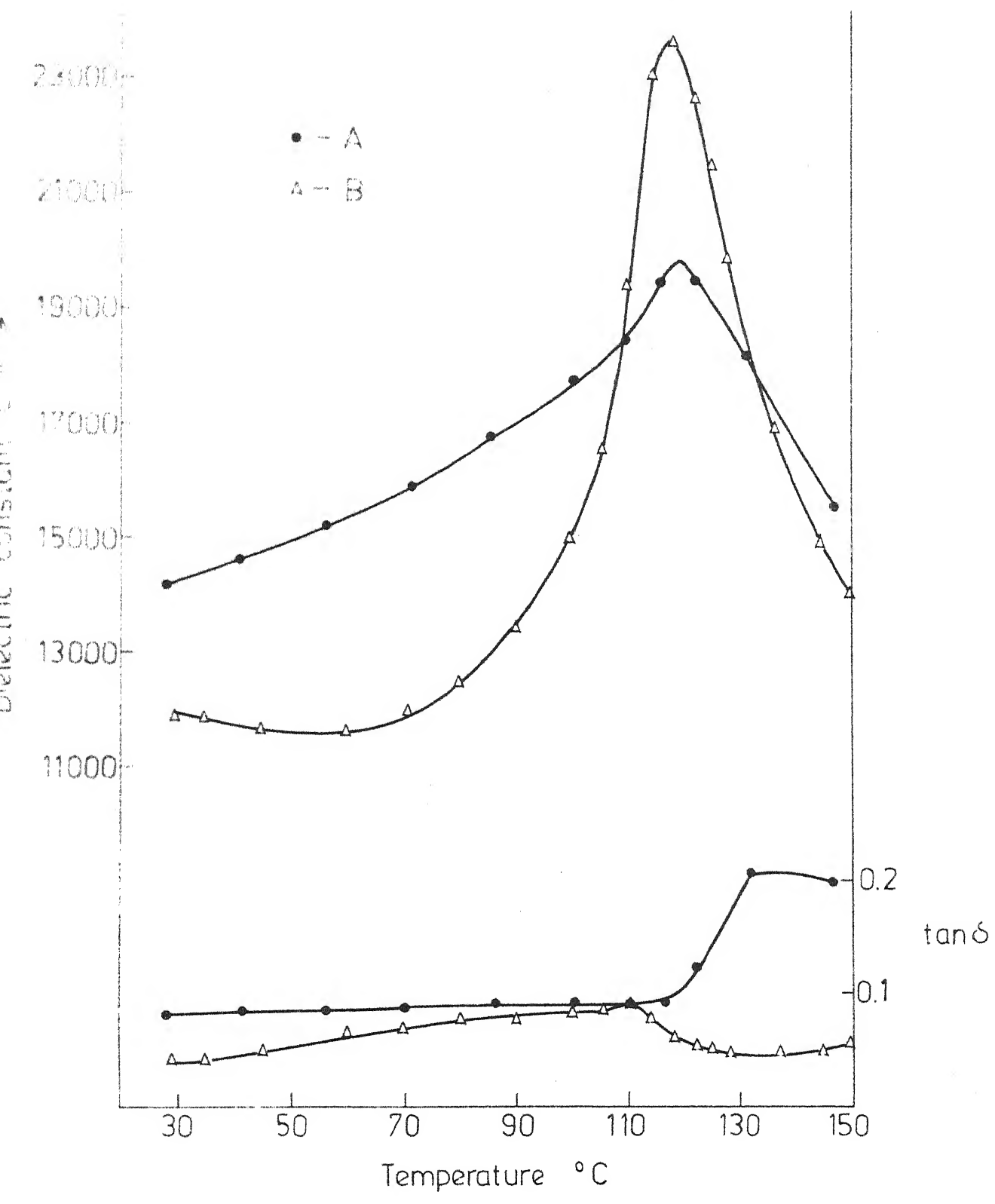

Fig. IV.19 ϵ Vs T curve for

A -- 0.4% La doped $BaTiO_3$ + glass G_2 coated on one surface and heat treated at 1100/15 min.

B -- 0.4% La doped $BaTiO_3$ + 0.05% Mn doped $BaTiO_3$ (heat treated at 1200 °C/1hr).

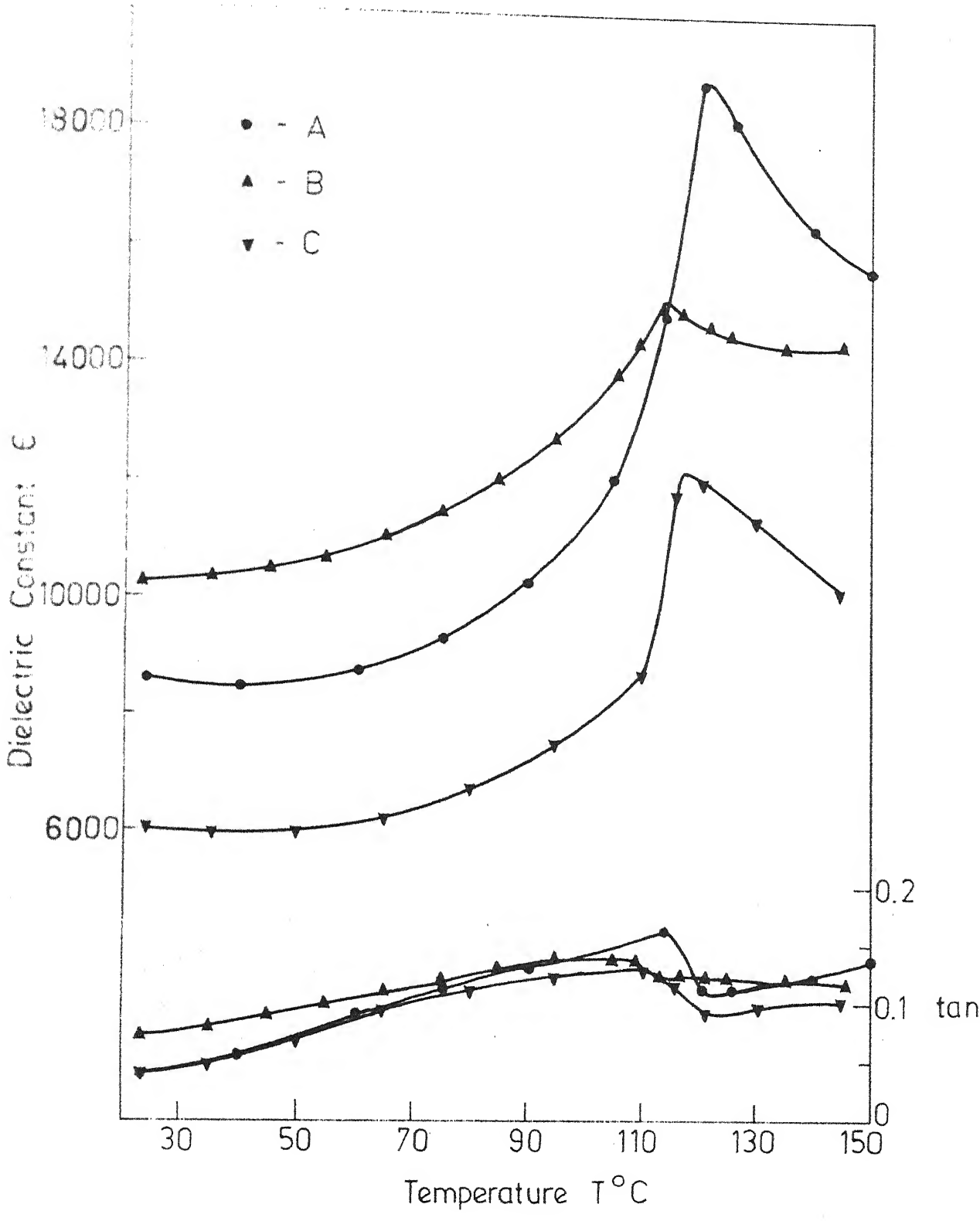

Fig. IV.20 ϵ Vs T curve of

A. 0.4 mole % La added S(II) 5-7μ $BaTiO_3$ + 1 wt %
(1100°C / 15 min)

B. 0.4 mole % La added S(II) 5-7μ $BaTiO_3$ + 3 wt %
(1000°C / 30 min)

C. 0.4 mole % La added S(II) 5-7μ $BaTiO_3$ + 5 wt %
(1100°C / 15 min)

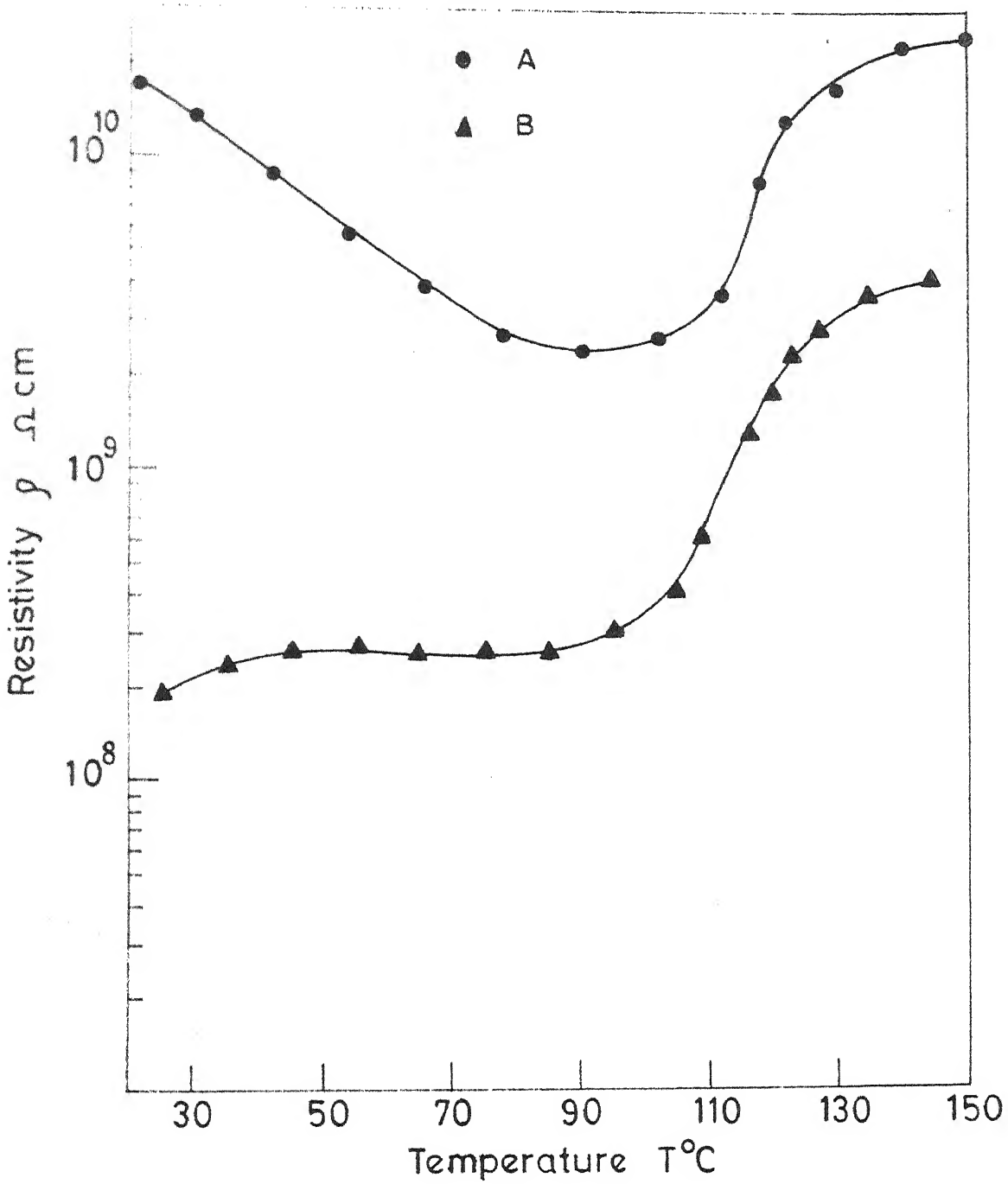

Fig.IV.21 ρ vs T curve of
A - 0.4 mole % La added s(II) 5-7 μ
$BaTiO_3$ + 5 wt % G_2 (1100°C/15 min.)
B - 0.4 mole % La added S(II) 5-7 μ
$BaTiO_3$ + 3 wt % G_2 (1000°C/30 min)

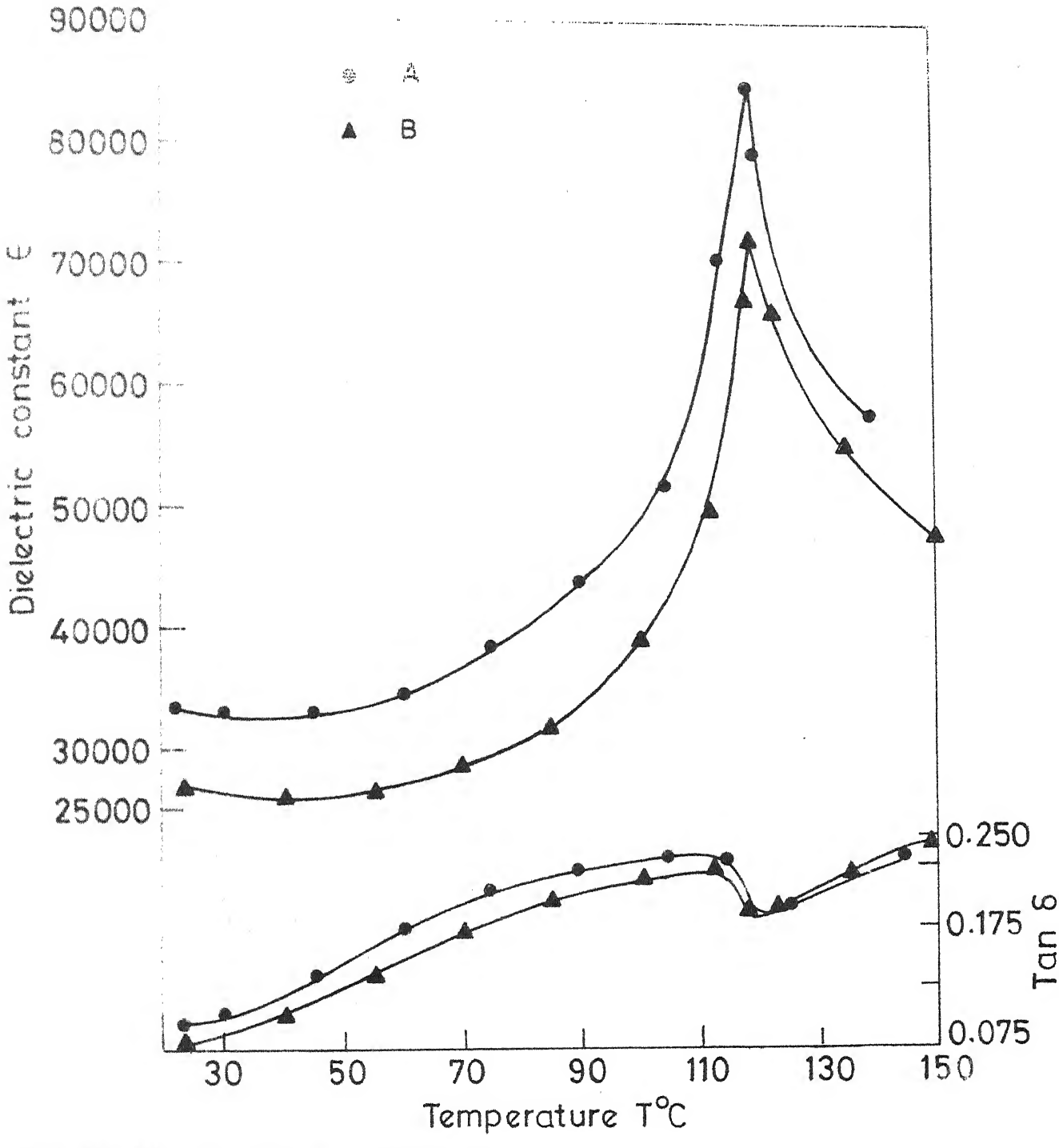

Fig. IV.22 ε vs T curve of

A-0.4 mole % La added S(II) 25-30 μ $BaTiO_3$ + 1 wt % Al_2O_3 + 3 wt % G_2 (1100°C/15 min.)

B-0.4 mole % La added S(II) 25-30 μ $BaTiO_3$ + 3 wt % G_2 (1100 °C/15 min.)

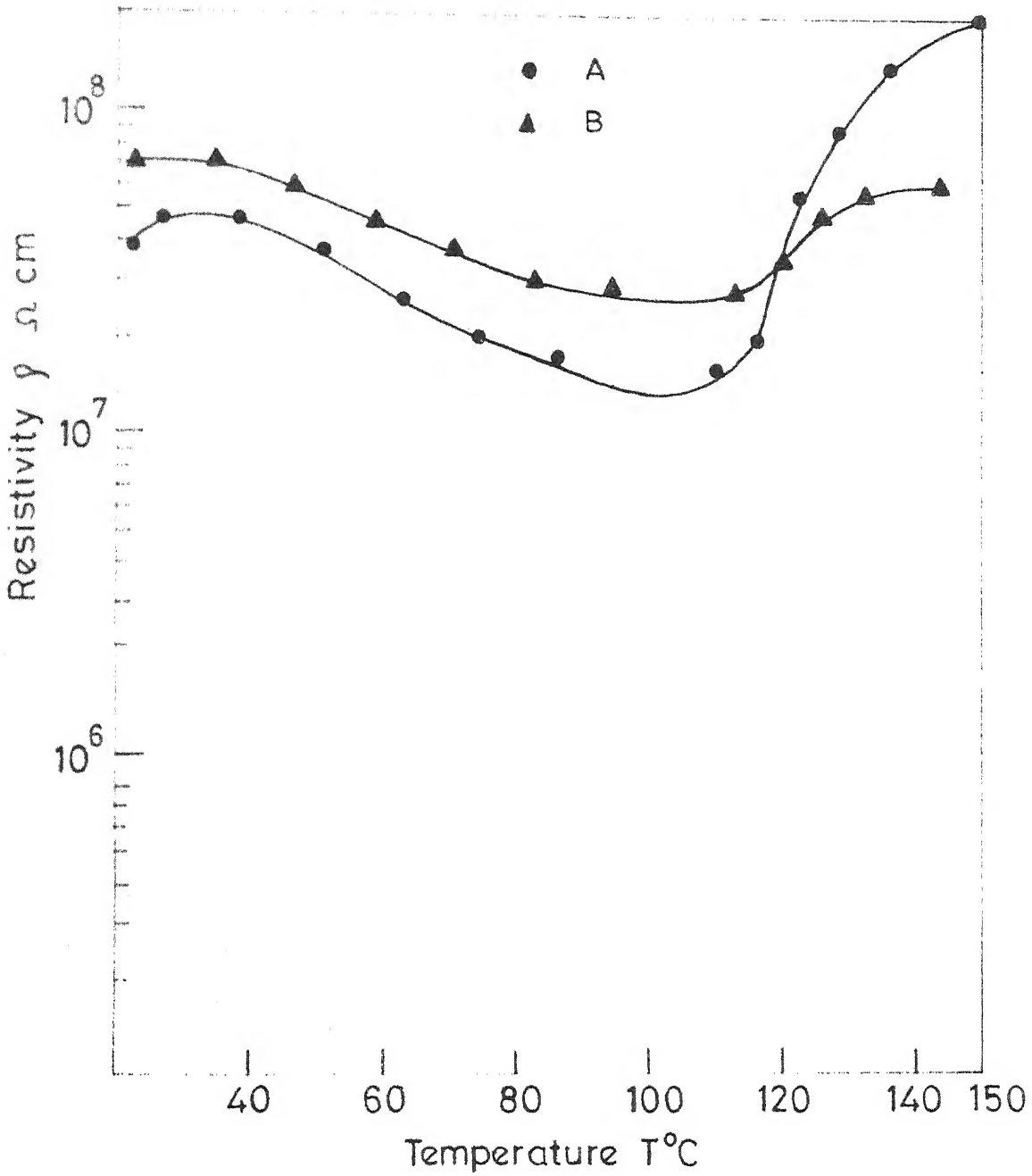

Fig. IV.23 ρ vs T curve of
A - 0.4 mole % La + 1 wt % Al_2O_3 added s(II) 25-30 μ $BaTiO_3$ + 3 wt % G_2 (1100°C/15 min.)

B - 0.4 mole % La added s(II) 25-30 μ + 3 wt % G_2 (1100°C/15 min.)

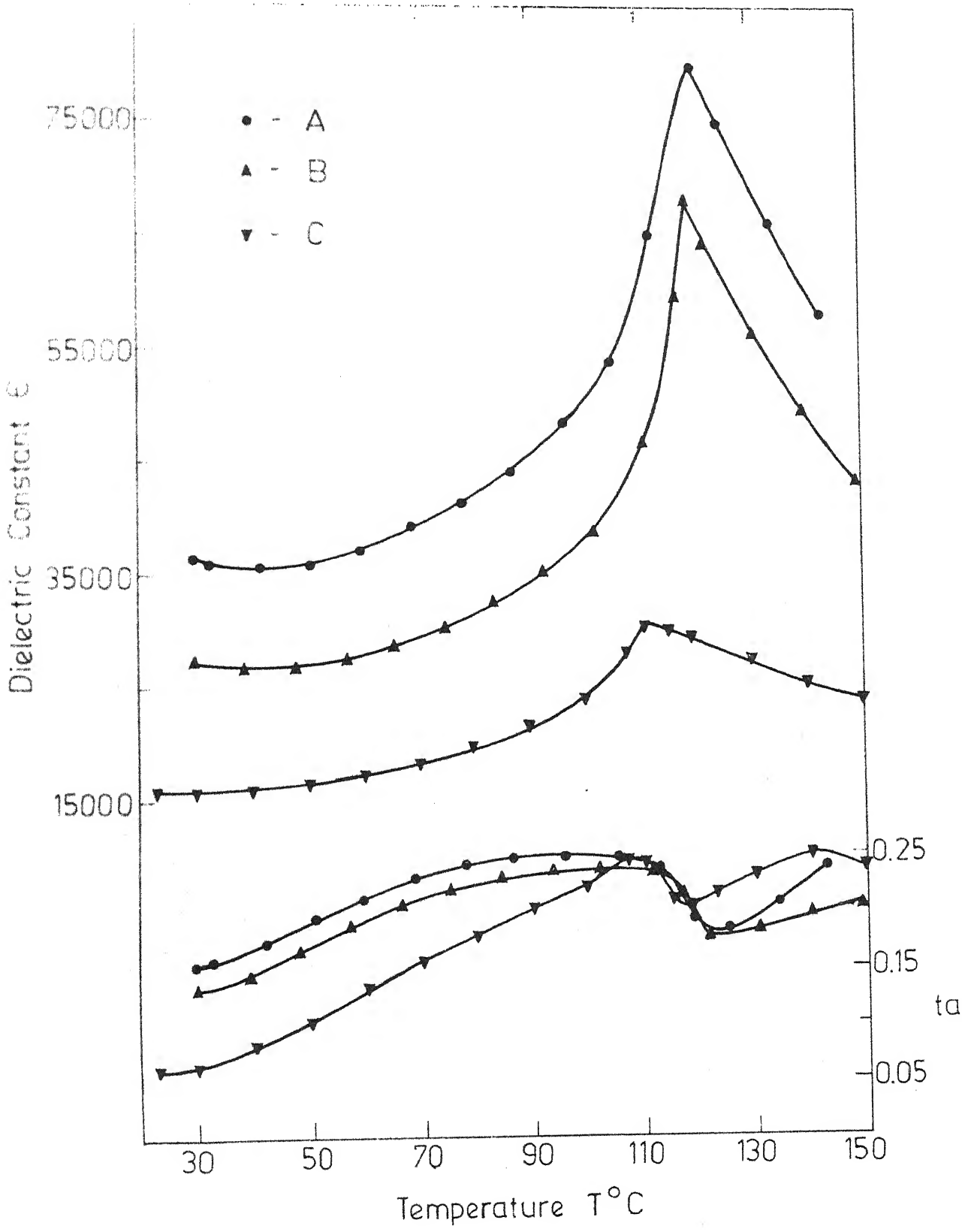

Fig. IV.24 ϵ Vs T curve of

A. 0.4 mole % La + 1 wt % Al_2O_3 added 25-30μ $BaTiO_3$ + 4 %
(1100°C / 15 min)

B. 0.4 mole % La + 1 wt % Al_2O_3 added 25-30μ $BaTiO_3$ + 4 %
(1100°C / 15 min)

C. 0.4 mole % La + 1 wt % Al_2O_3 added 25-30μ $BaTiO_3$ + 3 %

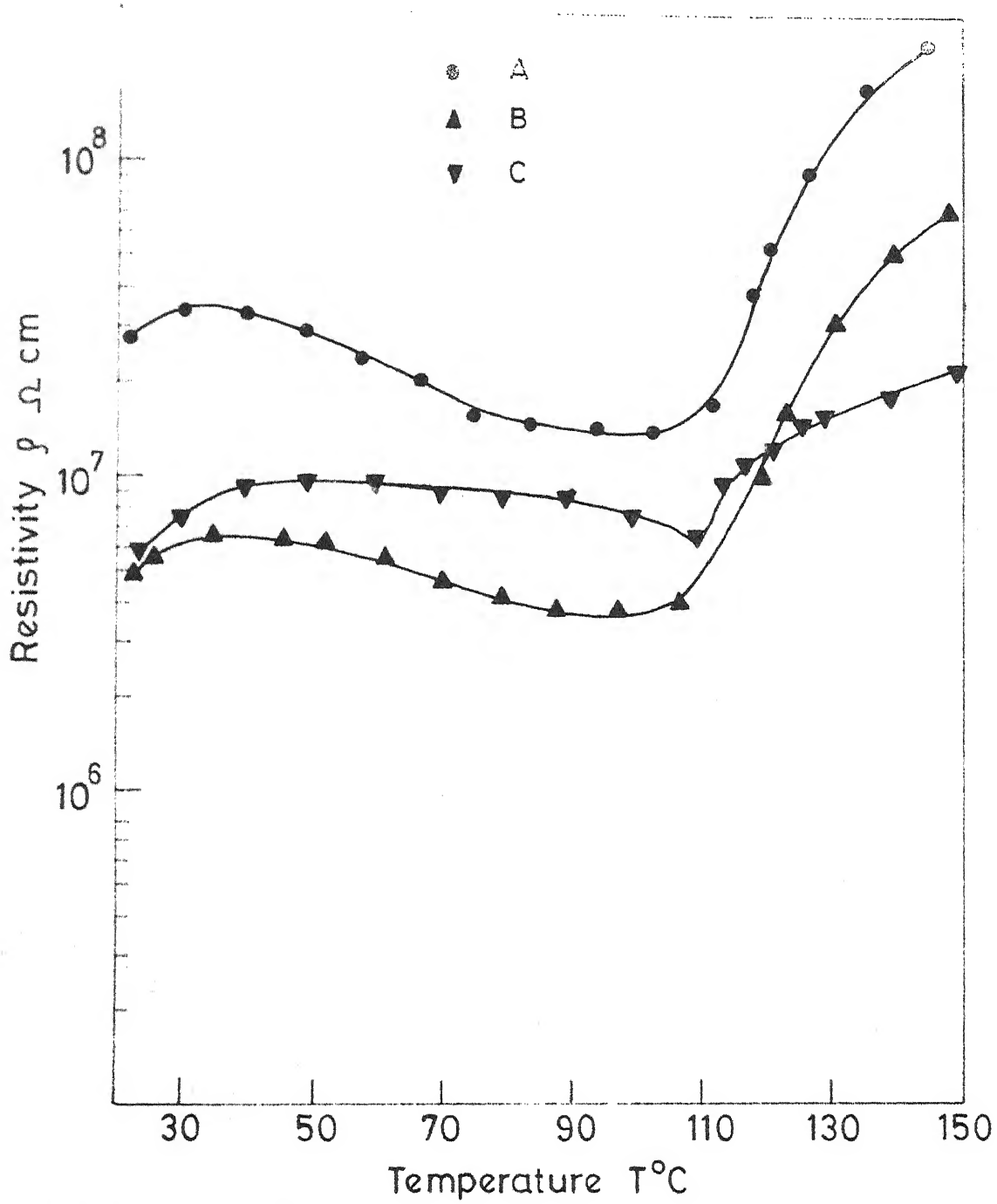

Fig.IV.25 ρ vs T curve of
A-0.4 mole % La + 1 wt % Al_2O_3 added S(II)
25-30 μ $BaTiO_3$ + 4 wt % G_1 (1100°C/15 min.)

B-0.4 mole % La + 1 wt % Al_2O_3 added S(II)
25-30 μ $BaTiO_3$ + 4 wt % G_2 (1100°C/15 min.)

C-0.4 mole % La + 1 wt % Al_2O_3 added S(II)
25-30 μ $BaTiO_3$ + 3 wt % G_2 (1000°C/30 min.)

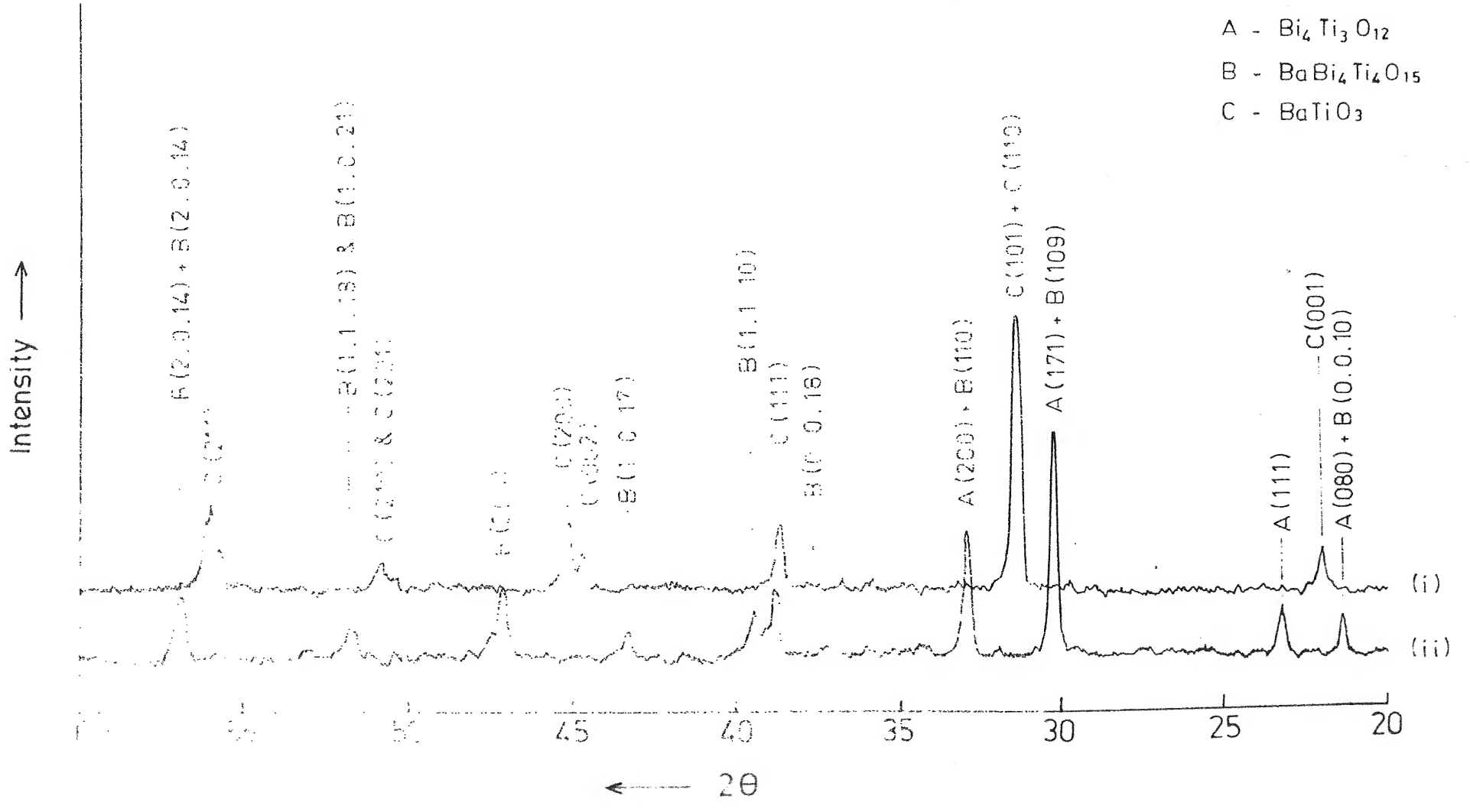

Fig. IV.26 X-ray deffraction patterns of S(II) 25-30 μ $BaTiO_3$ + G_2 coated samples.
(i) 1000°C treated sample.
(ii) 1100°C treated sample

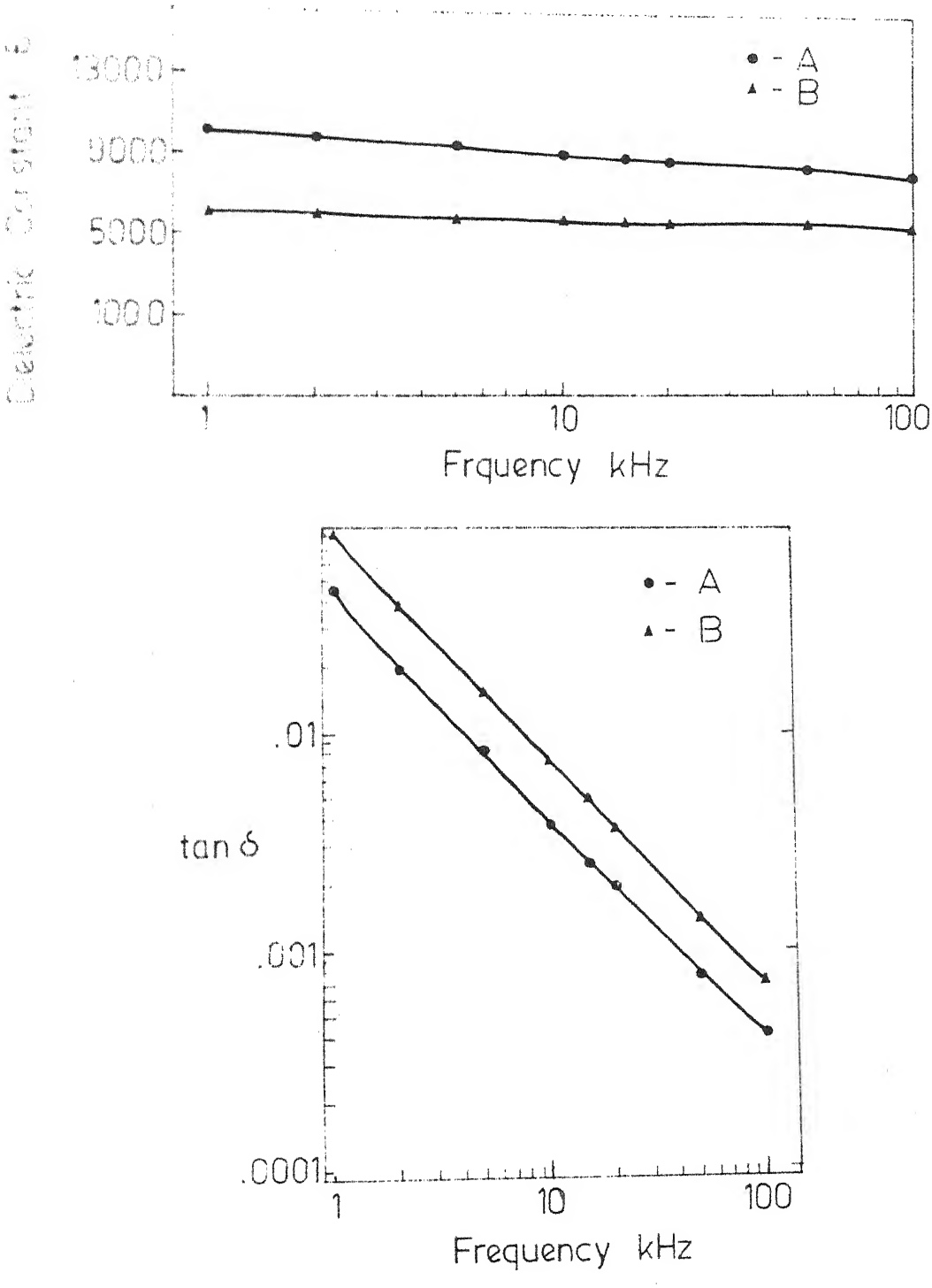

Fig. IV.27 Dielectric Constant Vs Frequency curves of

A - 0.4 mole % La added S(II) 5-7 μ $BaTiO_3$ + 3 wt % G_2 (1000°C/30 min)

B - 0.4 mole % La added S(II) 5-7 μ $BaTiO_3$ + 5 wt % G_2 (1100°C/15 min)

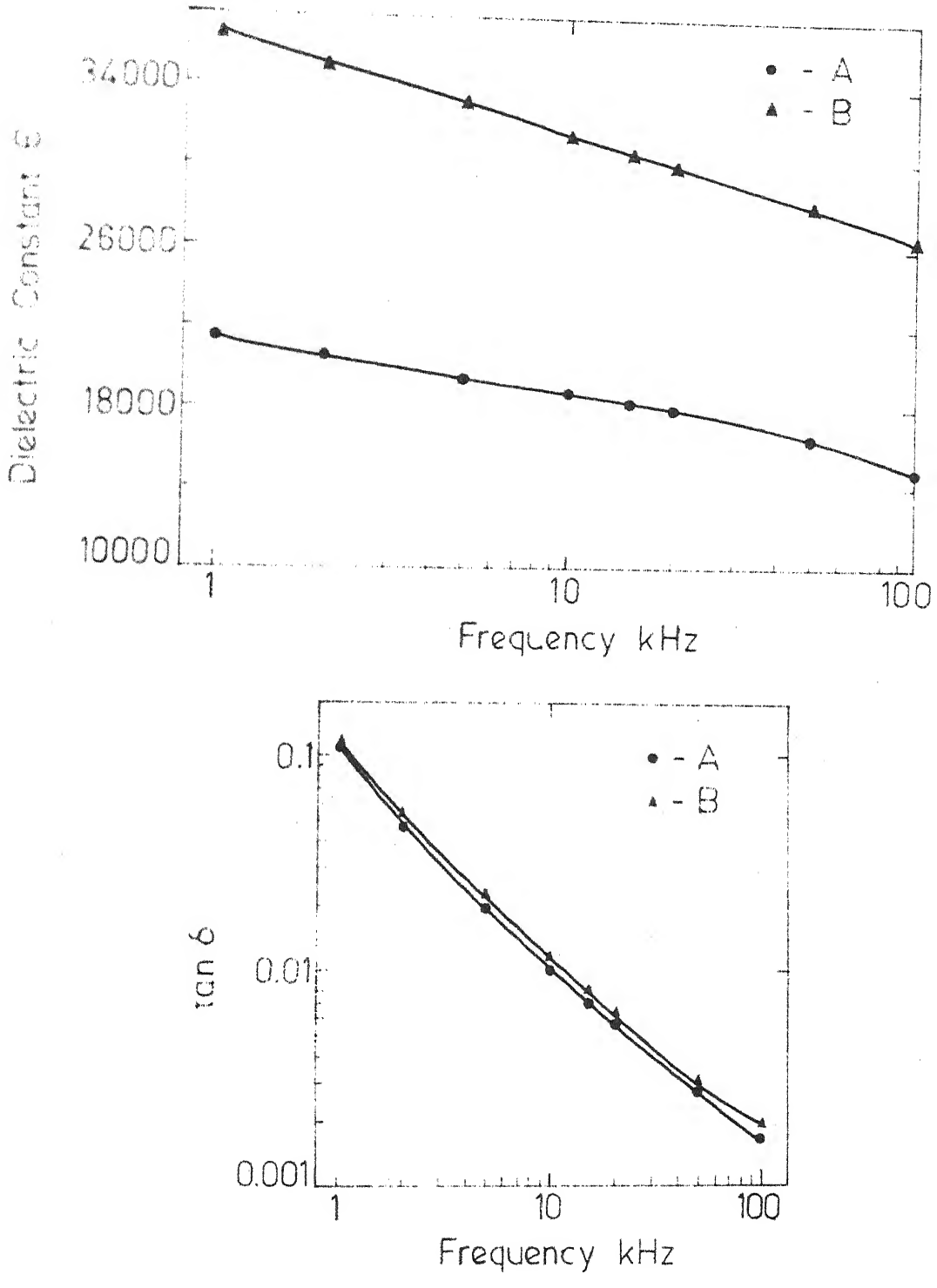

Fig. IV.28 Dielectric Constant Vs frequency curves of

A- 0.4 mole % La added S(II) 25-30 μ $BaTiO_3$ + 3 wt % G_2 (1100°C / 15 min)

B- 0.4 mole % La + 1 wt % Al_2O_3 added S(II) 25-30 μ $BaTiO_3$ + 3 wt % G_2 (1100°C / 15 min)

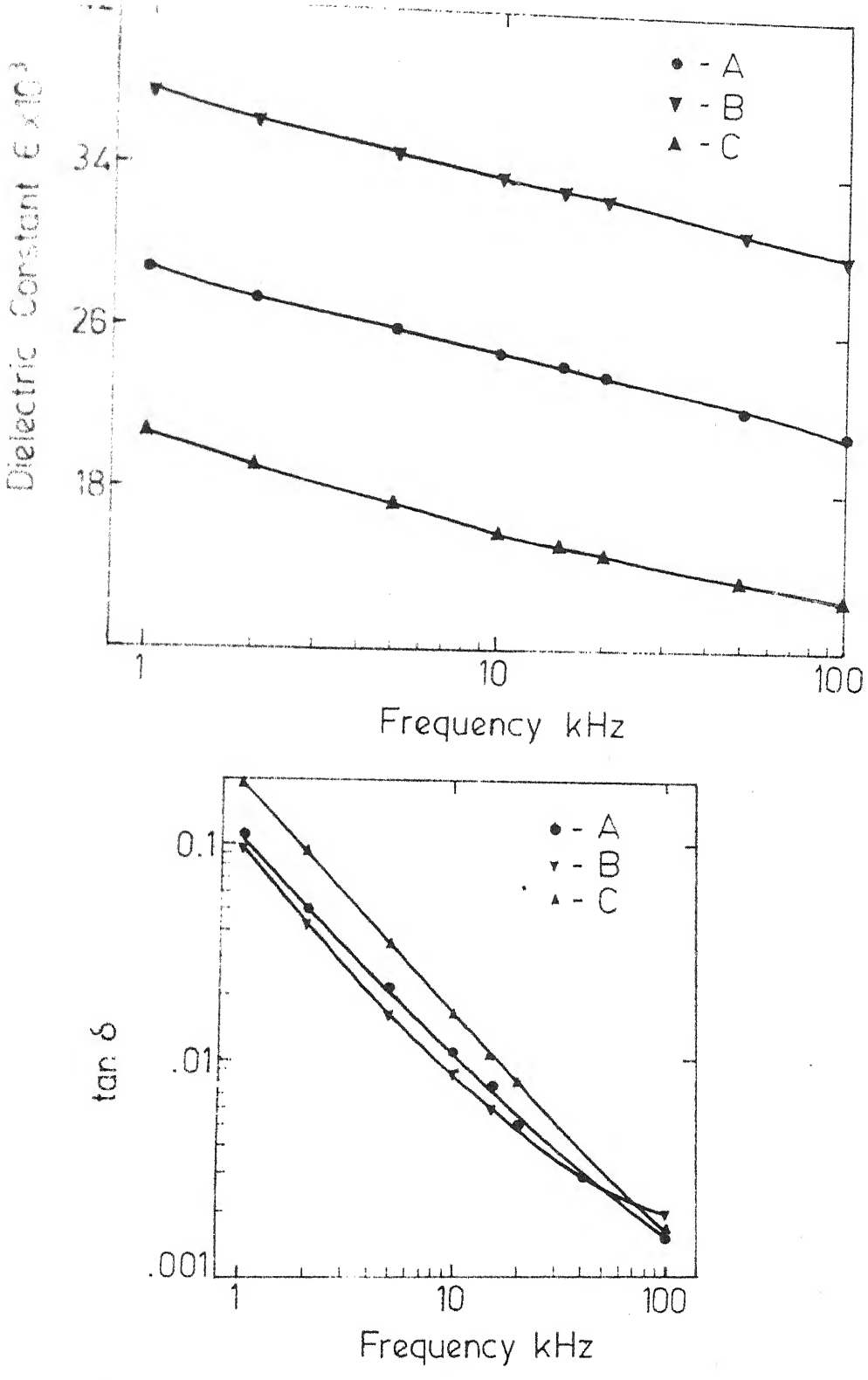

Fig. IV.29 Dielectric Constant Vs Frequency curves of

A- 0.4 mole % La + 1wt % Al_2O_3 added S(II) 25-30 μ $BaTiO_3$ + 4 wt % G_1 (1100°C / 15 min)

B- 0.4 mole % La + 1wt % Al_2O_3 added S(II) 25-30 μ $BaTiO_3$ + 4 wt % G_2 (1100°C / 15 min)

C- 0.4 mole % La + 1wt % Al_2O_3 added S(II) 25-30 μ $BaTiO_3$

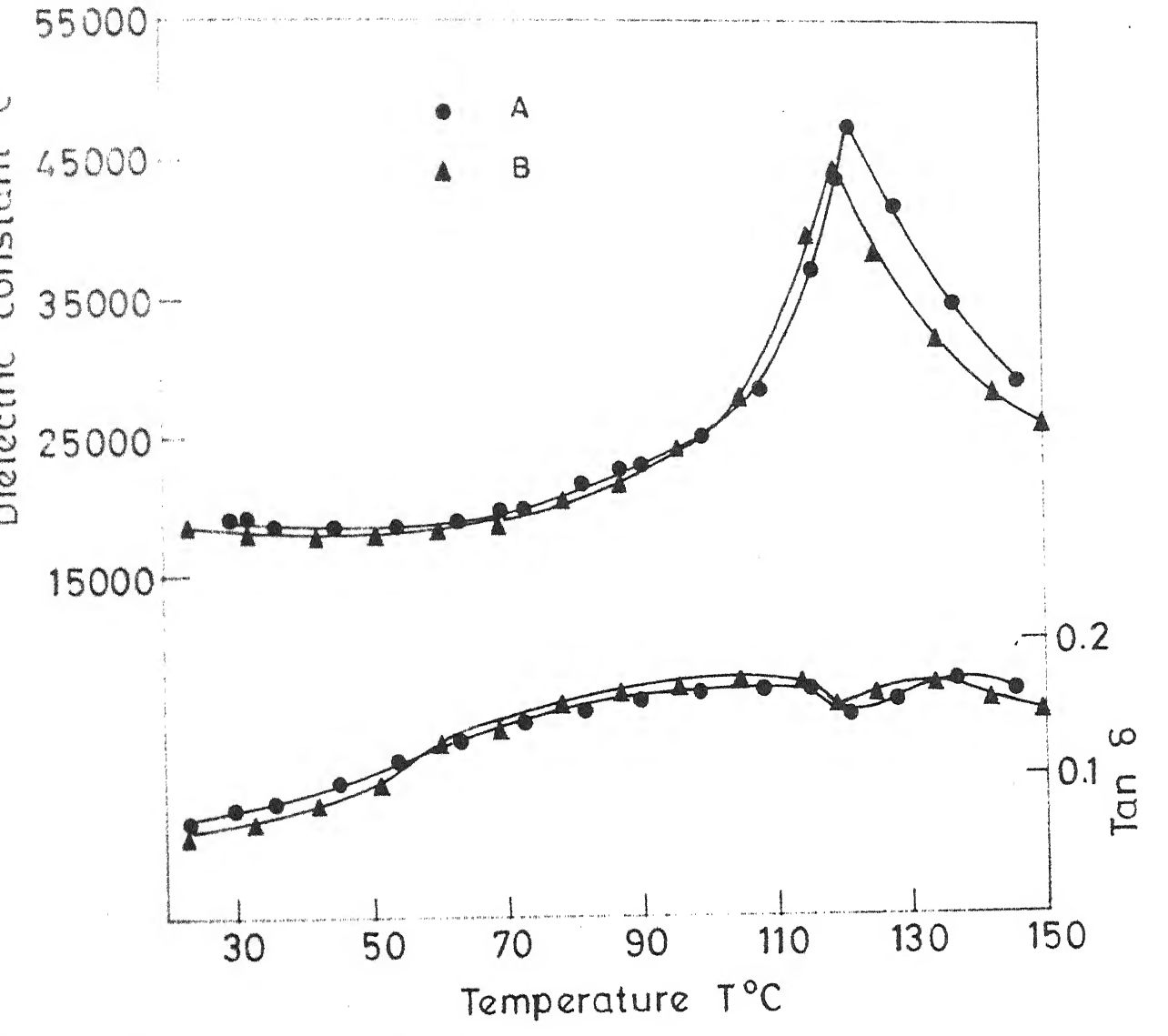

Fig. IV.30 ϵ vs T curve of

A – 0.4 mole % La + 1 wt % Al_2O_3 + 0.025 mole % Mn added S(II) 25–30 μ $BaTiO_3$ + 4 wt % G_1 (1100°C/15 min

B – 0.4 mole % La + 1 wt % Al_2O_3 + 0.025 mole % Mn added S(II) 25–30 μ $BaTiO_3$ + 4 wt % G_2 (1100°C/15 min

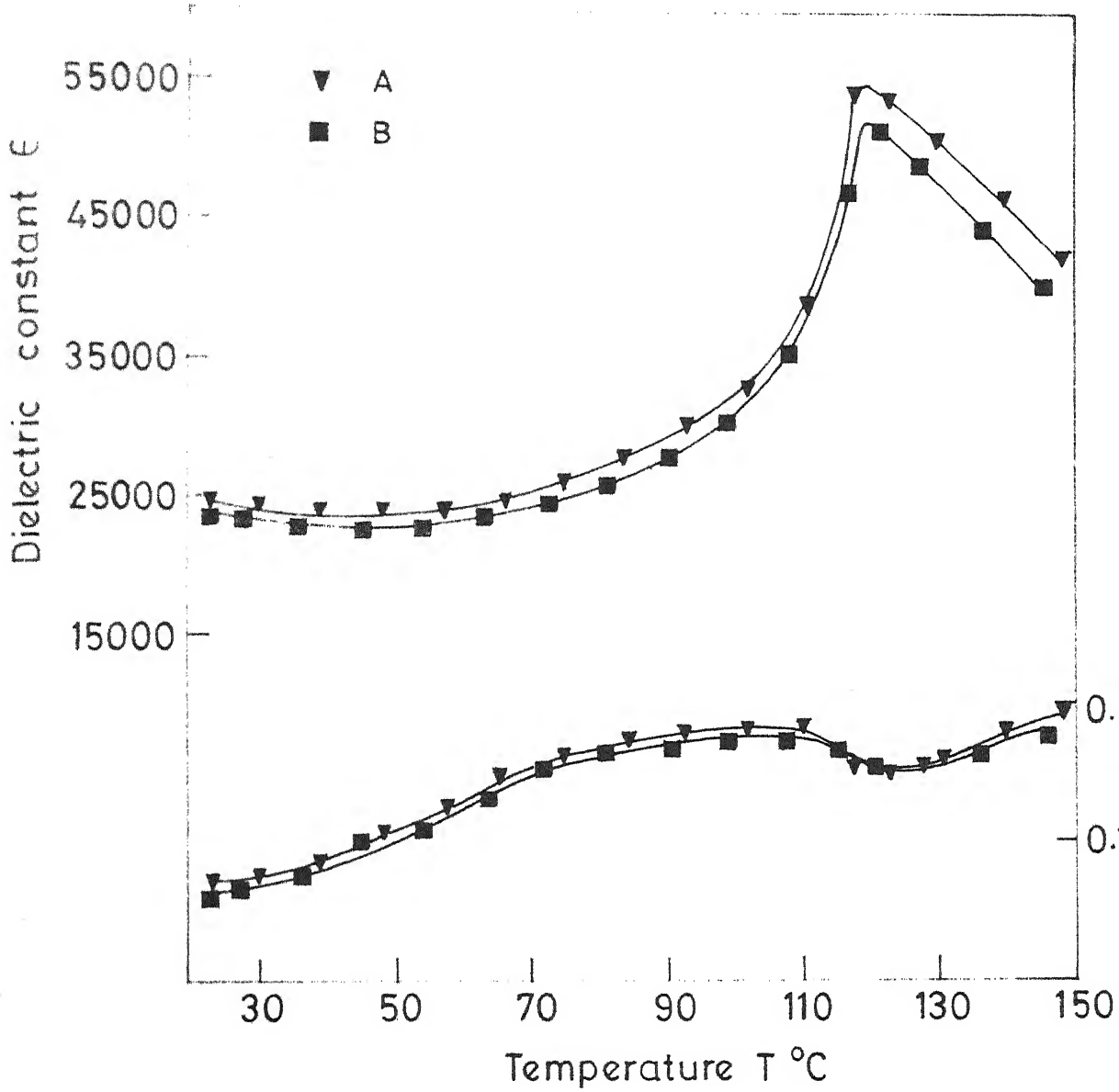

Fig. IV.31 ∈ vs T curve of

A-0.4 mole % La+1wt % Al_2O_3 added S(II) 25-

$BaTiO_3$ + 4 wt % G_1 (+ 0.025 mole % Mn) 1100°C/15

B-0.4 mole % La+1 wt % Al_2O_3 added S(II) 25-

$BaTiO_3$ + 4 wt % G_2 (+ 0.025 mole % Mn) 1100°C/15 m

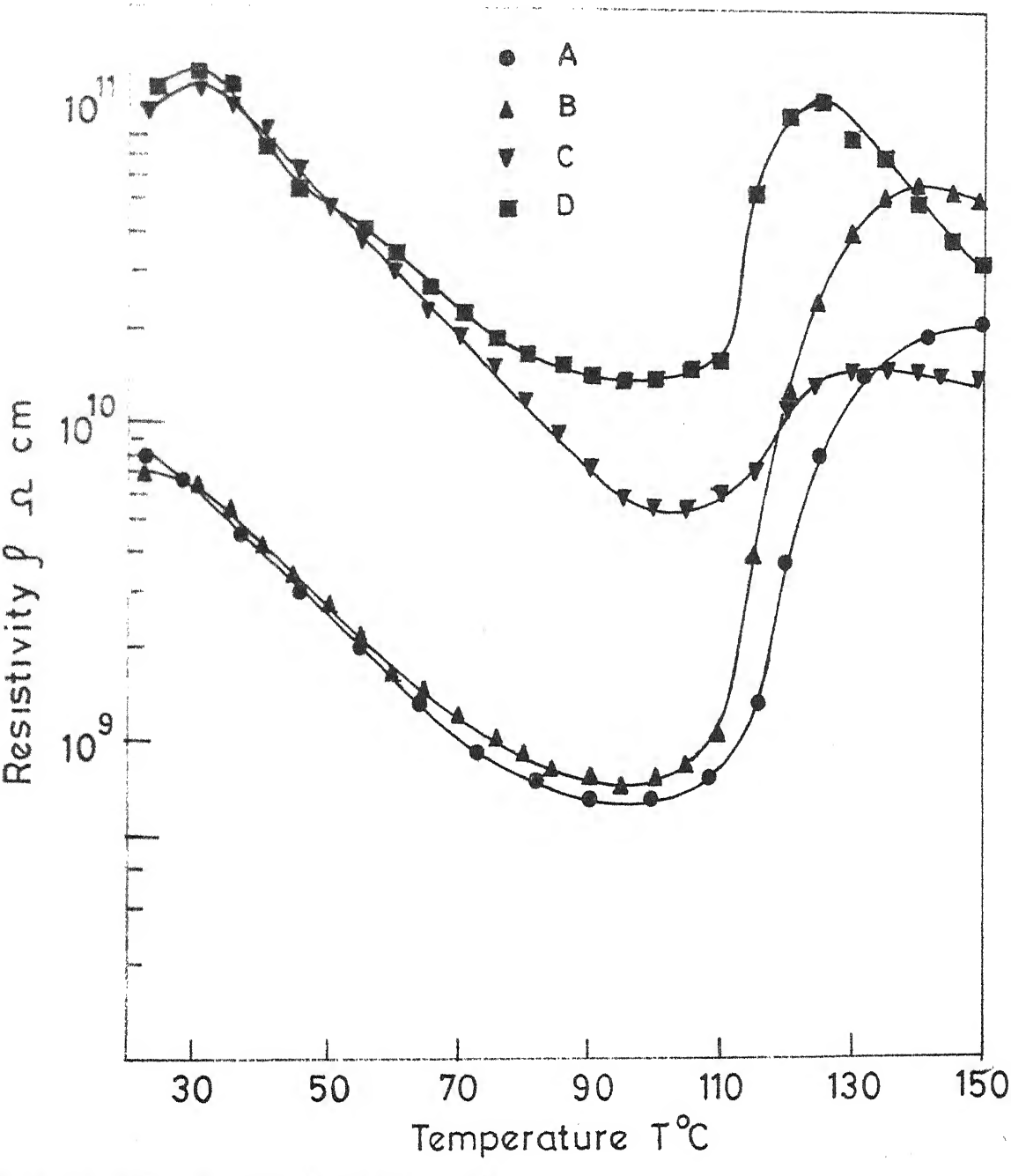

Fig. IV.32 ρ vs T curve of

A-0.4 mole % La+1wt % Al_2O_3+0.025 mole % Mn added S(II) 25-30 μ $BaTiO_3$+4wt % G_1(1100°C/15 min)

B-0.4 mole % La+1wt % Al_2O_3+0.025 mole % Mn added S(II) 25-30 μ $BaTiO_3$+wt % G_2(1100°C/15 min.)

C-0.4 mole % La+1wt % Al_2O_3 added S(II) 25-30 μ $BaTiO_3$+4 wt % G_1+0.025 mole % Mn (1100°C/15 min.)

D-0.4 mole % La+1wt % Al_2O_3 added S(II) 25-30 μ $BaTiO_3$+4wt % G_2+0.025 mole % Mn (1100°C/15 min.)

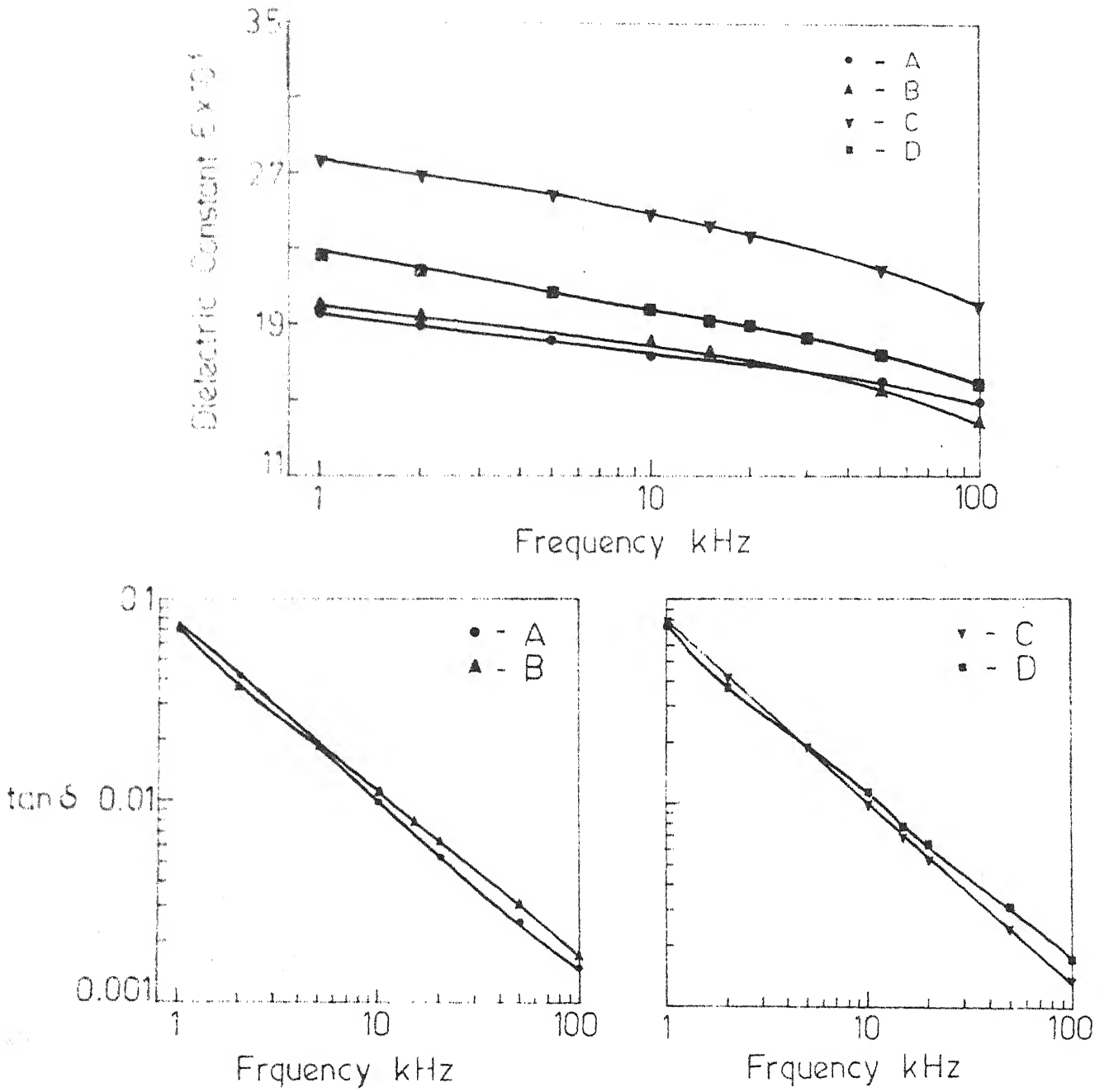

Fig. IV.33 Dielectric Constant Vs Frequency curves of

A - 0.4 mole % La + 1 wt % Al_2O_3 + 0.025 mole % Mn added S(II) 25-30 μ $BaTiO_3$ + 4 wt % G_1 (1100°C/15 min)

B - 0.4 mole % La + 1 wt % Al_2O_3 + 0.025 mole % Mn added S(II) 25-30 μ $BaTiO_3$ + 4 wt % G_2 (1100°C/15 min)

C - 0.4 mole % La + 1 wt % Al_2O_3 added S(II) 25-30 μ $BaTiO_3$ + 4 wt % G_1 (+0.025 mole% Mn) (1100°C/15 min)

D - 0.4 mole % La + 1 wt % Al_2O_3 added S(II) 25-30 μ $BaTiO_3$ + 4 wt % G_2 (+0.025 mole% Mn) (1100°C/15 min)

are observed. Among simultaneous and separate addition of Mn ions, later method produced overall better characteristics.

Further work can be done with the above knowledge, and with the following informations:

1. To get higher value of dielectric constant bigger particle size in 20-50 μ range (58), and lowest possible bulk resistance (59) are main criteria. With smaller particles lower resistivity is observed. Starting material had the average particle size value 4 μ. Bigger particles had the value in 17 to 19 μ range. So effect of intermediate [illegible] of starting material with additives (59) (to increase the grain size to the required value) to decrease the resistivity value below 9000 ohm-cm can be checked.

2. To decrease the resistivity value to a larger extent, effect of other dopants like Sb and Dy (59,38) and the effect of inert and reducing atmospheres (38,59) can be tried. Inert and reducing atmosphere will definitely improve the properties. But the preparation cost also will increase enormously.

3. G_1 glass with Mn produced better behaviour. Effect of higher concentration, preferably in steps of 0.005 mole % Mn rise, keeping G_1 concentration constant, can be checked. Many people report the better behaviour of CuO added samples (55,59). So its effect with G_1 glass can be studied and the effect of Mn and Cu ions can be compared.

Appendix I

A.1. Determination of Bismuth Oxide in Glass Sample (60):

A known quantity of the glass sample (about 500 mg) is dissolved in 10 ml of concentrated nitric acid by gentle heating and the solution is diluted to 250 ml. To 25 ml of the above solution, taken in a conical flask 3 to 4 drops of indicator solution (0.1% pyrocatechol violet) is added and diluted to about 100-150 ml. If the solution is not clear blue, dilute ammonia solution is added in dropwise until the violet colour changes to blue. Now the pH is checked and adjusted to about 2. The solution is titrated against 0.01 M EDTA solution until the colour changes to clear yellow. The pH is checked several times during the titration, especially in the vicinity of the end point. 1 ml of 0.01 M EDTA = 2.090 mg of Bi. From this amount of Bi_2O_3 is calculated.

A.2. Determination of Lanthanum in the Commercial Lanthanum Oxide:

About 250 mg of the oxide is dissolved in the minimum quantity of nitric acid (1 + 1) by gentle heating. The solution is made upto 250 ml. To 50 ml of the above solution excess of EDTA is added. EDTA will complex with the lanthanum present in the solution. The pH of the solution is adjusted first to 3 by 0.5 M ammonia and then to 5.5 to 5.9 by hexamine. The EDTA left after complexation is removed by titration with 0.01 M zinc solution to pink colour using xylenol orange as indicator. Excess of ammonium fluoride followed by 100-200 mg

ascorbic acid is added to the resulting solution, heated to 90-95°C, cooled and then liberated EDTA titrated against zinc solution to pink colour. 1 ml of 0.01 M EDTA complexed with lanthanum solution corresponds to 1.3891 g of La. From this the actual amount of La_2O_3 is calculated.

A.3. Determination of $TiCl_4$ in 10 ml of the Stock Solution (61)

10 ml of the stock solution is diluted to 250 ml. 20 ml of the above solution is pipetted out into a clean beaker, acidified with 20 ml concentrated hydrochloric acid and cooled to 10°C. To the cooled solution a freshly prepared 5 percent aqueous cupferron solution is added slowly and with constant vigorous stirring. First a yellow precipitate of titanium cupferrate is formed and the addition of cupferron reagent is continued till the formation of a white precipitate. The formation of the white precipitate indicates that the reagent is present in excess. The precipitate is removed by filtration while it is cold, through a No. 41 filter paper. This is washed several times with 10% by volume of hydrochloric acid containing 1.5 g of cupferron per litre, then twice with 5 N ammonia solution to remove excess of cupferron and finally once with water. The precipitate is ignited in a previously weighed silica crucible gently at first and then strongly. This is weighed as TiO_2. From this weight of TiO_2 the weight of $TiCl_4$ present in the solution is calculated.

79.9 g $TiCl_2$ corresponds to 189.9 g $TiCl_4$.

REFERENCES

1. J. Burn and G.H. Maher. J. Mat. Sci. 10, 645 (1963).
2. S.B. Desu, M.Tech. Thesis, I.I.T. Kanpur (1979).
3. S.B. Desu and E.C. Subbarao, J. Mat. Sci. 15, 2113 (1980).
4. S.B. Desu and E.C. Subbarao in Advances in Ceramics, Vol. 1, Am. Ceram. Soc. (1980).
5. Metals Hand Book, 8, 255.
6. E.C. Subbarao in Proc. Symp. on Sintering and Sintered Products, Bombay (1979).
7. S.M. Park, Ph.D. Thesis, Univ. of Illinois.
8. J.L. Mukherjee and H.S. Ravishankar in Proc. Symp. on Sintering and Sintered Products, Bombay (1979).
9. D. Hennings, Ber. Dtsch. Keram. Ges. 55, 359 (1978).
10. K. Ramesh Chowdary, M.Tech. Thesis, I.I.T. Kanpur (1981).
11. Von Hippal, Dielectrics and Wave, The M.I.T. Press (1966) p. 228.
12. I.A. Sauer and S.S. Flaschen, Proceedings of Electronic Components Symposium, 41 (1956).
13. O. Saburi, J. Phys. Soc. Japan, 14[9], 1159 (1959).
14. V.J. Tennery and R.L. Cook, J. Am. Ceram. Soc. 44[4], 187-93 (1961).
15. W. Heywang, ibid, 47[10], 484 (1964).
16. G.T. Mallick, Jr. and P.R. Emtage, J. App. Phys., 39[7], 3088-94 (1961).
17. H.A. Sauer and J.R. Fisher, J. Am. Ceram. Soc. 43[6], 297 (1960).
18. P.K. Gallagher, F. Schrey and F.V. Dimarcello, ibid, 46[8], 359 (1963).
19. W.R. Northover, ibid, 48[4], 173 (1965).
20. S. Hayakawa et.al., Am. Ceram. Soc. Bul., 45[2], 209 (1966).

[illegible]. [illegible]rouse and H. Sarahi, J. Amer. Cer. Soc. 54[6], 320 (1971).

[illegible]. F.K. Gallegher and F. Scherey, ibid, 46[12], 567 (1963).

[illegible]. F.Y. Tien and W.G. Carlson, ibid, 46[6], 297 (1963).

[illegible]. G.H. Jonker, Mater. Res. Bull. 2[4], 401 (1967).

[illegible]. P. Katsiroka, J. Am. Ceram. Soc. 55[2], 108 (1972).

[illegible]. M. Ueoka, Ferroelectrics, 7[1], 351 (1974).

[illegible]. P.W. Ryan and E.C. Subbarao, Applied Phys. Letters, 1[3], 69 (1963).

[illegible]. G. Goodman, J. Am. Ceram. Soc. 46[1], 48 (1963).

[illegible]. H.J. Haanstra and H. Ihrig, ibid, 63[5-6] (1980).

30. J.E. MacChasney and J.F. Potter, ibid, 48[1], 81 (1965).

31. G.T. Mallick, Jr. and P.R. Emtage, J. App. Phys. 39[7], 3088 (1968).

32. R. Wernicke, Advances in Ceramics, Vol. 1 (1981).

33. J. Daniels and R. Wernicke, Phylips Res. Rep. 31, 544 (1976).

34. R. Wernicke, Phys. Stat. Sol.(a), 47, 139 (1978).

35. H. Wichansky, Am. Ceram. Soc. Bull. 48[11], 998 (1970).

36. G. Goodman, Advances in Ceramics, Vol. 1 (1981).

37. R.M. Glaister, British Patent 849,938, Sept. 28, 1960.

38. S. Waku, Rev. Electr. Commun. Lab. 15[9-10], 689 (1967)

39. S. Waku et al., J. Phys. Soc. Jpn. 28, 457 (1967).

40. S. Waku, U. S. Patent 3,473,958, Oct. 21, 1969.

41. T. Prokopowicz, U. S. Patent 3,426,251, Feb. 4, 1969.

42. EIA Standard, RS-198-B. Electronic Industries Assn., Washington, D.C., 1971.

43. J. Volger, Progress in Semiconductors, Vol. 4, 207 (1960).

44. E.M. Levin, Phase Diagram for Ceramists (1964).

46. J.L. Murray, Am. Ceram. Soc. Bull. 37, 476 (1958).

47. L.E. Hase and Rustam Roy, J. Am. Ceram. Soc. 38, 476 (1958).

48. H.M. Landis, J. App. Phys. 36[6], 2000 (1965).

49. W.S. Clabaugh, E.M. Swiggard and R. Gilchrist, J. Res. NBS, 56, 289 (1956).

50. F. Kulcsar, J. Am. Ceram. Soc. 39[1], 13 (1956).

51. V.N. Eremenko and Yu. V. Naidich, 'Liquid Phase Sintering', A special research report translated from Russian consultants bureau.

52. W.D. Kingery, J. Appl. Phys. 30, 301 (1959).

53. J. Prince, C. Smittalls and S. Williams, J. Int. Met. 62, 287 (1938).

54. D.F. Rushman and M.A. Strivens, Trans. Faraday Soc. 42A, 231 (1946).

55. H.C. Graham, N.M. Tallen and K.S. Mazdiyasni, J. Am. Ceram. Soc. 52, 548 (1967).

56. W. Heywang and W. Wersing, Ferroelectrics, 7(1), 361 (1974).

57. J.C. Brice, Selected Topics in Solid State Physics, XII (1973).

58. S. Waku, 'Annual Report of Study Group on Applied Ferroelectrics in Japan', 27-154-984 (1979-4) (in Japanese).

59. K. Okazaki, Advances in Ceramics, Vol. 1, 23 (1981).

60. W. Heywang, J. Mater. Sci. 6, 1214 (1971).

61. H.A. Flaschka, EDTA Titrations.

62. Vogel, Quantitative Inorganic Chemical Analysis.

IPMS-1585- [illegible]